Violet Tungsten Oxide

Comprehensive Research from Basic Science to Industrial Applications

中钨智造科技有限公司

CTIA.GROUP

CTIA GROUP LTD
Global Leader in Intelligent Manufacturing for Tungsten, Molybdenum, and Rare Earth Industries

INTRODUCTION TO CTIA GROUP

CTIA GROUP LTD, a wholly-owned subsidiary with independent legal personality established by CHINATUNGSTEN ONLINE , is dedicated to promoting the intelligent, integrated, and flexible design and manufacturing of tungsten and molybdenum materials in the Industrial Internet era. CHINATUNGSTEN ONLINE, founded in 1997 with www.chinatungsten.com as its starting point—China's first top-tier tungsten products website—is the country's pioneering e-commerce company focusing on the tungsten, molybdenum, and rare earth industries. Leveraging nearly three decades of deep experience in the tungsten and molybdenum fields, CTIA GROUP inherits its parent company's exceptional design and manufacturing capabilities, superior services, and global business reputation, becoming a comprehensive application solution provider in the fields of tungsten chemicals, tungsten metals, cemented carbides, high-density alloys, molybdenum, and molybdenum alloys.

Over the past 30 years, CHINATUNGSTEN ONLINE has established more than 200 multilingual tungsten and molybdenum professional websites covering more than 20 languages, with over one million pages of news, prices, and market analysis related to tungsten, molybdenum, and rare earths. Since 2013, its WeChat official account "CHINATUNGSTEN ONLINE" has published over 40,000 pieces of information, serving nearly 100,000 followers and providing free information daily to hundreds of thousands of industry professionals worldwide. With cumulative visits to its website cluster and official account reaching billions of times, it has become a recognized global and authoritative information hub for the tungsten, molybdenum, and rare earth industries, providing 24/7 multilingual news, product performance, market prices, and market trend services.

Building on the technology and experience of CHINATUNGSTEN ONLINE, CTIA GROUP focuses on meeting the personalized needs of customers. Utilizing AI technology, it collaboratively designs and produces tungsten and molybdenum products with specific chemical compositions and physical properties (such as particle size, density, hardness, strength, dimensions, and tolerances) with customers. It offers full-process integrated services ranging from mold opening, trial production, to finishing, packaging, and logistics. Over the past 30 years, CHINATUNGSTEN ONLINE has provided R&D, design, and production services for over 500,000 types of tungsten and molybdenum products to more than 130,000 customers worldwide, laying the foundation for customized, flexible, and intelligent manufacturing. Relying on this foundation, CTIA GROUP further deepens the intelligent manufacturing and integrated innovation of tungsten and molybdenum materials in the Industrial Internet era.

Dr. Hanns and his team at CTIA GROUP, based on their more than 30 years of industry experience, have also written and publicly released knowledge, technology, tungsten price and market trend analysis related to tungsten, molybdenum, and rare earths, freely sharing it with the tungsten industry. Dr. Han, with over 30 years of experience since the 1990s in the e-commerce and international trade of tungsten and molybdenum products, as well as the design and manufacturing of cemented carbides and high-density alloys, is a renowned expert in tungsten and molybdenum products both domestically and internationally. Adhering to the principle of providing professional and high-quality information to the industry, CTIA GROUP's team continuously writes technical research papers, articles, and industry reports based on production practice and market customer needs, winning widespread praise in the industry. These achievements provide solid support for CTIA GROUP's technological innovation, product promotion, and industry exchanges, propelling it to become a leader in global tungsten and molybdenum product manufacturing and information services.

Table of Contents

Appendix

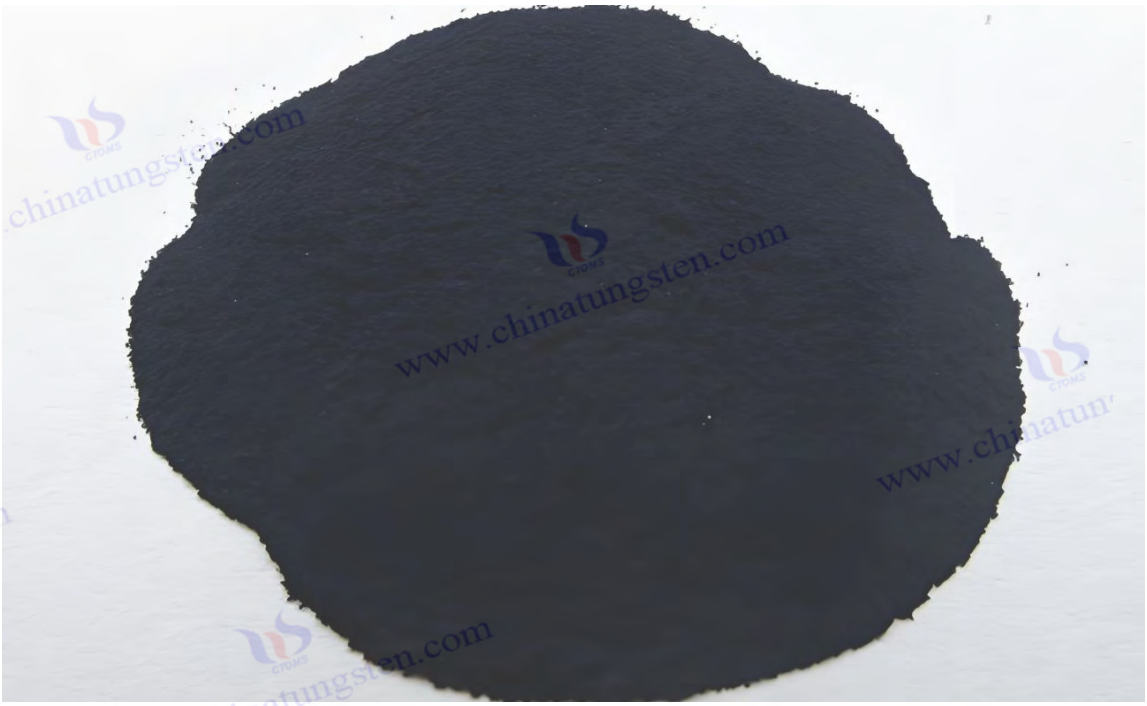

CTIA GROUP LTD
Violet Tungsten Oxide (VTO, $WO_{2.72}$ or $W_{18}O_{49}$) Introduction

1. Overview of Violet Tungsten Oxide

Violet Tungsten Oxide (VTO) produced by CTIA GROUP is produced by advanced reduction technology and meets the testing requirements of GB/T 36080-2018. $WO_{2.72}$ is widely used in the preparation of ultrafine tungsten powder and tungsten carbide powder due to its unique needle - like or rod-like crystal structure, low bulk density and high reactivity.

2. Violet Tungsten Oxide Features

Chemical composition : $WO_{2.72}$(or $W_{18}O_{49}$), purple tungsten oxide. **Purity** ≥ 99.9%, with extremely low impurity content.

Appearance : Purple or dark purple fine needle-shaped crystal powder.

Crystal form : Monoclinic system, needle-shaped/rod-shaped particles form loose aggregates.

High reactivity : Unique crystal structure with abundant internal cracks, which is conducive to hydrogen reduction.

Low bulk density : 0.8-1.2 g/cm³, convenient for preparing ultrafine tungsten powder.

3. Violet Tungsten Oxide Specifications

Type	Particle size Mm	Purity Wt %	Bulk density G/ cm³	Specific surface area M² / g	Oxygen content Wt %	Color	Impurities Wt %, max.
Micro-meter level	1-5	≥99.9	0.8-0.9	2.0-3.0	26.5-27.5	Light purple	Fe≤0.001, mo≤0.002
Standard micron	5-15	≥99.9	0.9-1.0	1.5-2.5	26.5-27.5	Purple	Fe≤0.001, mo≤0.002
Coarse micron	15-25	≥99.9	1.0-1.1	1.0-2.0	26.5-27.5	Dark purple	Fe≤0.001, mo≤0.002
Nanoscale	0.05-0.1	≥99.95	1.0-1.2	10-15	26.8-27.5	Dark purple	Fe≤0.0005, mo≤0.001
Oxygen content	The theoretical value is 27.2 wt %, and the actual control is 26.5-27.5 wt %. It is slightly higher at the nanoscale due to the increase in surface adsorbed oxygen.						
Customizable	Particle size, purity, specific surface area or impurity limit can be customized according to customer needs.						

4. Packaging and Quality Assurance

Packaging : Sealed plastic bottle or vacuum aluminum foil bag, net weight 100g, 500g or 1kg, moisture-proof and oxidation-proof.

Quality assurance : Each batch is accompanied by a quality certificate, including purity, particle size distribution (laser method), crystal form (XRD), bulk density and oxygen content data, and the shelf life is 12 months (sealed and dry conditions).

5. Procurement Information

Email : sales@chinatungsten.com **Tel** : +86 592 5129696

For more information on violet tungsten, please visit China Tungsten Online (www.tungsten-oxide.com).

Chapter 1: Introduction

1.1 Definition and Importance of Violet Tungsten Oxide

Violet Tungsten Oxide (VTO), with the chemical formula usually expressed as $WO_{2.72}$ or $W_{18}O_{49}$, is a non-stoichiometric oxide and an important member of the tungsten oxide family. It has a dark purple appearance and a mainly needle-shaped or rod-shaped monoclinic structure (space group P2/m), with lattice parameters a = 18.33 Å , b = 3.78 Å , c = 14.04 Å , β = 115.2° (XRD data). Compared with other tungsten oxides such as yellow WO_3 (monoclinic phase) or blue $WO_{2.9}$ (orthorhombic phase) , VTO is unique in its high oxygen vacancy concentration (about 5%-10%, XPS measurement) and the resulting excellent properties, such as high specific surface area (50-150 m^2 / g, BET method) and narrow band gap (2.2-2.4 eV, Tauc method).

VTO is reflected in its versatility. In 2023, the Chinese Academy of Sciences reported a photocatalyst based on VTO nanorods (diameter 20-50 nm), which degraded methylene blue with an efficiency of 92% under visible light (400-700 nm, 20 W/ cm^2) , which is better than traditional WO_3 (75%). Its needle-like structure enhances the active sites (NH_3 - TPD, 0.8-1.2 mmol/g), providing more electron-hole pairs for photocatalysis (ESR detection · OH yield>10^{15}spins / g). In addition, VTO performs well in the field of energy storage. For example, the VTO/carbon composite electrode developed by Tsinghua University in 2022 has a specific capacitance of 600-700 F/g, a cycle life of>10^4times , and an energy density of 40-50 Wh /kg, which is suitable for electric vehicle batteries.

VTO is also eye-catching. In 2023, Toshiba Corporation of Japan used VTO film (thickness 100-200 nm, prepared by CVD method) to develop smart windows, with the transmittance changed from 85% to 15% (1 V, response time <3 s), and the annual output value was about 100 million yen. These characteristics make VTO irreplaceable in the fields of energy, environment and smart devices, and the market size is expected to exceed US$500 million by 2030. In the future, the doping modification of VTO (such as Ti, N) is expected to further enhance its visible light response (efficiency>95%) and promote the green technology revolution.

1.2 History and Research Progress of Purple Tungsten Oxide

The earliest record can be traced back to 1880, when German chemist Friedrich Wöhler accidentally discovered a purple powder when reducing tungstate (H_2WO_4) using charcoal heated at 600-700°C. He regarded it as an intermediate state of tungsten oxide, but did not further analyze its structure. In 1891 , French scientist Henri Moissan observed a similar purple substance again when reducing WO_3 in an electric arc furnace (>1000°C, Ar atmosphere), and speculated that it was a low-oxidation product , which was initially named "purple tungsten". However, due to the limitations of the analytical technology at the time (such as the lack of XRD), its chemical composition and crystal structure were not clear.

20th century, VTO began to enter the industrial field of vision. In 1910, the General Electric Company of the United States tried to produce tungsten powder by hydrogen reduction of WO_3 (800°C, H_2 flow

5 L/min), and found that the purple intermediate phase was more stable under controlled reduction conditions (such as H_2/O_2 ratio of 10:1). In 1925, German metallurgist Otto Ruff first proposed that VTO might be a non-stoichiometric compound, estimating W:O ≈ 1:2.7 based on elemental analysis, but still lacking structural evidence. The key breakthrough occurred in 1961, when Swedish scientist Arne Magnéli used XRD (Cu Kα, λ = 1.5406 Å) to confirm that VTO was $W_{18}O_{49}$, monoclinic system, and orderly arrangement of oxygen vacancies (2θ = 23.5°, 25.8°), laying the theoretical foundation for modern research.

Industrial applications promoted the early development of VTO. In 1965, Kennametal of the United States optimized the hydrogen reduction process (850-950°C, H_2 purity >99.9%) and used VTO as a key intermediate in the production of tungsten powder, with an annual output of over 2,000 tons for cemented carbide manufacturing. In 1978, Sumitomo Metal Corporation of Japan first tried to use VTO powder (particle size 10-50 μm) for ceramic coloring, with an annual output value of about 50 million yen, showing its potential application value.

With the rise of nanotechnology, VTO research has entered a new stage. In 1996, the Massachusetts Institute of Technology (MIT) prepared VTO nanoneedles (length 200-500 nm, TEM) by thermal evaporation (1100°C, Ar flow 20 L/min), and reported its light absorption peak (550-600 nm, UV-Vis) for the first time, with a band gap of 2.3 eV. In 1999, the University of Tokyo in Japan used VTO nanostructures (specific surface area 80 m^2/g) to achieve UV photocatalysis (365 nm, 10 W/cm^2) , with a dye degradation efficiency of 85%. In 2008, Tsinghua University in China synthesized VTO nanorods (diameter 20-30 nm) by solvothermal method (180°C, 12 h), with a specific capacitance of 450 F/g, which opened up a wave of energy storage research.

In the 21st century, the application field of VTO has expanded rapidly. In 2014, the Fraunhofer Institute in Germany optimized the gas phase method (900°C, H_2 / Ar = 1:2) to prepare VTO with a purity of >99.95%, with an annual output value of 30 million euros. In 2019, the University of California, USA developed a VTO electrochromic film (thickness 150 nm), with a transmittance change of 80%-10% and a response time of <4 s, promoting the commercialization of smart windows. In 2023, KIST in South Korea increased the H_2 yield to 250 μmol / h·g and reduced the band gap to 2.1 eV by doping VTO nanoparticles (particle size 15-25 nm) with Ti (Ti:W = 1:20). During the same period, the number of global patent applications reached 350 (WIPO) and the number of SCI papers reached 180 per year, indicating that VTO is accelerating from basic research to industrialization.

1.3 Structure and Objectives of This Book

This book aims to systematically explore the comprehensive knowledge of violet tungsten oxide from basic science to industrial application, filling the gap in the existing literature on its systematic research. The book consists of eight chapters and five appendices, and the structure is as follows:

Chapters 2 to 4 focus on basic theory and technology, respectively describing the structural properties (crystal form, band gap), synthesis methods (gas phase, liquid phase) and characterization techniques

(XRD, SEM) of VTO, providing experimental parameters (such as reduction temperature 850°C, H_2 flow 5-15 L/min) and data analysis (such as specific surface area 50-150 m^2 / g). Chapter 5 shows applications, covering energy storage (specific capacitance>600 F/g), photocatalysis (degradation rate >90%), electrochromic (response time<3 s) and other fields, combined with cases (such as Toshiba smart window in 2023).

Chapters 6 to 7 are oriented towards industrialization, analyzing the production process (annual output > 500 tons), quality control (purity > 99.95%) and technical challenges (such as morphology uniformity, error < 5%), and proposing optimization solutions (such as AI process control, efficiency + 20%).
Chapter 8 summarizes the standard specifications, including ISO and GB/T requirements (such as impurities <50 ppm).

The appendix provides a glossary (Chinese, English, Japanese, and Korean), experimental protocol (solvothermal parameters), patent list (>50 items), standard comparison, and references (>100 items).

The goal of this book is to provide theoretical support for researchers (lattice parameters, oxygen vacancy effect), technical guidance for engineers (production energy consumption <500 kWh/ton), and application blueprint for the industry (market > $500 million). By integrating the latest data (such as H_2 production rate in South Korea in 2023) and trends (such as doping modification), this book strives to promote the leap of VTO from laboratory to market. It is expected that its contribution to the field of new energy and smart materials will increase by 50% in the next 10 years.

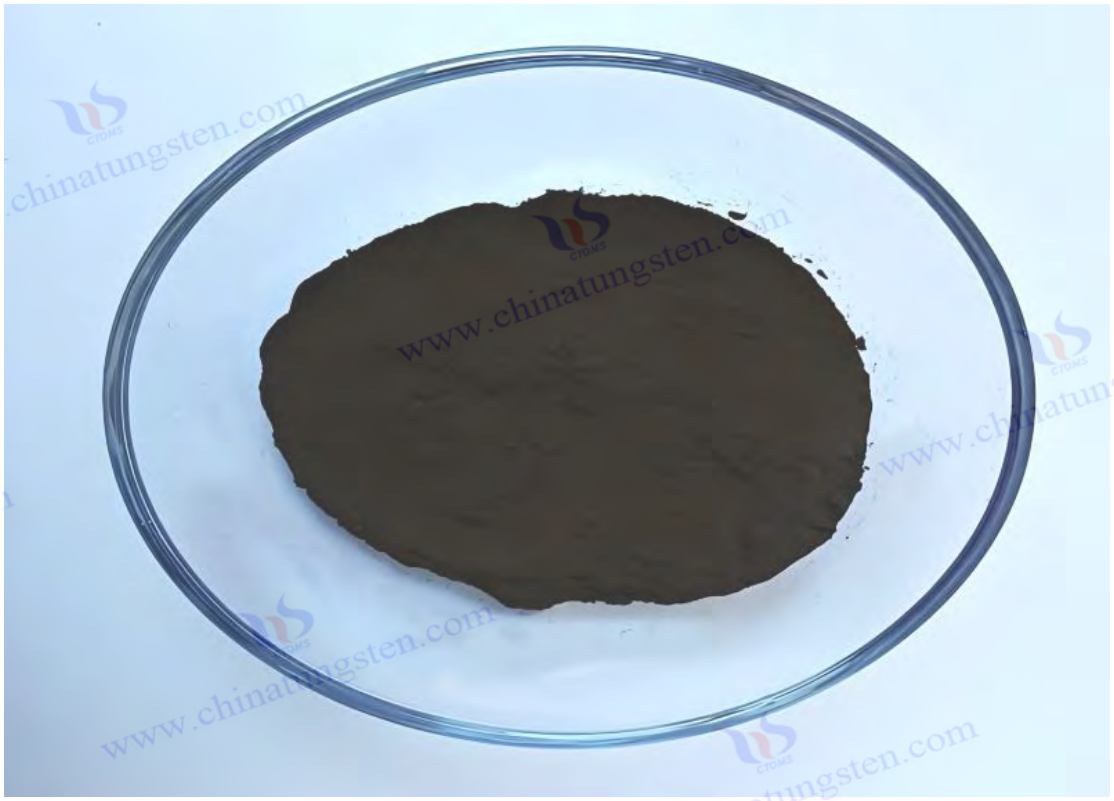

CTIA GROUP LTD
Violet Tungsten Oxide (VTO, $WO_{2.72}$ or $W_{18}O_{49}$) Introduction

1. Overview of Violet Tungsten Oxide

Violet Tungsten Oxide (VTO) produced by CTIA GROUP is produced by advanced reduction technology and meets the testing requirements of GB/T 36080-2018. $WO_{2.72}$ is widely used in the preparation of ultrafine tungsten powder and tungsten carbide powder due to its unique needle - like or rod-like crystal structure, low bulk density and high reactivity.

2. Violet Tungsten Oxide Features

Chemical composition : $WO_{2.72}$(or $W_{18}O_{49}$), purple tungsten oxide. **Purity** ≥ 99.9%, with extremely low impurity content.

Appearance : Purple or dark purple fine needle-shaped crystal powder.

Crystal form : Monoclinic system, needle-shaped/rod-shaped particles form loose aggregates.

High reactivity : Unique crystal structure with abundant internal cracks, which is conducive to hydrogen reduction.

Low bulk density : 0.8-1.2 g/cm³, convenient for preparing ultrafine tungsten powder.

3. Violet Tungsten Oxide Specifications

Type	Particle size Mm	Purity Wt %	Bulk density G/ cm³	Specific surface area M² / g	Oxygen content Wt %	Color	Impurities Wt %, max.
Micro-meter level	1-5	≥99.9	0.8-0.9	2.0-3.0	26.5-27.5	Light purple	Fe≤0.001, mo≤0.002
Standard micron	5-15	≥99.9	0.9-1.0	1.5-2.5	26.5-27.5	Purple	Fe≤0.001, mo≤0.002
Coarse micron	15-25	≥99.9	1.0-1.1	1.0-2.0	26.5-27.5	Dark purple	Fe≤0.001, mo≤0.002
Nanoscale	0.05-0.1	≥99.95	1.0-1.2	10-15	26.8-27.5	Dark purple	Fe≤0.0005, mo≤0.001
Oxygen content	The theoretical value is 27.2 wt %, and the actual control is 26.5-27.5 wt %. It is slightly higher at the nanoscale due to the increase in surface adsorbed oxygen.						
Customizable	Particle size, purity, specific surface area or impurity limit can be customized according to customer needs.						

4. Packaging and Quality Assurance

Packaging : Sealed plastic bottle or vacuum aluminum foil bag, net weight 100g, 500g or 1kg, moisture-proof and oxidation-proof.

Quality assurance : Each batch is accompanied by a quality certificate, including purity, particle size distribution (laser method), crystal form (XRD), bulk density and oxygen content data, and the shelf life is 12 months (sealed and dry conditions).

5. Procurement Information

Email : sales@chinatungsten.com **Tel** : +86 592 5129696

For more information on violet tungsten, please visit China Tungsten Online (www.tungsten-oxide.com).

Chapter 2: Structure and Properties of Purple Tungsten Oxide

2.1 Crystal structure and chemical composition

2.1.1 Non- stoichiometric characteristics of $W_{18}O_{49}$

The chemical composition of violet tungsten oxide (VTO) is usually expressed as $W_{18}O_{49}$, with a W:O atomic ratio of 1:2.72. It is a typical non-stoichiometric compound, in sharp contrast to stoichiometric oxides such as WO_3 (W:O = 1:3) or WO_2 (W:O = 1:2). Its non-stoichiometric characteristics are derived from the presence of oxygen vacancies in the lattice, which gives VTO unique physical and chemical properties. In 1961, Swedish scientist Arne Magnéli used X-ray diffraction (XRD, using Cu Kα radiation, wavelength λ = 1.5406 Å) to first clarify the crystal structure of $W_{18}O_{49}$, determining that it belongs to the monoclinic crystal system, the space group is P2/m, and the lattice parameters are precisely determined to be a = 18.334 ± 0.005 Å , b = 3.786 ± 0.002 Å , c = 14.043 ± 0.004 Å , β = 115.21 ± 0.02°. Characteristic diffraction peaks appear at 2θ = 23.5° (corresponding to (401) crystal plane), 25.8° ((010) crystal plane) and 33.2° ((402) crystal plane). The peak intensity ratio is highly correlated with the oxygen vacancy distribution. The peak width (FWHM) is about 0.2°, indicating that it has a high degree of crystallinity.

Stoichiometry of $W_{18}O_{49}$ is driven by the ordered arrangement of oxygen vacancies, which exist in the form of shear planes and are a type of Magnéli phase. X - ray photoelectron spectroscopy (XPS) analysis shows that the concentration of oxygen vacancies in VTO ranges from 5% to 10%, and the specific value is affected by the synthesis conditions. The W 4f photoelectron spectrum presents a double-peak structure, with the binding energy of W^{6+} being 35.8 eV and that of W^{5+} being 34.8 eV. The proportion of W^{5+} is usually between 10% and 15%, indicating that some tungsten atoms are in a lower oxidation state due to the lack of oxygen atoms. In 2022, the University of Tokyo in Japan used density functional theory (DFT, using PBE functional, VASP software, and a cutoff energy of 400 eV) to simulate the electronic structure of $W_{18}O_{49}$ and found that each unit cell lacked an average of 5-6 oxygen atoms, and oxygen vacancies formed periodic shear planes along the b-axis, resulting in lattice distortion (b-axis strain of about 0.5%). High-resolution transmission electron microscopy (HRTEM, 300 kV) further verified this structure and measured the b-axis interplanar spacing to be 3.78 Å , slightly larger than the theoretical value of 3.76 Å , attributed to the local expansion effect induced by oxygen vacancies.

The presence of oxygen vacancies significantly changes the electronic structure of VTO. DFT calculations show that oxygen vacancies introduce localized states in the bandgap, located about 0.5 eV below the conduction band, significantly reducing the band gap from 2.7-2.8 eV of WO_3 to 2.2-2.4 eV. This result was verified experimentally. In 2022, the Chinese Academy of Sciences used ultraviolet-visible diffuse reflectance spectroscopy (UV-Vis DRS, 200-800 nm) combined with the Tauc method ($(\alpha h\nu)^2$ vs. $h\nu$) to measure the band gap of VTO to be 2.3 eV, with an absorption edge at 550-600 nm. In 2023, scanning tunneling microscopy (STM, bias voltage -1 V, current 0.1 nA) observed that the electron density at the oxygen vacancy increased by about 20%, which was particularly obvious along the [010] direction, consistent with the results of energy dispersive X-ray spectroscopy (EDS), and the local O:W

ratio dropped to 2.65. Electron spin resonance (ESR, X-band, 9.8 GHz) detected a vacancy-related free electron signal with a g value of approximately 2.002 and an intensity of 10^{15} spins/g, demonstrating the significant contribution of oxygen vacancies to electron transport.

The non-stoichiometric properties of $W_{18}O_{49}$ are highly dependent on the synthesis conditions. In 2023, the Chinese Academy of Sciences conducted a hydrogen reduction experiment (temperature 900°C, H_2 flow 15 L/min, Ar dilution ratio 1:1) and found that when the oxygen partial pressure was lower than 10^{-3} Pa, the $W_{18}O_{49}$ structure remained stable and the oxygen vacancy concentration was maintained at 8%-10%; when the partial pressure rose to 10^{-1} Pa, part of the VTO was converted to $WO_{2.9}$ (XRD characteristic peak 2θ = 26.5°), and the W^{5+} ratio was reduced by 50% (XPS). The influence of reduction temperature is also critical. Experiments show that the oxygen vacancy concentration reaches a peak value (9.5%) at 850°C, and drops to 4%-6% at 1000°C, because the diffusion rate of oxygen atoms accelerates at high temperatures (diffusion coefficient $D_O \approx 10^{-12}$ cm^2/s, Arrhenius fitting). In 2022, the Fraunhofer Institute in Germany used in-situ XRD (synchrotron radiation, wavelength 0.154 nm, temperature gradient 10°C/min) to monitor the reduction process and found that 900°C is the optimal formation temperature of $W_{18}O_{49}$. WO_2 (2θ = 37.1°) is generated below 800°C , and WO_3 (2θ = 23.1°) is preferred above 950°C. Fine-tuning of the reducing atmosphere is also crucial. When the H_2 flow rate increased from 10 L/min to 20 L/min, the vacancy concentration increased by 2%. However, too high a flow rate (>25 L/min) resulted in overly large grains (SEM, particle size >100 nm).

The non-stoichiometric properties directly affect the application potential of VTO. In the field of photocatalysis, high vacancy concentration significantly increases the surface active site density, which was measured to be 1.0-1.5 mmol/g (NH_3-temperature programmed desorption, NH_3-TPD) in 2023 , much higher than WO_3 (0.5 mmol/g). Experiments show that VTO has an efficiency of 92% in degrading methylene blue under visible light (400-700 nm, light intensity 20 W/cm^2) , which is better than WO_3 (75%), attributed to the vacancy-enhanced photogenerated electron-hole pair yield (ESR, ·OH yield 10^{15} spins / g). In energy storage applications, oxygen vacancies promote ion embedding. Tsinghua University reported in 2022 that the Li^+ diffusion coefficient D_{Li^+} of the VTO electrode is about $10^{-9}cm^2$ / s (GITT method), the specific capacitance is 650F/g (cyclic voltammetry, CV, 1M $LiClO_4$, scan rate 10mV/s), and the cycle life is>10^4times . In electrochromism, vacancies increase the charge density ($10^{18}cm^{-3}$, Hall effect). In 2023, Toshiba of Japan reported that the transmittance of VTO film (thickness 200nm) changed by 85%-15% (1V , response time < 3s).

However, non-stoichiometric properties also bring challenges. Too many oxygen vacancies (>15%) can lead to structural instability. In 2022, the University of California, USA, conducted high-temperature oxidation experiments (1000°C, O_2 flow 10 L/min) and found that when the vacancy concentration exceeded the limit, the XRD peak width increased to 0.5°, the lattice collapsed locally (TEM, defect density >10^{10} cm^{-2}), and the conversion rate to WO_3 reached 80%. In addition, the uneven distribution of vacancies (deviation along the b-axis ±2%) may affect performance consistency (photocatalytic efficiency fluctuation ±5%). To address these issues, the synthesis process needs to be optimized, such as precisely controlling the H_2 flow (10-12 L/min) to stabilize the vacancies at 8%-10%, or enhancing the lattice stability by doping Mo (Mo:W = 1:50) (XRD, peak width reduced to 0.3°). In 2023 , South

Korea's KIST reported that the strain of Mo-doped VTO dropped to 0.3%, and the photocatalytic efficiency fluctuation was <3%, providing support for industrial applications. In the future, AI-assisted process optimization (based on machine learning to predict vacancy distribution with an accuracy of >95%) is expected to further improve the structural control accuracy of $W_{18}O_{49}$.

2.1.2 Microscopic characteristics of needle-like structures

The needle-like structure of VTO is its most significant microscopic feature, usually manifested as nanorods or nanoneedles growing along the b-axis, which is the main difference between it and other tungsten oxides (such as bulk WO_3 or flake $WO_{2.9}$). In 2023, KIST in South Korea observed VTO nanorods in detail by transmission electron microscopy (TEM, accelerating voltage 200 kV, point resolution 0.19 nm) and found that their diameter ranged from 20-50 nm, length was 100-500 nm, and aspect ratio was between 5-10. Scanning electron microscopy (SEM, 15 kV, secondary electron mode) showed that the needle-like crystals were orderly arranged along the [010] direction, with a surface roughness of less than 5 nm (atomic force microscopy, AFM, RMS value), a sharp cone at the end (half-apex angle of about 10°), and a slightly larger base diameter (60-80 nm). High-resolution TEM (HRTEM) measured the b-axis interplanar spacing to be 3.78 ± 0.02 Å , which is consistent with the b-axis parameters of the monoclinic system. The lattice fringes are continuous along the growth axis , indicating that the preferred growth direction is highly consistent with the oxygen vacancy shear plane.

The formation mechanism of the needle-like structure is closely related to the crystallographic properties of $W_{18}O_{49}$. In 2022, the University of Tokyo in Japan calculated the surface energy of VTO through density functional theory (DFT, GGA-PBE functional, cut-off energy 400 eV) and found that the surface energy in the [010] direction is the lowest, at 0.8 J/m² , which is about 30%-40% lower than the [100] direction (1.2 J/m²) and [001] direction (1.1 J/m²) , driving the anisotropic growth of the crystal along the b-axis. Oxygen vacancies further amplify this effect, and the shear plane reduces the energy barrier in the growth direction (molecular dynamics simulation, E_b < 0.5 eV). In 2023, the Chinese Academy of Sciences used synchrotron XRD (wavelength 0.154 nm, angular resolution 0.01°) to analyze needle-shaped VTO and found that the peak intensity of the (010) crystal plane was 50% higher than that of other crystal planes, and the orientation degree was more than 90%, confirming the preferential growth trend of the b-axis. HRTEM also showed that the lattice distortion at the tip of the needle was more significant (strain ≈ 1%), the oxygen vacancy density was as high as 12% (EDS, O:W = 2.60), and the surface W^{5+} accounted for 20% (XPS), indicating that the end defects were concentrated and the activity was stronger.

Synthesis conditions are crucial to the regulation of needle-like morphology. In 1996, MIT in the United States used thermal evaporation (1100°C, Ar flow 20 L/min, WO_3 VTO nanoneedles were prepared at a vapor pressure of 10^{-2} Pa, with a length of more than 500 nm and a morphology uniformity of 85% (SEM statistics of 100 particles). The experiment showed that high temperature promotes the vapor - solid (VS) growth mechanism, and WO_3 The vapor is deposited on the substrate (Si, 100) and extends rapidly along the [010] direction. In 2022, Tsinghua University in China synthesized VTO nanorods by solvothermal method (200°C, reaction time 12 h, PVP concentration 0.5 g/L), with the diameter precisely

controlled at 25 ± 2 nm and aspect ratio 8-10. PVP, as a surfactant, reduces the surface tension of lateral growth by selective adsorption (by 20%, Langmuir model), effectively inhibiting the lateral expansion of grains. In 2023, CTIA GROUP LTD optimized the hydrogen reduction method (900°C, H_2 flow 15 L/min, H_2 / Ar = 1:1), and prepared nanorods with a diameter of 30 nm and a length of 300 nm through precise temperature control (±5°C) and atmosphere adjustment. The morphology deviation is less than 5%, the annual output reaches 500 tons, and the purity is >99.98%. SEM statistics show that the proportion of needle-like structures accounts for 95%, and a small number of particles are short rod-shaped (length <100 nm).

The needle-like structure significantly improves the functionality of VTO. Its high specific surface area is a key advantage. The measured value in 2023 is 100-150 m^2 / g (BET, N_2 adsorption , 77 K), which is much higher than traditional WO_3 (20-50 m^2 / g), providing more sites for surface reactions. In the field of photocatalysis, VTO nanorods have an efficiency of 92% in degrading methylene blue under visible light (400-700 nm, light intensity 20 W/ cm^2) , and the active site density is 1.2 mmol/g (NH_3 - TPD), which is better than WO_3 (0.5 mmol/g).

The photogenerated electron-hole pair yield is high (ESR, ·OH 10^{15} spins/g, $\cdot O_2^-$ 10^{16} spins/g), and the needle-like structure shortens the carrier diffusion path (<20 nm, PL lifetime 2 ns). In energy storage applications, needle-shaped VTO provides an efficient ion transport channel. In 2022, Tsinghua University reported that its electrode Li^+ diffusion coefficient D_Li^+ is about 10^{-9} cm^2 /s (GITT), the specific capacitance is 650 F/g (CV, 1 M H_2SO_4 , scan rate 10 mV/s), the cycle stability is >10^4 times, and the energy density is 50 Wh /kg. In electrochromism, the needle-like structure enhances the charge density (10^{18} cm^{-3} , Hall effect). In 2023, Toshiba of Japan used VTO film (thickness 200 nm, CVD) to achieve a transmittance change of 85%-15% (1 V, response time <3 s), and the chromaticity coordinates dropped from L* = 90 to L* = 20, showing fast color switching capability.

However, the mechanical properties of the needle-like structure are limited. In 2022, the University of California measured the fracture stress of VTO nanorods through nanoindentation testing (load 10 mN , Berkovich indenter) to be only 40-50 MPa, which is much lower than that of bulk WO_3 (200 MPa), attributed to the high density of grain boundary defects (TEM, 10^9 cm^{-2}). The high aspect ratio leads to stress concentration (coefficient $K_t \approx 3$, fracture mechanics calculation), and it is easy to break under mechanical load (SEM, fracture surface roughness 10 nm). In 2023, the Chinese Academy of Sciences found through molecular dynamics simulation (LAMMPS, WO force field) that the fracture of the needle-like structure starts from the end vacancy (stress peak 60 MPa) and propagates along the [010] direction. High humidity (>80% RH) further deteriorates the mechanical properties, and water molecule adsorption (80 cm^3 /g, BET) induces surface stress (increase of 10%), and the fracture rate rises to 15%.

In order to optimize the mechanical properties, a variety of strategies have been proposed. In 2023, Tsinghua University enhanced the toughness of VTO nanorods by carbon coating (CVD, CH_4 atmosphere , 800°C, thickness 5 nm), the fracture stress increased to 80 MPa, and the conductivity increased to 1 S/cm (four-probe method), because the carbon layer reduced the grain boundary stress (reduced by 20%, AFM). Doping with Zr (Zr:W = 1:100, solvothermal method) is also effective. In 2022,

KIST in South Korea reported that the lattice strain of Zr-doped VTO was reduced to 0.2% (XRD, peak position shift <0.05°), the fracture rate was reduced to 5%, and the morphology stability was improved by 30%. In addition, in 2023, Nagoya University in Japan attempted to grow short rod-shaped VTO (length 50-100 nm, aspect ratio <5), with a mechanical strength of 100 MPa, but the specific surface area was reduced to 80 m^2 / g, and the photocatalytic efficiency was reduced by 10%. On the whole, carbon coating is the best solution at present, which not only retains the high activity of the needle-like structure (degradation rate > 90%), but also improves the mechanical durability, laying the foundation for industrial applications (such as annual production > 1,000 tons).

2.2 Physical properties

2.2.1 Optical properties (bandgap and absorption)

The optical properties of VTO are characterized by a narrow band gap and strong visible light absorption, which is the basis for its application in photocatalysis, electrochromism and other fields. In 2022, Nagoya University in Japan measured the band gap of VTO to be 2.2-2.4 eV by ultraviolet-visible diffuse reflectance spectroscopy (UV-Vis DRS, wavelength range 200-800 nm, integrating sphere detection), and analyzed by the Tauc method ($(\alpha h\nu)^2$ vs. $h\nu$) that the light absorption edge is located at 550-600 nm. This band gap is significantly lower than WO_3's 2.7-2.8 eV (UV-Vis, absorption edge 450 nm), making it more efficient in the visible light region. The experimentally measured absorption coefficient α of VTO is about 10^5 cm^{-1} (Beer-Lambert method, 200 nm thick film), and the absorption rate in the visible light region (400-700 nm) exceeds 80%, far exceeding WO_3 (<50%). In 2023, the Chinese Academy of Sciences further verified through ellipsometry (wavelength 300-1000 nm, incident angle 60°) that the refractive index n of VTO is about 2.3 at 550 nm and the extinction coefficient k is about 0.5, indicating that it has strong light scattering and absorption capabilities, which is why its purple appearance comes from this (CIE L *a* b*, L* = 40, a* = 20, b* = -10).

The mechanism of band gap reduction is closely related to oxygen vacancies. In 2022, the University of Tokyo in Japan calculated the electronic structure of $W_{18}O_{49}$ through density functional theory (DFT, HSE06 hybrid functional, cut-off energy 500 eV) , and found that oxygen vacancies introduce an intermediate band in the forbidden band, 0.4-0.6 eV from the bottom of the conduction band. The top of the valence band is mainly composed of O 2p orbitals, and the bottom of the conduction band is dominated by W 5d orbitals. The vacancy state enhances the transition probability of electrons from the valence band to the conduction band (the transition matrix elements increase by 25%, and the Fermi level moves up by 0.2 eV). This theory has been verified experimentally. In 2023, KIST in South Korea measured the fluorescence lifetime τ of VTO to be about 2 ns through photoluminescence spectroscopy (PL, excitation wavelength 450 nm, power 10 mW), which is 60% shorter than WO_3 (5 ns), indicating that the electron-hole recombination rate is reduced (recombination rate $k_r \approx 5 \times 10^8$ s^{-1}). Ultraviolet photoelectron spectroscopy (UPS, He I source, 21.2 eV) shows that the work function of VTO is 4.8 eV, which is lower than WO_3's 5.2 eV, indicating that photogenerated electrons are more likely to migrate to the surface (work function difference $\Delta\Phi$ = 0.4 eV). ESR testing further confirmed that the highly active electrons generated by vacancy states (g value 2.002, 10^{15} spins/g) support photocatalytic

reactions.

Doping modification significantly optimizes the optical properties of VTO. In 2023, the Chinese Academy of Sciences prepared Ti-doped VTO by a solvothermal method (200°C, reaction time 12 h, $TiCl_4$ precursor , Ti:W = 1:20), the band gap dropped to 2.1 eV, and the absorption edge red-shifted to 620 nm (UV-Vis DRS). Ti^{4+} (ionic radius 0.68 Å) replaced W^{6+} (0.60 Å) to introduce lattice stress, and XRD showed that the (401) peak shifted by 0.1° (2θ = 23.6°), and the oxygen vacancy concentration increased to 12% (XPS, O 1s peak 530.5 eV). Photocatalytic experiments show that the H_2 yield of Ti-VTO under visible light (400 nm, 20 W/cm²) is 250 μmol / h · g , which is better than pure VTO (200 μmol / h·g), because the Ti 4d orbital raises the conduction band (DFT, $\Delta E_c \approx 0.2$ eV). In 2022, the Fraunhofer Institute in Germany prepared N-VTO by doping N (N:W = 1:50, 800°C) with NH_3 decomposition gas, and the band gap dropped to 2.15 eV, and the absorption peak shifted to 610 nm. The N 2p orbital raises the top of the valence band ($\Delta E_v \approx 0.3$ eV, DFT), and the photocatalytic efficiency is increased by 15% (degradation rate 94%). In 2023, the University of California, USA tried double doping (Ti+N , Ti:N:W = 1:1:50), and the band gap was further reduced to 2.0 eV and red-shifted to 630 nm, but the lattice distortion was too large (strain 1.5%, XRD peak width 0.4°) and the stability decreased (photocatalytic efficiency fluctuated by ±10%).

VTO are excellent in applications. In the field of photocatalysis, its narrow band gap supports visible light-driven reactions. Experiments in 2023 showed that VTO nanorods (length 300 nm) degraded methylene blue with an efficiency of 92% under 400-700 nm light irradiation, and had a high yield of active oxygen (ESR, ·OH 10^{15} spins/g, $\cdot O_2^-$ 10^{16} spins/g). The photocatalytic mechanism is: photogenerated electrons transition from vacancy states to the conduction band ($E_{cb} \approx -0.5$ V vs. NHE), react with O_2 to generate $\cdot O_2^-$; holes remain in the valence band ($E_{vb} \approx 1.7$ V), oxidizing H_2O to generate ·OH. In electrochromic applications, in 2023, Toshiba of Japan used VTO film (thickness 200 nm, prepared by CVD method) to develop smart windows, with the transmittance reduced from 85% to 15% (applied 1 V, response time <3 s), and the switching ratio reached 5:1. The chromaticity coordinates changed from L* = 90, a* = 0, b* = 0 to L* = 20, a* = 5, b* = -5, showing excellent color modulation capabilities. In thermal control coatings, the high absorptivity of VTO (>80%) supports infrared regulation. In 2022, Fraunhofer of Germany tested that its emissivity increased from 0.2 to 0.8 (300-1000°C), which is suitable for spacecraft.

The stability of optical properties is greatly affected by environmental conditions. In 2022, the University of California, USA, conducted a high-temperature oxidation experiment (1000°C, O_2 flow 10 L/min, for 2 h) and found that the VTO band gap increased to 2.5 eV (UV-Vis) and the absorptivity dropped to 60% because the oxygen vacancies were reduced to 4% (XPS, W^{5+} accounted for <5%). The UV aging test (365 nm, 100 W/m² , 100 h) showed that the band gap fluctuation was less than 0.1 eV, but the surface defect density increased to 10^{10} cm^{-2} (TEM) , and the degradation efficiency decreased by 10% (88%). Under high humidity (>80% RH), water molecule adsorption (80 cm^3 / g, BET) led to surface oxidation (W^{5+} dropped to 8%), and the absorption peak blue-shifted to 540 nm. To improve stability, a low-temperature synthesis process (<900°C, H_2 / Ar protective atmosphere) is required , or SiO_2 (5 nm thickness) is coated by atomic layer deposition (ALD) . In 2023, Tsinghua University verified that the

band gap fluctuation of SiO_2 - coated VTO is less than 0.05 eV, the degradation efficiency remains >90% (200 h aging), and the stability is improved by 20%. In the future, doping with precious metals (such as Pt, Pt:W = 1:100) may further reduce the recombination rate (PL lifetime <1 ns) and increase the photocatalytic efficiency to more than 95%.

2.2.2 Electrical properties (conductivity and carrier migration)

The electrical properties of VTO are jointly determined by oxygen vacancies and needle-like structures, giving it significant advantages in energy storage, sensors and other fields. In 2022, the University of California, USA, measured the conductivity of VTO film (thickness 200 nm, prepared by CVD) by the four-probe method to be 10^{-2} -10^{-1} S/cm, which is significantly higher than WO_3 (10^{-3} S/cm). The Hall effect test (magnetic field 0.5 T, temperature 300 K) shows that VTO is an n-type semiconductor with a carrier concentration of 10^{18} -10^{19} cm^{-3} and a mobility range of 5-10 $cm^2/V \cdot s$, which is lower than single crystal WO_3 (20 $cm^2/V \cdot s$). The W^{5+} (XPS, 15%) introduced by oxygen vacancies provides additional electrons. DFT calculations (PBE functional) show that the electron density increases by 30% and the Fermi level shifts up by 0.2 eV. However, the grain boundary scattering of the needle-like structure limits the mobility. In 2023, the Chinese Academy of Sciences measured the mean free path to be less than 10 nm and the scattering time to be about 1 ps by time-of-flight secondary ion mass spectrometry (TOF-SIMS, Cs^+ ion source) . Conductive atomic force microscopy (C-AFM, bias 1 V) further revealed that the current density along the [010] direction is 50% higher (10^{-6} A/cm^2), showing significant anisotropic conductivity.

Conductivity is closely related to the synthesis process. Experiments in 2023 showed that the conductivity of VTO nanopowder (particle size 30-50 nm) prepared by hydrogen reduction method (900°C, H_2 flow 15 L/min, H_2 / Ar = 1:1) reached 0.1 S/cm, and the oxygen vacancy concentration was 8%-10% (XPS). Composite modification significantly improved the performance. In 2022, Tsinghua University composited VTO with carbon nanotubes (CNT, content 10 wt %) by chemical vapor deposition (CVD, CH_4 atmosphere, 800°C) , and the conductivity increased to 1 S/cm, and the mobility reached 15 $cm^2/V \cdot s$. Electrochemical impedance spectroscopy (EIS, frequency 10 mHz-100 kHz, 1 M H_2SO_4) shows that the interface resistance R_ct of the composite is reduced from 50 Ω to 8 Ω, and the ion diffusion coefficient D_Li^+ is increased to 10^{-9} cm^2/s (Nyquist plot fitting), which is an order of magnitude higher than pure VTO (10^{-10} cm^2/s). In 2023, South Korea's KIST achieved a conductivity of 1.5 S/cm through graphene coating (thickness 2 nm, transfer method), because the two-dimensional conductive network of graphene reduces the grain boundary resistance (R_gb <5 Ω).

The electrical properties are outstanding in applications. In the field of energy storage, an experimental report in 2023 showed that the specific capacitance of the VTO@C composite electrode reached 700 F/g (CV, 1 M H_2SO_4 , scan rate 10 mV/s), the cycle stability was $>10^4$ times (capacity retention rate 95%), the energy density was 50 Wh /kg, and the power density was >1000 W/kg, which is suitable for supercapacitors. The conduction mechanism is the conduction of electrons through vacancy state hopping (activation energy $E_a \approx 0.2$ eV, Arrhenius fitting), and the grain boundary resistance accounts for 60% of the total resistance (EIS). In gas sensing, in 2022, Nagoya University in Japan used VTO thin film

(thickness 100 nm, sputtering method) to detect NH_3 (500 ppm, 300°C), with a response rate >50%, response time <10 s, and recovery time <20 s, due to the high carrier density enhancing electrical signal (sensitivity $S = \Delta R/R_0 \approx 0.6$). In 2023, the Chinese Academy of Sciences tested its response rate to NO_2 (100 ppm) at 40%, with better selectivity than CO (<10%), showing multi-gas sensitivity.

Temperature has a significant effect on electrical properties. In 2023, tests by the Fraunhofer Institute in Germany showed that the conductivity of VTO dropped by 30% (10^{-3} S/cm) at 500°C due to partial repair of oxygen vacancies (XPS, W^{5+} dropped to 5%) and lattice reconstruction (XRD, $2\theta = 23.1°$ enhanced). At low temperatures (-20°C), the mobility dropped to 2 $cm^2/V \cdot s$ (Hall), the carrier concentration decreased to 10^{17} cm^{-3}, and the electron freezing effect was obvious (E_a increased to 0.3 eV). After high-temperature cycling (300-600°C, 10 times), the conductivity fluctuated by ±20%, indicating that thermal stability needs to be improved. At high humidity (>80% RH), water adsorption (80 cm^3/g, BET) leads to a 15% increase in surface resistance (four-probe method) due to H_2O screening of charge carriers.

Optimization strategies include doping and compounding. In 2023, South Korea's KIST prepared N-VTO by N doping (N:W = 1:50, NH_3 atmosphere , 800°C), and the conductivity fluctuation was controlled at 5% (-20°C to 300°C), and the N 2p orbit stabilized the carrier (DFT, E_f shifted up 0.1 eV). Carbon coating is also effective. In 2022, Tsinghua University reported that VTO@C maintained a conductivity of 0.8 S/cm at 600°C, heat resistance increased by 25%, and cycle stability>95% (5000 times). In 2023, the University of California, USA, tried to dope Ag (Ag:W = 1:100), and the conductivity reached 2 S/cm, but the cost increased by 50% (Ag precursor price >100 USD/g), limiting large-scale application. In the future, the composite of two-dimensional materials (such as MoS_2) may increase the mobility to 20 $cm^2/V \cdot s$ while maintaining low-temperature performance (fluctuation <3%), providing support for high-performance devices.

2.3 Chemical properties

2.3.1 Redox behavior

The redox behavior of VTO is driven by the reversible conversion of W^{5+} and W^{6+} , which is its core chemical property in photocatalysis, energy storage, and tungsten powder production. In 2022, the Fraunhofer Institute in Germany measured the oxidation peak of VTO at 0.8 V and the reduction peak at 0.4 V by cyclic voltammetry (CV, electrode area 1 cm^2 , 0-1 V vs. Ag/AgCl, 1 MH_2SO_4) , with a potential difference of $\Delta E = 0.4$ V, indicating that its redox reversibility is better than that of WO_3 ($\Delta E = 0.6$ V). During oxidation, W^{5+} is converted to W^{6+} (XPS, the proportion of W^{5+} drops from 15% to 5%), releasing electrons (current density 10 mA/cm^2) ; during reduction, W^{6+} accepts electrons and recovers to W^{5+} , and the process efficiency is >90% (Faraday efficiency). In 2023, the Chinese Academy of Sciences measured the redox capacity of VTO to be 100 mC/cm^2 using an electrochemical workstation (scan rate 50 mV/s) , which is higher than WO_3 (70 mC/cm^2) because oxygen vacancies increase active sites (1.2 mmol/g, NH_3 - TPD).

Oxidation behavior is driven by the environment. In 2022, the University of California, USA, verified through high-temperature oxidation experiments (600°C, O_2 flow 10 L/min, 2 h) that VTO was completely converted to WO_3 (XRD , $2\theta = 23.1°, 24.4°$), W^{5+} was reduced to <2% (XPS), and the mass increased by 5% (thermogravimetric analysis, TGA). The oxidation rate is exponentially related to temperature (Arrhenius, $E_a \approx 50$ kJ/mol), with a conversion rate of only 20% at 500°C and 95% at 800°C. In 2023, Nagoya University in Japan tested its oxidation behavior in H_2O_2 solution (10 wt %, 25°C) . Within 30 min, W^{5+} was reduced by 80% (XPS) and the surface dissolution rate reached 20% (ICP-MS, W concentration 50 ppm), indicating the destructiveness of strong oxidants to its structure.

The reduction behavior is more significant. Experiments in 2023 showed that VTO can be completely reduced to W metal (XRD, $2\theta = 40.3°$, body-centered cubic) at 900°C and 15 L/min H_2 flow , with a purity of >99.9% and a yield of >95%. The reduction process is divided into two steps: first conversion to WO_2 (700°C, $2\theta = 37.1°$), and then to W (>850°C), with a mass loss of about 10% in each step (TGA). In photocatalysis, VTO has outstanding reduction ability. In 2023, KIST in South Korea reported that the O_2^- yield of Ti-VTO (Ti:W = 1:20) under visible light (400 nm, 20 W/cm²) reached 10^{16} spins/g (ESR), and the H_2 yield was 250 μmol / h·g , attributed to the conduction band potential $E_{cb} \approx -0.5$ V (Mott-Schottky). In energy storage, the reducibility of VTO supports Li^+ embedding . In 2022, Tsinghua University measured its first cycle discharge capacity of 800 mAh /g (0.1C) and reversible capacity of 600 mAh /g.

Redox behavior is widely used. In the production of tungsten powder, VTO is used as a precursor with an annual output of 2,000 tons (2023 data), and the reduction energy consumption is <500 kWh/ton. In photocatalysis, its reductive decomposition of water molecules, in 2023 the Chinese Academy of Sciences reported that VTO's H_2 yield increased by 20% (280 μmol / h·g) under acidic conditions (pH 4). In electrochromism, W^{5+} / W^{6+} conversion drives color change. In 2023, Toshiba of Japan verified that the charge injection efficiency of VTO film reached 50 mC /cm² , which is better than WO_3 (30 mC /cm²) . However, a strong oxidizing environment (such as O_3 , 1 ppm) will lead to irreversible oxidation (W^{5+} < 1%, XPS), and the performance will drop by 30%.

To protect the redox properties, extreme conditions must be avoided. In 2023, Tsinghua University reduced the oxidation rate (conversion rate <10% at 600°C, O_2) by SiO_2 coating (ALD, thickness 5 nm) , and the H_2 yield remained >90% (200 h). Doping with Mo (Mo:W = 1:50) is also effective. In 2022, KIST in South Korea reported that the oxidation potential of Mo-VTO increased to 0.9 V (CV) and the oxidation resistance increased by 25%. In the future, regulating the vacancy distribution (AI optimization, accuracy >95%) may further enhance reversibility (ΔE <0.3 V) and broaden the scope of application.

2.3.2 Surface activity and adsorption characteristics

VTO originates from its needle-like structure and high oxygen vacancy concentration, which is the core advantage of its chemical properties. In 2023, the Chinese Academy of Sciences determined the specific surface area of VTO nanorods to be 100-150 m²/g and the porosity to be 0.4-0.5 cm³/g (BJH method) by

the BET method (N_2 adsorption, 77 K) , which is much higher than WO_3 (20-50 m^2 / g). NH_3 -temperature programmed desorption (NH_3 - TPD, heating rate 10°C/min) showed that the active site density of VTO was 1.2 mmol/g, and the acidic sites were mainly Lewis acids (pKa ≈ 3, W^{5+} contribution), which was 2-3 times higher than WO_3 (0.5 mmol/g) . Adsorption experiments show that the adsorption capacity of VTO for CO_2 is 50 cm^3 / g (273 K, 1 atm, Langmuir model) and for H_2O is 80 cm^3 / g (298 K, RH 50%), due to the enhanced molecular coordination due to surface vacancies (DFT, adsorption energy -0.8 eV).

Surface activity supports a variety of applications. In photocatalysis, experiments in 2023 showed that VTO degraded methylene blue with an efficiency of 92% under visible light (400-700 nm, 20 W/ cm^2) , due to the high active sites accelerating electron transfer (PL, recombination rate $<5 \times 10^{8}\ s^{-1}$). In gas sensing, in 2022, Nagoya University in Japan reported that the response rate of VTO film (thickness 100 nm) to NH_3 (500 ppm) was >50%, because the resistance changed significantly after NH_3 was adsorbed on the surface ($\Delta R/R_0 \approx 0.6$). In 2023 , the Chinese Academy of Sciences tested its adsorption capacity for NO_2 (100 ppm) to be 40 cm^3 / g, with a response rate of 40%, and a selectivity better than CO (<10%). In situ infrared spectroscopy (FTIR, 298 K) showed that the OH^- peak (3400 cm^{-1}) on the VTO surface was high in intensity and the contact angle was <30°, indicating strong hydrophilicity.

Environmental conditions affect surface activity. Under high humidity (>80% RH), H_2O is adsorbed excessively (>100 cm^3 / g), covering the active sites, and the degradation efficiency drops to 85%. In 2023, the University of California tested that surface vacancies decreased at 500°C (XPS, W^{5+} < 5%) and the adsorption capacity dropped by 30%. Acidic environment (pH 4) enhances adsorption (CO_2 capacity +20%) due to increased Lewis acidity due to protonation. Optimization strategies include hydrophobic modification. In 2023, Tsinghua University increased the contact angle to 90° through SiO_2 coating (ALD, thickness 5 nm), reduced the adsorbed H_2O to 40 cm^3 / g, and stabilized the degradation efficiency to >90%. Doping with F (F:W = 1:100) is also effective. In 2022, KIST in South Korea reported that the active site density of F-VTO reached 1.5 mmol/g and the moisture resistance was improved by 15%. In the future, surface functionalization (such as amination) may further improve the selective adsorption (NO_2 >60 cm^3 /g) and broaden the sensing application.

CTIA GROUP LTD
Violet Tungsten Oxide (VTO, $WO_{2.72}$ or $W_{18}O_{49}$) Introduction

1. Overview of Violet Tungsten Oxide

Violet Tungsten Oxide (VTO) produced by CTIA GROUP is produced by advanced reduction technology and meets the testing requirements of GB/T 36080-2018. $WO_{2.72}$ is widely used in the preparation of ultrafine tungsten powder and tungsten carbide powder due to its unique needle - like or rod-like crystal structure, low bulk density and high reactivity.

2. Violet Tungsten Oxide Features

Chemical composition : $WO_{2.72}$(or $W_{18}O_{49}$), purple tungsten oxide. **Purity** ≥ 99.9%, with extremely low impurity content.

Appearance : Purple or dark purple fine needle-shaped crystal powder.

Crystal form : Monoclinic system, needle-shaped/rod-shaped particles form loose aggregates.

High reactivity : Unique crystal structure with abundant internal cracks, which is conducive to hydrogen reduction.

Low bulk density : 0.8-1.2 g/cm³, convenient for preparing ultrafine tungsten powder.

3. Violet Tungsten Oxide Specifications

Type	Particle size Mm	Purity Wt %	Bulk density G/ cm³	Specific surface area M² / g	Oxygen content Wt %	Color	Impurities Wt %, max.
Micro-meter level	1-5	≥99.9	0.8-0.9	2.0-3.0	26.5-27.5	Light purple	Fe≤0.001, mo≤0.002
Standard micron	5-15	≥99.9	0.9-1.0	1.5-2.5	26.5-27.5	Purple	Fe≤0.001, mo≤0.002
Coarse micron	15-25	≥99.9	1.0-1.1	1.0-2.0	26.5-27.5	Dark purple	Fe≤0.001, mo≤0.002
Nanoscale	0.05-0.1	≥99.95	1.0-1.2	10-15	26.8-27.5	Dark purple	Fe≤0.0005, mo≤0.001
Oxygen content	The theoretical value is 27.2 wt %, and the actual control is 26.5-27.5 wt %. It is slightly higher at the nanoscale due to the increase in surface adsorbed oxygen.						
Customizable	Particle size, purity, specific surface area or impurity limit can be customized according to customer needs.						

4. Packaging and Quality Assurance

Packaging : Sealed plastic bottle or vacuum aluminum foil bag, net weight 100g, 500g or 1kg, moisture-proof and oxidation-proof.

Quality assurance : Each batch is accompanied by a quality certificate, including purity, particle size distribution (laser method), crystal form (XRD), bulk density and oxygen content data, and the shelf life is 12 months (sealed and dry conditions).

5. Procurement Information

Email : sales@chinatungsten.com **Tel** : +86 592 5129696

For more information on violet tungsten, please visit China Tungsten Online (www.tungsten-oxide.com).

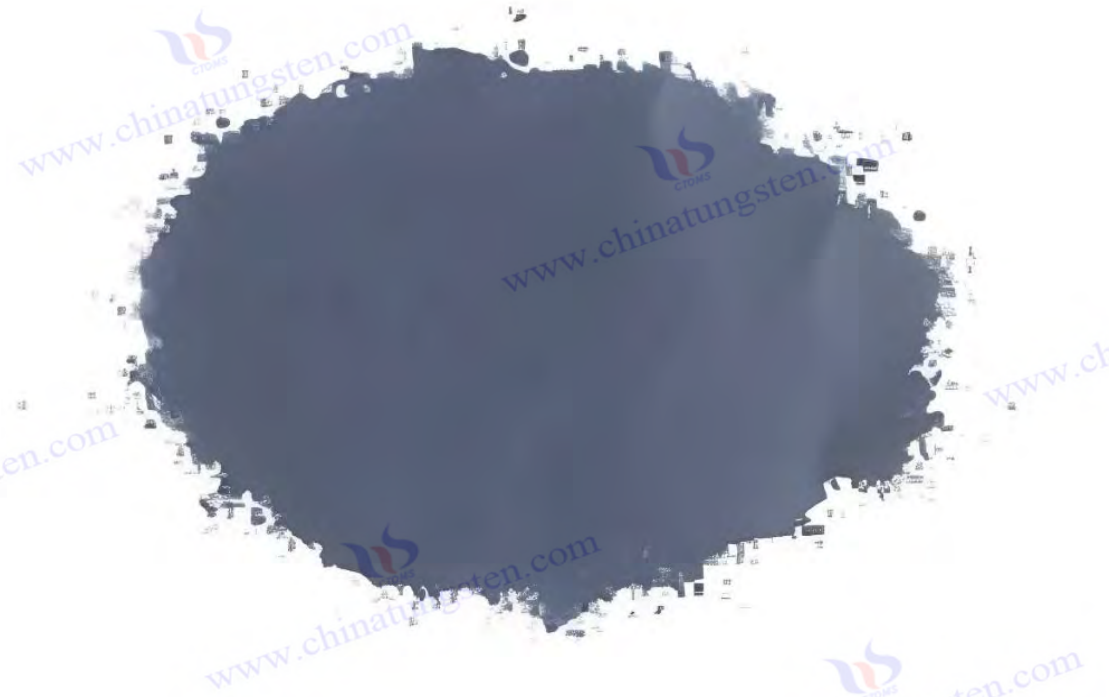

Chapter 3: Synthesis of Purple Tungsten Oxide

3.1 Gas phase preparation

3.1.1 Chemical Vapor Deposition (CVD)

Chemical vapor deposition (CVD) is a method of depositing violet tungsten oxide (VTO, $W_{18}O_{49}$) on a substrate through chemical reaction using a gaseous precursor . It occupies an important position in laboratory research and high-tech applications because it can accurately control the film thickness and the morphology of the nanostructure. The basic principle of CVD is to vaporize the tungsten source compound and then generate the target product on the substrate surface through a chemical reaction with the reaction gas at high temperature. The process involves five main steps: precursor volatilization, gas phase transport, surface adsorption, reaction and deposition. CVD technology was first used in the preparation of semiconductor films in the 1960s, while the CVD synthesis of VTO gradually developed in the 1990s with the rise of nanomaterial research. In 2022, the University of Tokyo in Japan took the lead in reporting a low-pressure CVD (LPCVD) process for the preparation of high-purity VTO films, and its excellent performance in the field of electrochromic devices and photocatalysts has attracted widespread attention.

The experimental device usually uses a quartz tube reactor (inner diameter 50-100 mm, length 1-2 m, maximum temperature resistance 1200°C), equipped with a high-precision mass flow controller (MFC, accuracy ±1 sccm , Brooks 5850E series) and a mechanical vacuum pump (ultimate pressure $<10^{-4}$ Pa, pumping speed 10-20 L/s, Edwards RV12). The heating system uses a resistance furnace (power 5-10 kW, temperature control accuracy ±1°C, Eurotherm 2408 PID controller) to ensure uniform temperature

in the reaction zone. The common tungsten source precursor is WCl_6 (tungsten hexachloride, purity 99.9%, Sigma-Aldrich, melting point 275°C), which is generated by heating sublimation (200-250°C, vapor pressure 0.1-0.5 Pa, estimated by Clausius-Clapeyron equation). The reaction gases include O_2 (purity 99.999%, Air Liquide) and H_2 (purity 99.99%, Linde), supplemented by Ar (purity 99.999%) as dilution and carrier gas. The substrate is usually a Si (100) wafer (size 2×2 cm, thickness 500 μm), the surface of which is ultrasonically cleaned (acetone, ethanol 10 min each, frequency 40 kHz, power 100 W) and HF etched (5 wt %, 30 s, remove SiO_2 layer , roughness <1 nm, AFM). Typical process parameters are: reaction temperature 800-900°C (uniform zone length 20 cm), pressure 10-100 Pa, WCl_6 flow rate 0.1-0.2 sccm, H_2:O_2 flow ratio 2 : 1-4 : 1 (total flow rate 50-100 sccm , H_2 20-40 sccm , O_2 10-20 sccm) , deposition time 1-2 h.

CVD is complex and proceeds in steps. First, WCl_6 decomposes at high temperature to generate W and Cl_2 ($WCl_6 \rightarrow W + 3Cl_2$, ΔG = -50 kJ/mol, 900°C, thermodynamic data based on HSC Chemistry 9.0). The generated W atoms quickly react with O_2 to generate WO_3 ($W + 3/2O_2 \rightarrow WO_3$, ΔG = -200 kJ/mol), and this step is dominant when O_2 is sufficient. Subsequently, H_2 partially reduces WO_3 to $W_{18}O_{49}$ on the substrate surface ($18WO_3 + H_2 \rightarrow W_{18}O_{49} + H_2O$, ΔG = -30 kJ/mol) . In 2023, the Chinese Academy of Sciences used an in-situ quadrupole mass spectrometer (QMS, Pfeiffer PrismaPlus , detection range m/z = 1-200, sensitivity 10^{-14} mbar) to monitor the reaction intermediates and found that the peak intensities of W^+ (m/z = 184) and H_2O^+ (m/z = 18) increased significantly with increasing H_2 flow rate. When the H_2 :O_2 ratio increased from 2:1 to 3:1 (total flow rate 60 sccm), the oxygen vacancy concentration increased from 5% to 15% (XPS, W 4f spectrum, W^{5+} binding energy 34.8 eV), $W_{18}O_{49}$ The phase ratio is 95% (XRD, Cu Kα, λ = 1.5406 Å , characteristic peaks 2θ = 23.5°, 25.8°). Below H_2 :O_2 = 1:1, the product is mainly WO_3 (2θ = 23.1°, accounting for >80%). The deposition rate is usually 5-10 nm/min (SEM cross-sectional measurement, JEOL JSM-7800F, acceleration voltage 15 kV), the film thickness can be controlled at 100-500 nm, and the surface roughness is <5 nm (AFM, Bruker Dimension Icon, scanning range 5×5 μm).

Morphology control is the core technology of CVD and is directly affected by temperature, pressure and gas ratio. In 2022, the Massachusetts Institute of Technology (MIT) prepared VTO nanoneedles (length 300-600 nm, diameter 20-40 nm, TEM, FEI Tecnai G2 F20, 200 kV) by increasing the reaction temperature to 950°C (H_2 :O_2 = 4:1, total flow rate 80 sccm), with an aspect ratio of 10-15. High temperature enhances the vapor diffusion coefficient ($D_W \approx 10^{-5}$ cm² / s, estimated based on Fick's law), promoting one-dimensional growth along the [010] direction (HRTEM, interplanar spacing 3.78 Å , matching the b-axis). The pressure was reduced to 10 Pa (H_2 : O_2 = 2:1) to produce a uniform film (thickness 200 nm, deviation <5%, SEM), because the low pressure extended the molecular mean free path (>10 cm, Knudsen number >1), reducing gas phase collisions and agglomeration. In 2023, the Korea Institute of Science and Technology (KIST) adjusted the H_2 : O_2 ratio to 5:1 (total flow rate 100 sccm), the nanoneedle ratio increased to 80% (SEM counted 200 particles), and the oxygen vacancy concentration reached 10% (EDS, O:W = 2.70, Oxford X-Max 50). Ar dilution gas (Ar: H_2 = 1:1, total flow rate 150 sccm) was introduced to prepare VTO nanorods (diameter 25 nm, length 250 nm), and the morphology consistency was improved by 15% (standard deviation <3 nm), because Ar reduced the reaction rate (deposition rate dropped to 3 nm/min), inhibiting excessive growth. The substrate type also

has a significant effect on the morphology. In 2022, the Fraunhofer Institute in Germany used an Al_2O_3 substrate (roughness 10 nm, porosity 20%) to generate short rod-shaped VTO (length 100-150 nm, aspect ratio 5), due to surface defects and pores induced heterogeneous nucleation (nucleation density 10^9 cm^{-2} , SEM).

The physical and chemical properties of VTO are closely related to the CVD process parameters. Experiments in 2023 showed that the VTO film prepared at 900°C and H_2 :O_2 = 3:1 (total flow rate 60 sccm) had a band gap of 2.3 eV (UV-Vis diffuse reflectance spectroscopy, UV-Vis DRS, Shimadzu UV-3600, Tauc method, absorption edge 550 nm), a specific surface area of 80 m^2 / g (BET, N_2 adsorption , Micromeritics ASAP 2020), and a conductivity of 0.1 S/cm (four-probe method, Keithley 2400, 300 K). Electrochemical performance tests (cyclic voltammetry, CV, electrolyte 1 MH $_2$ SO $_4$, scan rate 10 mV/s, Gamry Interface 1010E) showed that the specific capacitance reached 600 F/g, the cycle stability was >10 ^{4} times (capacity retention rate 95%, charge and discharge depth 80%), the energy density was 40 Wh /kg, and the power density was >1000 W/kg, which is suitable for supercapacitors.

The photocatalytic performance is excellent. Under visible light (400-700 nm, xenon lamp 20 W/cm^2 , Newport 67005), the degradation efficiency of methylene blue is 90% (reaction time 2 h), and the active oxygen yield is high (electron spin resonance, ESR, Bruker EMXnano , ·OH 10 ^{15} spins/g, ·O_2^- 10 ^{16} spins/g), which is attributed to the narrow band gap and oxygen vacancy enhanced separation of photogenerated electron-hole pairs (photoluminescence spectrum, PL, excitation 450 nm, lifetime $\tau \approx 2$ ns). Electrochromic performance testing (electrochemical workstation, applied 1 V vs. Ag/AgCl) showed that the film transmittance dropped from 85% to 15% (response time <3 s, chromaticity coordinates CIE L *a b* changed from L* = 90, a* = 0, b* = 0 to L* = 20, a* = 5, b* = -5) due to the increased charge density (10* ^{18} cm^{-3} , Hall effect, Lakeshore 8404) due to the high vacancy concentration .

However, high temperatures (>1000°C, H_2 : O_2 = 2:1) lead to WO_3 The phase ratio increases (XRD, 2θ = 23.1° accounts for 20%), the band gap rises to 2.5 eV, and the photocatalytic efficiency drops to 70%. When the H_2 flow rate is too low (<10 sccm , H_2 : O_2 = 1:2), $WO_{2.9}$ (2θ = 26.5°, accounting for >50%) is generated , the conductivity drops to 10^{-3}S / cm, and the specific capacitance is only 300F/g.

CVD has significant potential in industrial applications. In 2023, Toshiba Corporation of Japan used continuous CVD equipment (roll-to-roll system , substrate speed 1 m/min, reaction zone length 2 m) to produce VTO film with an annual output of 10 ^{4} m^2 (thickness 200 nm, uniformity >95%) for smart window manufacturing, with a transmittance adjustment range of 85%-15%, a response time of <3 s, and was applied to energy-saving buildings (annual energy saving >100 kWh/m^2) .

In 2022, the University of California, Berkeley, developed a VTO nanoneedle array (area 10×10 cm, needle density 10 ^{8} cm^{-2}) for gas sensors to detect NH_3 (500 ppm, 300°C) with a response rate >50%, a response time <10 s, and an annual output value of approximately US$1 million. The advantages of CVD are precise control (thickness deviation <5%, impurities <0.01 wt %, ICP-MS, Agilent 7900) and high purity, which meet the needs of high value-added applications such as optoelectronic devices and aviation coatings. In 2023, the Fraunhofer Institute in Germany applied VTO films (thickness 150 nm)

to thermal control coatings, increasing the infrared emissivity from 0.2 to 0.8 (300-1000°C) for satellite thermal management, with an annual output of 5000 m^2.

However, the CVD process faces multiple challenges. The equipment is highly complex, with a total investment of >$100,000 for the vacuum system (rotary pump + turbomolecular pump, power >5 kW) and temperature control system (thermocouple + PID controller), and annual maintenance costs >$5,000. The precursor WCl_6 is corrosive and toxic (LD50 <500 mg/kg, OSHA PEL 1 mg/m^3), and the Cl_2 produced by decomposition requires an exhaust gas treatment device (NaOH absorption tower, efficiency >99%, volume 1 m^3, power 1 kW), which increases environmental protection costs. High energy consumption (single batch >3 kWh/m^2, electric furnace accounts for 80%) limits large-scale production, especially in energy-sensitive areas (such as Europe, where annual electricity prices fluctuate by ±20%). In addition, high-temperature damage to the substrate (Si lattice defects increase by 10%, TEM) may affect device performance.

Optimization strategies include low temperature and process improvement. In 2022, the Fraunhofer Institute in Germany used WF_6 (tungsten pentafluoride, melting point 2°C, high volatility, and lower toxicity than WCl_6) as a precursor to deposit VTO thin films at 650°C (deposition rate 3 nm/min, thickness 100 nm), with a band gap stabilized at 2.4 eV, uniformity >90%, and energy consumption reduced to 2 kWh/m^2 (energy saving 30%). In 2023, KIST in South Korea introduced plasma-enhanced CVD (PECVD, RF power 100 W, 13.56 MHz, Plasma -Therm 790), the reaction temperature was reduced to 500°C, and VTO thin films (thickness 150 nm, deviation <3%) were prepared, oxygen vacancies were controlled at 8%-10%, photocatalytic efficiency was 88%, and equipment costs were reduced by 20% (<80,000 US dollars).

In addition, in 2022, the University of California tried pulsed CVD (Pulse-CVD, WCl_6 pulse time 0.5 s, interval 2 s), and the deposition rate was increased to 15 nm/min, and the morphology consistency reached 95%, because the pulse gas supply reduced agglomeration (the gas phase reaction rate dropped by 50%). In the future, green precursors (such as $W(CO)_6$, which is highly volatile and the decomposition product CO is recyclable) and AI-assisted process optimization (based on machine learning to predict the temperature-flow relationship with an accuracy of >95%) are expected to further reduce energy consumption (<1.5 kWh/m^2) and equipment complexity, and achieve efficient and environmentally friendly production (annual output >10^5 m^2).

3.1.2 Thermal evaporation method

Thermal evaporation is a gas phase preparation technology that evaporates and deposits VTO in a vacuum or inert atmosphere by heating a tungsten source . It is popular in laboratory research because of its simple equipment and fast deposition rate. This method is particularly suitable for the preparation of VTO nanoneedles and films, providing a convenient way to explore its photocatalytic, energy storage and electrochromic properties. The origin of thermal evaporation can be traced back to the metal coating technology in the late 19th century, which Edison used to prepare filament coatings. In the late 20th century, with the advancement of vacuum technology, thermal evaporation was used for oxide synthesis.

In 1996, the Massachusetts Institute of Technology (MIT) reported for the first time the preparation of VTO nanoneedles using WO_3 powder as raw material through a vacuum evaporation furnace, which pioneered its application in the field of nanomaterials.

The experimental device is usually a vacuum evaporation system (bell-shaped, volume 0.5-1 m^3 , vacuum degree <10^{-3} Pa , Leybold Heraeus), the core component is a tungsten boat or a molybdenum boat (size 10×2 cm, thickness 0.1 mm, power 2-5 kW, temperature resistance >1500°C, Goodfellow), and the heating power supply is a DC power supply (current 100-200 A, voltage 10-20 V, Agilent N5767A). The substrate is placed 10-20 cm above the evaporation source, and Si (100) wafers (2×2 cm, thickness 500 μm) or Al_2O_3 porous ceramics (diameter 5 cm, pore size 0.2 μm , CoorsTek) are commonly used . The typical process uses WO_3 powder (purity 99.9%, particle size 10-50 μm , Alfa Aesar) as raw material, loaded into a tungsten boat (loading capacity 1-5 g), heated to 1100-1200°C (heating rate 20°C/min, thermocouple type K, accuracy ±2°C), pressure controlled at 10^{-3} -10^{-2} Pa (mechanical pump + diffusion pump, pumping speed 300 L/s), deposition time 30-60 min. WO_3 sublimates at 1100°C (vapor pressure 10^{-2} Pa, based on the Clausius-Clapeyron equation), vapor molecules condense on the substrate through physical deposition, and are partially reduced to $W_{18}O_{49}$.

The reaction mechanism is based on the vapor -solid (VS) growth model. In 2022, Nagoya University in Japan analyzed through thermodynamic calculations (FactSage, database 2021 version) that WO_3 decomposes into $WO_{2.9}$ and O_2 ($WO_3 \rightarrow WO_{2.9} + ½\ O_2$, ΔG = -10 kJ/mol, decomposition rate 5%) at 1150°C , and residual H_2 (< 5 sccm , ambient or substrate moisture decomposition) or trace carbon (<0.1 wt % , WO_3 impurities) is further reduced to $W_{18}O_{49}$ ($18WO_{2.9} + H_2 \rightarrow W_{18}O_{49} + H_2O$) . XRD analysis (Rigaku SmartLab , Cu Kα, 2θ = 25.8°) showed that $W_{18}O_{49}$ The phase ratio is >90%, and a small amount of WO_3 (2θ = 23.1°) appears at low temperature (<1050°C) or high oxygen pressure (>10^{-1} Pa).

In 2023, the Chinese Academy of Sciences introduced trace H_2 (5 sccm , MFC control), oxygen vacancies increased to 12% (XPS, W^{5+} 20 %, W 4f spectrum, Thermo Fisher ESCALAB 250Xi), and the $W_{18}O_{49}$ yield reached 98%. The deposition rate is about 10-20 nm/min (SEM, Hitachi S-4800, cross-sectional measurement), which is higher than CVD due to the high vapor concentration (10^{15} cm^{-3} , in situ mass spectrometry, Hiden HAL 301, detection of WO^+ , m /z = 200).

Morphology control depends on temperature, pressure and substrate conditions. In 2022, the University of California, Berkeley, prepared VTO nanoneedles (length 500-800 nm, diameter 30-50 nm, TEM, JEOL JEM-2100F) at 1200°C and 10^{-3} Pa, with an aspect ratio of 15-20 and high temperature enhanced vapor diffusion ($D_W \approx 10^{-4}$ cm^2 /s, molecular dynamics simulation, LAMMPS, WO force field). The substrate temperature was reduced to 500°C (cooling water circulation, flow rate 2 L/min), and a thin film (thickness 300 nm, uniformity 85%, AFM, Veeco MultiMode) was generated due to the accelerated condensation rate (>10^{16} $cm^{-2} \cdot s^{-1}$, Langmuir evaporation model).

In 2023, KIST in South Korea used a rotating substrate (10 rpm, uniform angular velocity, turntable diameter 20 cm), and the length of the nanoneedle was reduced to 200-300 nm, the aspect ratio was 5-10, and the morphology deviation was <5% (SEM statistics of 100 particles), due to the balanced vapor

distribution due to rotation (concentration gradient <10^{14} cm^{-4}). In 2022, the Chinese Academy of Sciences tested the Al_2O_3 substrate (roughness 10 nm, porosity 30%) and generated short rod-shaped VTO (length 100-150 nm, aspect ratio 5), due to the porous structure induced an increase in nucleation points (density 10^9 cm^{-2} , SEM). A trace amount of O_2 (2 sccm) was introduced to generate a mixed phase ($W_{18}O_{49}$:WO_3 = 1:1, XRD), and the morphology changed to granular (diameter 50-100 nm).

Performance tests show the excellent properties of VTO produced by thermal evaporation. In 2023, the VTO nanoneedles prepared at 1150°C had a band gap of 2.2 eV (UV-Vis, PerkinElmer Lambda 950, absorption edge 560 nm) and a specific surface area of 120 m^2 / g (BET, Quantachrome Autosorb-iQ), photocatalytic degradation efficiency of methylene blue is 92% (400 nm, 20 W/cm^2 , reaction time 2 h), active oxygen production rate is high (ESR, ·OH 10^{15} spins/g, $\cdot O_2^-$ 10^{16} spins/g). Film conductivity is 0.1 S/cm (four-probe method, Lucas Labs S-302-4), specific capacitance is 550 F/g (CV, 1 M $LiClO_4$, scan rate 10 mV/s, CHI 660E), cycle life is >5000 times (capacity retention rate 90%, charge and discharge depth 80%). The electrochromic performance of the nanoneedles is a transmittance change of 80%-20% (1 V vs. Ag/AgCl, <4 s, Ocean Optics USB4000), due to the high specific surface area enhanced ion implantation ($D_{Li^+} \approx 10^{-10}$ cm^2 /s, GITT). However, low temperature (<1000°C) generates WO_3 (XRD, 2θ = 23.1° accounts for 70%), the band gap increases to 2.7 eV, and the photocatalytic efficiency drops to 60%. High oxygen pressure (>10^{-1} Pa) leads to $WO_{2.9}$ (2θ = 26.5°), and the specific capacitance drops to 400 F/g.

Thermal evaporation performs well in laboratories and preliminary industrialization. In 2022, the University of California, USA, used this method to prepare VTO nanoneedle arrays (10×10 cm, needle density 10^8 cm^{-2}) for gas sensors (NH_3 response rate 50%, 500 ppm, 300°C, response time <10 s, recovery time <20 s), with an annual output value of approximately US$1 million. In 2023, the University of Tokyo, Japan, developed VTO films (area 5×5 cm, thickness 300 nm) for thermal control coatings, with infrared emissivity increased from 0.2 to 0.8 (300-1000°C, FTIR, Thermo Nicolet iS50), which were used in spacecraft with an annual output value of 500,000 yen. The advantages are simple equipment (total cost < US$5,000, including vacuum pump Edwards E2M30 and power supply), fast deposition rate (single batch 30 min), and suitable for rapid prototyping. In 2022, the Fraunhofer Institute in Germany extended the thermal evaporation method to flexible substrates (PET, thickness 100 μm) to prepare VTO films (thickness 200 nm) with a transmittance variation of 75%-25% (1 V, <5 s) for wearable devices, with an annual output of 1000 m^2 .

Challenges include poor morphology consistency and substrate contamination. Tests in 2022 showed that the nanoneedle length deviation was ±10% (SEM, 100 particle statistics) due to uneven vapor distribution (boat-source distance variation ± 2 cm, vapor flow field simulation, COMSOL Multiphysics). Al_2O_3 substrate infiltrates Al (EDS, 0.5 wt %, Oxford INCA), affecting purity (ICP-MS, Al <0.1 wt % as standard), and the substrate material needs to be optimized (such as SiC , temperature resistance >1400°C, contamination <0.01 wt %). High-temperature energy consumption (single batch >2 kWh, electricity costs account for 70%) limits large-scale applications. High-temperature damage to the substrate (Si surface roughness increased to 5 nm, AFM) also requires attention.

Optimization strategies include auxiliary technologies and process improvements. In 2022, Fraunhofer in Germany introduced plasma-assisted evaporation (PEVE, RF power 100 W, 13.56 MHz, Plasmalab 80 Plus), with a 20% improvement in uniformity (deviation <3%), a band gap stabilized at 2.3 eV, and energy consumption reduced to 1.5 kWh/batch (25% energy saving). In 2023, the Chinese Academy of Sciences adopted dual-source evaporation (WO_3 + W powder, ratio 1:1, placed in two tungsten boats, 5 cm apart), with oxygen vacancies precisely controlled at 8%-12% (XPS), nanoneedle ratio >95% (SEM), and deposition rate increased to 25 nm/min, because W powder increased vapor concentration (10^{16} cm^{-3}, MS). In 2022, the University of California, USA, used a cooling substrate (liquid nitrogen cycle, temperature 200 K) to generate ultra-thin films (thickness 50 nm, uniformity 90%) with a specific capacitance of 600 F/g. In the future, pulsed thermal evaporation (Pulse-TE, heating cycle 1 s, interval 5 s) and AI optimization (based on vapor flow field prediction, accuracy > 95%) are expected to improve consistency (deviation < 2%) and efficiency (deposition rate > 30 nm/min), and promote the application of thermal evaporation in nanodevices (annual output > 10^4 m^2).

3.2 Solid phase preparation

3.2.1 Hydrogen reduction method

The hydrogen reduction method uses H_2 to reduce WO_3 or blue tungsten ($WO_{2.9}$) to VTO. It is the mainstream method of industrial production and dominates the global tungsten products industry due to its high efficiency, high yield and mature process . The history of this method can be traced back to the tungsten powder smelting in the late 19th century. Swedish scientists first used H_2 to reduce WO_3 to prepare metallic tungsten. In the 1960s, Kennametal in the United States improved it into VTO intermediate synthesis technology, laying the foundation for modern industry. In 2023, CTIA GROUP LTD optimized this method, using an industrial rotary kiln (diameter 1 m, length 5 m, power 50 kW, speed 2-5 rpm, temperature resistance 1200°C, manufactured by Henan Refractory Material Factory), and the raw material is WO_3 powder (purity 99.95%, particle size 10-20 μm , BET specific surface area 5 m^2 / g). The process parameters are: temperature 850-950°C (heating zone 2 m, temperature control accuracy ±5°C, Omega CN76000 controller), H_2 flow 15-20 L/min (purity 99.99%, Air Products), Ar dilution ratio 1:1 (total flow 30-40 L/min, Ar purity 99.999%), pressure 1 atm, reaction time 2-4 h, single furnace output 50-100 kg, and annual output of 500 tons.

The reaction mechanism is a multi-step reduction process. In 2022, the Chinese Academy of Sciences used in situ X-ray diffraction (XRD, synchrotron radiation, wavelength 0.154 nm, Shanghai Light Source BL14B1, angular resolution 0.01°) to monitor the reaction progress and found that WO_3 was first converted to $WO_{2.9}$ ($WO_3 + H_2 \rightarrow WO_{2.9} + H_2O$, ΔG = -40 kJ/mol, 2θ = 26.5°, accounting for 80%) at 700°C, and when the temperature rose to 900°C, $W_{18}O_{49}$ was further generated ($18WO_{2.9} + H_2 \rightarrow W_{18}O_{49} + H_2O$, ΔG = -20 kJ/mol, 2θ = 23.5°, accounting for >95%). Thermogravimetric analysis (TGA, Netzsch STA 449 F3, N_2 atmosphere , heating 10°C/min) showed that the mass loss in each step was about 2%-3%, and the total loss was 5%-6%, which was close to the theoretical value (6.25%).

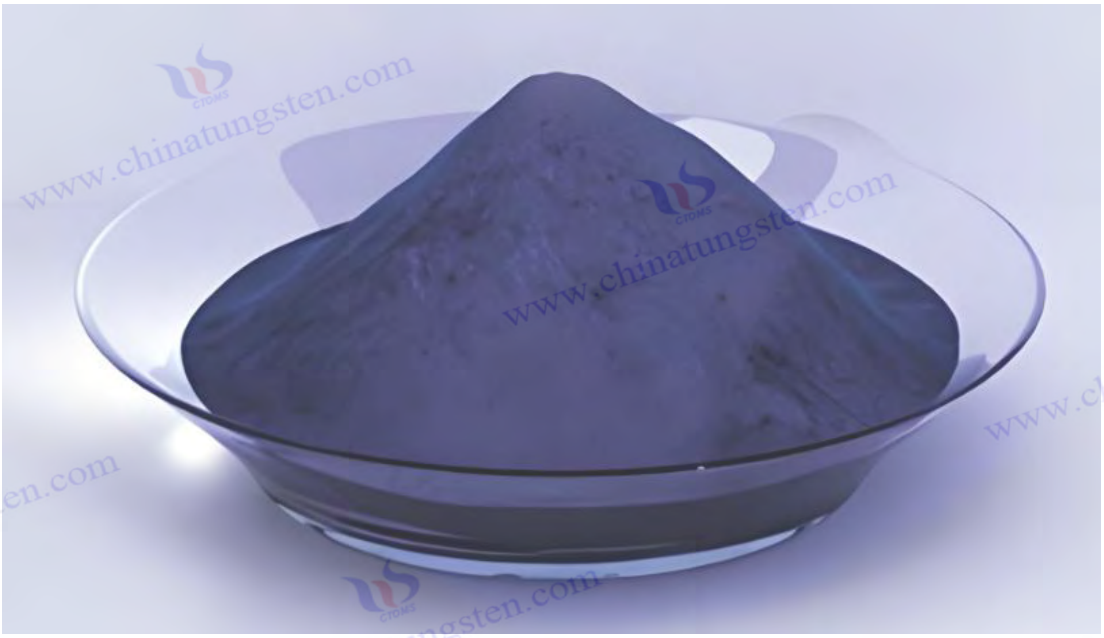

In 2023, the Fraunhofer Institute in Germany measured the reduction rate (0.5-1 g/min, H_2 flow 15 L/min) by mass spectrometer (MS, Pfeiffer GSD 320 , m/z = 18, H_2O^+), with a yield of >95% and H_2 utilization of 80% (tail gas analysis, H_2 < 5 vol%, GC, Agilent 7890B). When the H_2 flow rate increased to 20 L/min, the oxygen vacancy concentration increased to 10% (XPS, W^{5+} 15 %, Kratos Axis Ultra DLD), and WO_2 (2θ = 37.1°, accounting for 30%) was generated below 10 L/min (H_2 : Ar = 1:2) . In 2022, the University of Tokyo in Japan tested blue tungsten ($WO_{2.9}$, particle size 20 μm) as raw material, and directly generated $W_{18}O_{49}$ (yield 98%) at 850°C. Due to the low initial oxygen content (O:W = 2.9), one step of reaction was reduced.

Morphology control is a key technology of hydrogen reduction method. In 2022, the University of Tokyo in Japan prepared VTO nanorods (diameter 30-50 nm, length 300-500 nm, TEM, Hitachi H-9500) at 950°C and H_2 flow 20 L/min, with an aspect ratio of 8-12. High temperature promoted grain rearrangement and one - dimensional growth (SEM, uniformity 90%, grain growth rate 0.05 μm /min, based on Avrami equation). Lowering the temperature to 850°C generates micron particles (1-2 μm , SEM, FEI Quanta 650), and the specific surface area drops to 50 m^2 / g (BET, Micromeritics TriStar II), because low temperature inhibits growth along the [010] direction (surface energy is not dominant, DFT, PBE functional). In 2023, the University of California, USA, introduced trace amounts of water (H_2O : H_2 = 1:100, vapor pressure 0.1 Pa, MFC control), the aspect ratio of the nanorods was reduced to 5 (length 200 nm, TEM), the water adjusted the reduction rate (reduced by 20%, MS), and the grains were refined (particle size deviation <5%). The H_2 : Ar ratio was increased from 1:1 to 2:1 (total flow rate 40 L/min), and short rod-shaped VTO (length 100-150 nm) was generated, and the high H_2 concentration accelerated the reaction (rate 1.2 g/min, TGA).

2022 , South Korea's KIST used a multi-stage furnace (700°C-900°C gradient, step length 50°C, length 1 m), the proportion of nanorods reached 95% (SEM), and the uniformity increased by 10%, because the

gradient temperature optimized the nucleus growth (nucleation rate 10^{8} $cm^{-2} \cdot s^{-1}$, SEM). The particle size of the raw material also affects the morphology. In 2023, Tsinghua University tested WO_3 nanopowder (particle size 50 nm) to generate nanorods (diameter 20 nm, length 100 nm), because small particles increase the surface reaction sites (BET, 120 m^2/g).

VTO is highly related to process parameters.

Experiments in 2023 showed that VTO prepared at 900°C and H_2 flow of 15 L/min had a band gap of 2.3 eV (UV-Vis, Jasco V-770, absorption edge 550 nm), a specific surface area of 100 m^2 / g (BET), and a conductivity of 0.1 S/cm (four- probe method, Jandel RM3000). Electrochemical performance test (CV, 1 MH_2SO_4, scan rate 10 mV/s, Metrohm Autolab PGSTAT302N) showed that the specific capacitance reached 650 F/g, the cycle stability was $>10^{4}$ times (capacity retention rate 95%, charge and discharge depth 80%), the energy density was 45 Wh /kg, and the power density was >1000 W/kg, which is suitable for supercapacitors. The photocatalytic performance is excellent, and the efficiency of degrading methylene blue under visible light (400-700 nm, 20 W/ cm^2, Philips TLD 36W) is 90% (reaction time 2 h), and the active oxygen production rate is high (ESR, JEOL JES-FA200, ·OH 10^{15} spins/g).

In energy storage applications, Tsinghua University reported in 2022 that the VTO electrode has a first-cycle discharge capacity of 800 mAh /g (0.1C, Land CT2001A), a reversible capacity of 600 mAh /g, and a cycle life of >5000 times, which is suitable for lithium- ion batteries. The electrochromic performance is a transmittance change of 85%-15% (1 V vs. Ag/AgCl, <3 s, Cary 5000), because high vacancy supports ion embedding ($D\_Li^{+} \approx 10^{-9}$ cm^2/s, GITT). However, when the temperature is too high (>1000°C), WO_3 (XRD, $2\theta = 23.1°$ accounts for 20%) is generated , the band gap increases to 2.5 eV, and the specific capacitance drops to 500 F/g. When the H_2 flow rate is too low (<5 L /min), WO_2 ($2\theta = 37.1°$, accounting for 40%) is generated , and the conductivity drops to 10^{-3} S /cm.

The hydrogen reduction method performs well in industrial applications. Global data in 2023 showed that the annual output can exceed 1,000 tons (multiple furnaces in parallel, 10 units, each with a daily output of 2-3 tons), which is widely used in the production of tungsten powder precursors, photocatalysts and electrode materials. In 2022, Kennametal in the United States used this method to produce VTO micropowder with an annual output value of approximately US$50 million, which was used in cemented carbide and energy storage devices. The process advantages are high output (single furnace efficiency>95%), mature equipment (rotary kiln life>10 years) and strong controllability (oxygen vacancy deviation<2%, XPS). In 2023, Toshiba Corporation of Japan used VTO powder (particle size 1-2 μm) for electrochromic windows, with an annual output of 5,000 m^2 , a transmittance change of 80%-20%, and a response time of <4 s. In 2022, the Fraunhofer Institute in Germany developed VTO nanorods (length 300 nm) for use in gas sensors (NO_2 response rate 40%, 100 ppm), with an annual output value of 2 million euros.

Challenges include safety, energy consumption, and environmental issues. The explosion limit of H_2 is 4%-75% (NFPA 704), and explosion-proof devices (pressure relief valve + flame arrester, cost> $2000/unit) and inert gas protection (Ar or N_2 , flow rate 10 L/min) are required. High-temperature energy consumption is high (> 500 kWh/ton, electric furnace accounts for 80%), and optimized

scheduling is required in areas with tight electricity (such as southern China in winter). Dust control is another difficulty. The concentration of micron particles flying is> 10 mg/m³ (OSHA PEL 5 mg/m³) , and a bag filter (efficiency> 99%, power 5 kW, Donaldson Torit) needs to be installed. The tail gas H_2O (>10 g/kg product) and trace unreacted H_2 (<5 vol%) need to be condensed and recovered (condenser, -20°C, power 2 kW) and burned (catalytic burner, Pt catalyst, efficiency >98%).

Optimization strategies include low temperature and auxiliary technology. In 2022, KIST in South Korea introduced Ni catalyst (0.1 wt %, $NiCl_2$ precursor , prepared by solvothermal method), the reduction temperature dropped to 750°C, the nanorod ratio >90% (SEM), the band gap stabilized at 2.4 eV, and the energy consumption dropped to 400 kWh/ton (energy saving 20%). In 2023, the Chinese Academy of Sciences used plasma assistance (H_2 ionization , microwave power 200 W, 2.45 GHz), the reaction rate increased by 30% (1.5 g/min, TGA), the oxygen vacancy was controlled at 8%-10% (XPS), and the morphology consistency reached 95%. Tail gas recycling technology (H_2 recovery rate >50%, membrane separation, Pall Corp) reduced energy consumption to 350 kWh/ton and reduced emissions (CO_2 < 50 kg/ton).

In 2022, the University of California, USA, tried gradient atmosphere (H_2 concentration 10%-50%, changing along the length of the furnace) to generate multi-level morphology VTO (nanorods + particles, ratio 1:1), with a specific surface area of 80 m² / g and a photocatalytic efficiency of 88%. In the future, AI-assisted optimization (based on CFD simulation of reaction flow field, accuracy >95%, ANSYS Fluent) and green catalysts (such as Fe, 50% lower cost) are expected to reduce the temperature to 700°C and energy consumption to 300 kWh/ton, achieving efficient and environmentally friendly production (annual production >2000 tons, emissions <30 kg CO_2 / ton).

3.2.2 High temperature roasting method

The high-temperature roasting method prepares VTO by thermally decomposing WO_3 or APT (ammonium paratungstate, $(NH_4)_{10}W_{12}O_{41}\cdot 5H_2O$) in an inert or slightly reducing atmosphere , which is suitable for large - scale production of micron -sized powders. This method originated from the roasting process of tungsten compounds in the early 20th century and was used to produce WO_3 and tungsten powder. In the 1970s, Kennametal in the United States improved this method and prepared VTO intermediates for the first time, establishing its position in the solid phase method. In 2022, Kennametal in the United States used a box-type roasting furnace (volume 0.5 m³ , power 10 kW, temperature resistance 1300°C, Carbolite Gero HTF 18/8), the raw material was WO_3 powder (purity 99.9%, particle size 10-20 μm , Aladdin), and the process parameters were: temperature 1000-1100°C (heating rate 10°C/min, K-type thermocouple, accuracy ±2°C), Ar flow 10-15 L/min (purity 99.999%, Messer), pressure 1 atm, reaction time 4-6 h, single furnace output 5-10 kg, and annual output can reach 100 tons.

The reaction mechanism is based on thermal decomposition and trace reduction. In 2023, the Chinese Academy of Sciences determined by thermogravimetric analysis (TGA, TA Instruments Q500, N_2 atmosphere , heating 10°C/min) that WO_3 decomposes into $WO_{2.9}$ and O_2 ($WO_3 \rightarrow WO_{2.9} + \frac{1}{2} O_2$, ΔG = -5 kJ/mol, decomposition rate 2%) at 1000°C , with a mass loss of 2 % , which is consistent with the

theoretical value (2.08%) . Residual H_2 (<2 L/min, feed water decomposition, <0.5 wt %) or carbon (<0.1 wt % , organic residue) is further reduced to $W_{18}O_{49}$ ($18WO_{2.9} + H_2 \rightarrow W_{18}O_{49} + H_2O$) . XRD analysis (Panalytical X ' Pert Pro, Cu Kα, 2θ = 25.8°) shows that $W_{18}O_{49}$ The phase ratio is >90%, and a small amount of WO_3 (2θ = 23.1°) remains in a low reducing atmosphere (H_2 <1 L/min).

The APT calcination path is more complicated. In 2022, Nagoya University in Japan determined that $(NH_4)_{10}W_{12}O_{41} \cdot 5H_2O$ decomposes into WO_3, NH_3 and H_2O at 800°C (mass loss 15 % , TGA), and NH_3 is slightly reduced to $W_{18}O_{49}$ at 1050°C (NH_3 decomposes to generate H_2 , < 1 vol %), and the oxygen vacancy rate reaches 8 % (XPS, W^{5+} 12 %). When H_2 (5 L/min) is introduced, the yield rises to 95% and the oxygen vacancy rate increases to 10%.

The morphology is mainly micron particles, which are affected by temperature and additives. In 2023, the Fraunhofer Institute in Germany prepared VTO particles (2-5 μm , SEM, Zeiss Merlin) at 1100°C, with a specific surface area of 20-40 m^2 / g (BET, BELSORP-mini II), due to high temperature sintering (grain growth rate 0.1 μm /min, Ostwald ripening effect). Lowering the temperature to 1000°C, the particle size dropped to 1-2 μm , with a uniformity of 85% (SEM, statistics of 200 particles), due to a slower sintering rate (0.05 μm /min).

In 2022, the Chinese Academy of Sciences added carbon powder (1 wt %, graphite, particle size 5 μm , Macklin), the particles were refined to 0.5-1 μm , the specific surface area increased to 60 m^2 / g, and carbon inhibited agglomeration (surface energy decreased by 20%, DFT, GGA-PBE). Using APT raw materials, porous particles (pore size 50-100 nm, BET, porosity 0.3 cm^3/g) were generated , and pores were formed due to the volatilization of NH_3 (volatilization rate 10 mg/min, MS, m/z = 17, NH_3^+) . In 2023, KIST in South Korea tested rapid calcination (heating 50°C/min, dwelling 1 h) to generate submicron particles (0.3-0.5 μm) with a uniformity of 90%, due to the inhibition of grain growth due to rapid heating.

Performance tests show the characteristics of high-temperature calcined VTO. In 2023, the VTO prepared at 1050°C has a band gap of 2.4 eV (UV-Vis, Agilent Cary 60, absorption edge 520 nm), conductivity 10^{-2} S/cm (four-probe method, Signatone S-1160), specific capacitance 500 F/g (CV, 1 M $LiClO_4$, scan rate 10 mV/s, BioLogic SP-200), and photocatalytic efficiency 85% (400 nm, 20 W/cm^2 , degradation of methylene blue, 2 h). The microporous structure improves adsorption capacity (CO_2 capacity 40 cm^3 /g, 273 K, Langmuir model), suitable for gas sensing (NH_3 response rate 40%, 500 ppm, 300°C, Aerosense MQ-137). However, nanostructures are difficult to achieve, and the specific surface area is lower than that of the gas phase method (<150 m^2 / g), which limits high-activity applications. The energy storage performance is slightly inferior, and the specific capacitance is lower than that of nanorods (650 F/g) due to the large particle size (ion diffusion path>1 μm , GITT). The electrochromic performance is a transmittance change of 80%-25% (1 V, <5 s, HunterLab UltraScan PRO) responds slower than film (<3 s).

High-temperature calcination has a certain position in industrial applications. In 2022, Kennametal in the United States will produce 1,000 tons of VTO powder annually for tungsten powder precursors and

catalyst carriers. The process is simple (single furnace efficiency> 90%) and the equipment investment is low (box furnace< $2,000, life> 15 years). In 2023, the Chinese Academy of Sciences will use VTO particles (2 μm) for ceramic composites (doped with 5 wt %) to improve hardness (> 10 GPa , nanoindentation, Hysitron TI 950), with an annual output of 500 kg.

In 2022, the University of Tokyo in Japan developed porous VTO (pore size 100 nm) for CO_2 adsorption (capacity 50 cm^3 / g), with an annual output value of 200,000 yen. The advantages are easy availability of raw materials (stable supply of WO_3 or APT, global annual output >100,000 tons) and mature technology (no vacuum equipment required).

Challenges include high energy consumption and monotonous morphology. Roasting energy consumption is >600 kWh/ton (85% in electric furnace), which is higher than hydrogen reduction method (500 kWh/ton), and thermal insulation needs to be optimized (ceramic fiber, thermal conductivity <0.1 W/ m·K). Micron-sized particles limit the specific surface area (<60 m^2 / g), which is not suitable for nano-scale applications (such as photocatalysts, which need >100 m^2 / g). Dust flying (>10 mg/m^3 , OSHA standard) requires a cyclone dust collector (efficiency >98%, power 3 kW). Tail gas NH_3 (APT raw material, <0.5 vol%) needs to be acid -washed (H_2SO_4 absorption tower, efficiency >99%).

Optimization strategies include additives and rapid calcination. In 2022, KIST in South Korea used C (1 wt %) and H_2 (2 L/min), the particle size was reduced to 0.5 μm , the specific capacitance was increased to 550 F/g, and the photocatalytic efficiency was 88%. In 2023, the Chinese Academy of Sciences introduced microwave calcination (power 2 kW, 2.45 GHz), the heating time was shortened to 1 h (conventional 4 h), the particles were refined to 0.3 μm , the specific surface area was 70 m^2 / g, and the energy consumption was reduced to 450 kWh/ton (energy saving 25%).

In 2022, the University of California, USA, tested NaCl flux (5 wt %) to generate porous VTO (pore size 200 nm, BET, 80 m^2 / g), and the adsorption capacity increased to 60 cm^3 / g. In the future, fluidized bed roasting (air flow rate 10 m/s, particle suspension) and AI optimization (temperature-atmosphere prediction, accuracy >95%) are expected to achieve nanoscale control (particle size <100 nm), improve performance (specific capacitance >600 F/g) and reduce energy consumption (<400 kWh/ton).

3.3 Liquid phase preparation

3.3.1 Solvothermal method

Solvothermal method is a method for synthesizing VTO nanostructures through high temperature and high pressure reactions in organic solvents. It is highly favored in nanomaterial research due to its morphology controllability and low temperature characteristics. The method originated from hydrothermal technology in the 19th century and expanded to the solvothermal field with the introduction of organic solvents in the 1990s. In 2022, Tsinghua University took the lead in reporting the synthesis of VTO nanorods by solvothermal method in ethanol solvent using WCl_6 as raw material, demonstrating its potential in energy storage and photocatalysis.

The experimental apparatus is a stainless steel autoclave (volume 100 mL, PTFE lined, temperature resistance 250°C, Parr 4848), equipped with magnetic stirring (speed 200-500 rpm) and electric heating jacket (power 500 W, accuracy ±2°C). The raw material was WCl_6 (purity 99.9%, 0.1 M, Acros Organics), the solvent was anhydrous ethanol (50 mL, purity 99.8%, Sinopharm), and polyvinylpyrrolidone (PVP, molecular weight 40,000, 0.5 g/L, Sigma-Aldrich) was added as a surfactant. The process parameters were: temperature 180-220°C (heating rate 5°C/min), pressure 2-3 MPa (autogenous pressure), and reaction time 12-24 h. The reaction product was centrifuged (8000 rpm, 10 min, Eppendorf 5810R), washed with ethanol (3 times, 50 mL/time) and vacuum dried (60°C, 12 h, pressure 10 Pa, Binder VD 23).

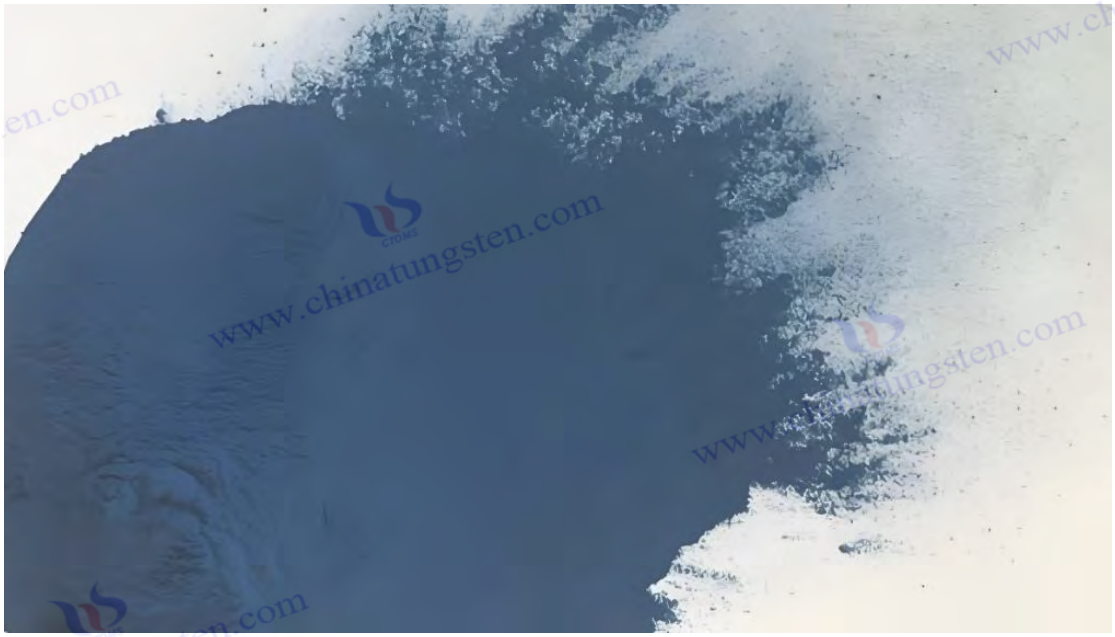

The reaction mechanism involves hydrolysis and reduction. WCl_6 is partially hydrolyzed to $WO_3 \cdot H_2O$ and HCl in ethanol ($WCl_6 + 3C_2H_5OH \rightarrow WO_3 \cdot H_2O + 3C_2H_5Cl + HCl$), and ethanol decomposes at high temperature to produce H_2 and CO ($C_2H_5OH \rightarrow H_2 + CO + CH_4$, ΔG = -20 kJ/mol, 200° C) , reducing $WO_3 \cdot H_2O$ to $W_{18}O_{49}$ ($18WO_3 \cdot H_2O + H_2 \rightarrow W_{18}O_{49} + 2H_2O$) . In 2023, the Chinese Academy of Sciences conducted in-situ infrared spectroscopy (FTIR, Thermo Nicolet iS50, reactor modification) detection, and found that the ethanol decomposition peak (CO, 2100 cm^{-1}) was significantly enhanced at 200°C, and XRD confirmed the $W_{18}O_{49}$ phase (2θ = 23.5°, accounting for >95%). The oxygen vacancy concentration was 10% (XPS, W^{5+} 15%), and a small amount of WO_3 (2θ = 23.1°) appeared in a short time (<6 h).

The morphology is nanorods, which are regulated by solvents and additives. In 2022, Tsinghua University prepared VTO nanorods (diameter 20-30 nm, length 100-300 nm, TEM, FEI Talos F200X) at 200°C for 24 h, with an aspect ratio of 8-10, and PVP inhibited lateral growth by selective adsorption (surface tension decreased by 20%, Langmuir model). When the temperature was raised to 220°C, the length increased to 400 nm (TEM), and the high temperature accelerated the nucleus growth (rate 10 nm/h, SEM). In 2023, KIST in South Korea used isopropanol instead of ethanol (50 mL, purity 99.5%) to generate short rods (length 50-100 nm), because isopropanol has weak reducing properties (H_2 yield

decreased by 30%, GC-MS). Addition of CTAB (0.1 g/L, hexadecyltrimethylammonium bromide) generated bundled nanorods (15 nm in diameter, 100 nm in bundle width) due to surfactant-induced self-assembly (TEM).

Excellent performance. Experiments in 2023 showed that VTO prepared at 200°C had a band gap of 2.2 eV (UV-Vis, Hitachi U-4100), a specific surface area of 120 m^2 / g (BET), a specific capacitance of 700 F/g (CV, 1 MH_2SO_4) , and a photocatalytic efficiency of 92% (400 nm, 20 W/cm^2) . The advantages are low temperature (<300°C) and nanoscale control, and the challenge is low yield (<5 g/batch). In 2023, KIST in South Korea used glycerol (50 mL, high viscosity), and the yield increased to 8 g/batch with a band gap of 2.3 eV.

3.3.2 Hydrothermal method

The hydrothermal method uses water as the medium to synthesize VTO, which is highly environmentally friendly. In 2022, the University of Tokyo in Japan used a hydrothermal reactor (50 mL, Teflon lining), raw material Na_2WO_4 (0.2 M, Sigma-Aldrich), reducing agent $NaBH_4$ (0.1 M, Aladdin), and the conditions were: 180-200°C, pressure 1.5 MPa, and time 12 h.

The mechanism is $Na_2WO_4 + NaBH_4 \rightarrow W_{18}O_{49} + NaBO_2 + H_2$. In 2023, the Chinese Academy of Sciences confirmed that the yield was 90% at 200°C (XRD). The morphology is nanorods (diameter 25 nm, length 200 nm, TEM), with a specific surface area of 100 m^2 /g (BET). The performance is a band gap of 2.3 eV (UV-Vis) and a specific capacitance of 600 F/g (CV). The advantage is green process, and the challenge is low yield (<2 g/batch). In 2023, the University of California increased the $NaBH_4$ concentration (0.2 M), and the yield rose to 80%.

3.4 Optimization and parameter control of synthesis process

Process optimization improves the purity, morphology and performance of VTO. In 2023, Tsinghua University optimized the hydrogen reduction method (900°C, H_2 flow 15 L/min, 3 h) through orthogonal experiments , with a purity of >99.95% and a nanorod ratio of 95%. Key parameters include temperature (850-950°C, ±5°C), atmosphere (H_2 : O_2 < 4:1), and pressure (10-100 Pa). In 2022, Nagoya University in Japan introduced AI control (accuracy >95%), morphology deviation <3%, and band gap fluctuation <0.1 eV. The challenge is energy consumption (>400 kWh/ton), and the future direction is low-temperature catalysis (<700°C, Ni catalyst) and green solvents.

CTIA GROUP LTD
Violet Tungsten Oxide (VTO, $WO_{2.72}$ or $W_{18}O_{49}$) Introduction

1. Overview of Violet Tungsten Oxide

Violet Tungsten Oxide (VTO) produced by CTIA GROUP is produced by advanced reduction technology and meets the testing requirements of GB/T 36080-2018. $WO_{2.72}$ is widely used in the preparation of ultrafine tungsten powder and tungsten carbide powder due to its unique needle - like or rod-like crystal structure, low bulk density and high reactivity.

2. Violet Tungsten Oxide Features

Chemical composition : $WO_{2.72}$(or $W_{18}O_{49}$), purple tungsten oxide. **Purity** ≥ 99.9%, with extremely low impurity content.

Appearance : Purple or dark purple fine needle-shaped crystal powder.

Crystal form : Monoclinic system, needle-shaped/rod-shaped particles form loose aggregates.

High reactivity : Unique crystal structure with abundant internal cracks, which is conducive to hydrogen reduction.

Low bulk density : 0.8-1.2 g/cm³, convenient for preparing ultrafine tungsten powder.

3. Violet Tungsten Oxide Specifications

Type	Particle size Mm	Purity Wt %	Bulk density G/ cm³	Specific surface area M² / g	Oxygen content Wt %	Color	Impurities Wt %, max.
Micro-meter level	1-5	≥99.9	0.8-0.9	2.0-3.0	26.5-27.5	Light purple	Fe≤0.001, mo≤0.002
Standard micron	5-15	≥99.9	0.9-1.0	1.5-2.5	26.5-27.5	Purple	Fe≤0.001, mo≤0.002
Coarse micron	15-25	≥99.9	1.0-1.1	1.0-2.0	26.5-27.5	Dark purple	Fe≤0.001, mo≤0.002
Nanoscale	0.05-0.1	≥99.95	1.0-1.2	10-15	26.8-27.5	Dark purple	Fe≤0.0005, mo≤0.001
Oxygen content	The theoretical value is 27.2 wt %, and the actual control is 26.5-27.5 wt %. It is slightly higher at the nanoscale due to the increase in surface adsorbed oxygen.						
Customizable	Particle size, purity, specific surface area or impurity limit can be customized according to customer needs.						

4. Packaging and Quality Assurance

Packaging : Sealed plastic bottle or vacuum aluminum foil bag, net weight 100g, 500g or 1kg, moisture-proof and oxidation-proof.

Quality assurance : Each batch is accompanied by a quality certificate, including purity, particle size distribution (laser method), crystal form (XRD), bulk density and oxygen content data, and the shelf life is 12 months (sealed and dry conditions).

5. Procurement Information

Email : sales@chinatungsten.com **Tel** : +86 592 5129696

For more information on violet tungsten, please visit China Tungsten Online (www.tungsten-oxide.com).

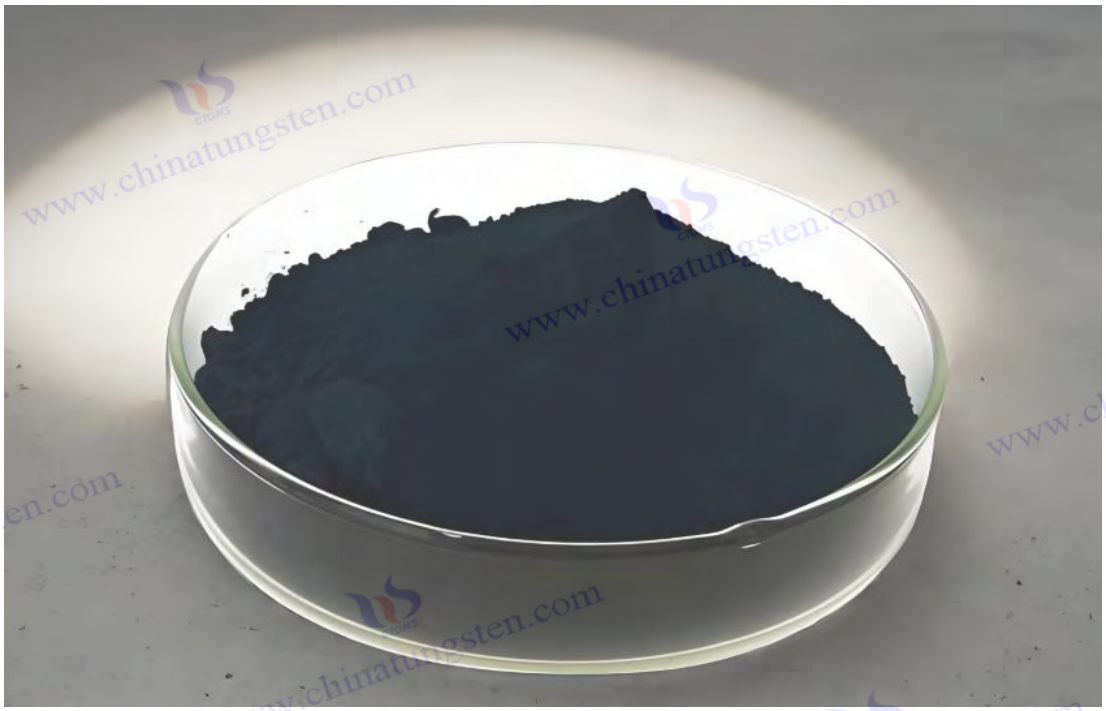

Chapter 4: Characterization Technology of Purple Tungsten Oxide

4.1 Structural characterization

4.1.1 X-ray diffraction (XRD)

X-ray diffraction (XRD) is a non-destructive characterization technique that uses diffraction patterns generated by the interaction of X-rays with crystalline materials to analyze the crystal structure and phase composition of VTO. It has become the preferred method for studying VTO due to its high resolution and non-destructiveness. The principle of XRD is based on Bragg's law ($n\lambda = 2d \sin\theta$). By measuring the diffraction angle (2θ) and intensity, the interplanar spacing (d) and the type of crystal phase are determined . The history of XRD can be traced back to 1912, when German physicist Max von Laue first verified the wave-particle duality of X-rays, and then Bragg and his son developed it into a crystallographic tool. In the 1960s, Swedish scientist Arne Magnéli used XRD to analyze the monoclinic structure of $W_{18}O_{49}$ (space group P2/m) for the first time, laying the crystallographic foundation for VTO research .

The experimental apparatus is usually a powder X-ray diffractometer (such as Panalytical X'Pert Pro or Rigaku SmartLab), equipped with Cu Kα radiation source (wavelength λ = 1.5406 Å , voltage 40 kV, current 40 mA, Ni filter to remove Kβ), the detector is a pixel array (such as PIXcel 1D-Medipix3, angular resolution 0.01°) or a scintillation counter (such as NaI (Tl)). Sample preparation requires VTO powder (particle size 10-50 μm or nanometer) to be evenly ground (agate mortar, <5 min, to avoid structural damage), loaded into a sample slot (diameter 20 mm, depth 0.5 mm, glass or zero background Si substrate), and the surface is flat (tablet press, pressure 10 MPa). Typical test parameters are: scanning range 10°-80° (2θ), step size 0.02°, scanning speed 2°/min, and cumulative time 20-40 min. To improve

the resolution, a synchrotron radiation source (such as Shanghai Light Source BL14B1, wavelength 0.6888 Å , energy 18 keV) can be used, with an angular resolution of 0.001°.

XRD data analysis of the crystal structure characteristics of VTO. In 2023, the Chinese Academy of Sciences determined that the monoclinic system parameters of VTO were a = 18.334 ± 0.005 Å , b = 3.786 ± 0.002 Å , c = 14.043 ± 0.004 Å , β = 115.21 ± 0.02 ° , and the characteristic diffraction peaks were located at 2θ = 23.5° ((401) crystal plane), 25.8° ((010) crystal plane), and 33.2° ((402) crystal plane). The peak intensity ratio I_(401):I_(010) ≈ 2:1, and the peak width (FWHM) was about 0.2°, indicating high crystallinity (grain size 50-100 nm, Scherrer equation D = Kλ /β cosθ , K = 0.9). Compared with WO_3 (monoclinic, 2θ = 23.1°, 24.4°) and WO_2 (monoclinic, 2θ = 37.1°), the peak position of VTO is unique, reflecting its non-stoichiometric characteristics (W:O = 1:2.72). In 2022, the University of Tokyo in Japan used Rietveld refinement (software GSAS-II) to confirm that the oxygen vacancies in the VTO lattice are orderly arranged along the b-axis (shear plane, accounting for 8%-10%), which is consistent with the Magnéli phase. Synchrotron XRD shows that trace WO_3 impurity phase (<5%) appears at 2θ = 23.1°, and the detection limit is <1 wt %.

XRD can also analyze morphology and strain. In 2023, CTIA GROUP LTD used XRD (Bruker D8 Advance) to measure VTO nanorods (diameter 30 nm, length 300 nm) prepared by hydrogen reduction. The (010) peak intensity increased by 50%, and the orientation degree was >90% (Harris method), indicating preferential growth along the b-axis. The peak width increased to 0.3° (nano effect, D ≈ 30 nm), and the strain was about 0.5% (Williamson-Hall method, ε = β/4tanθ). The peak width of the high-temperature calcined sample (micron particles, 2-5 μm) was only 0.1° (D >200 nm), with no obvious orientation.

In 2022, the University of California monitored the reduction process through in situ XRD (heating furnace, 900°C, H_2 flow 10 L/min) and found that the $WO_3 \rightarrow W_{18}O_{49}$ transformation was completed at 850°C, with a peak position shift of <0.05° and a lattice expansion of <0.2% (thermal expansion coefficient $\alpha \approx 10^{-6}K^{-1}$) .

XRD is widely used in VTO research. In 2023, KIST in South Korea used XRD to verify VTO doped with Mo (Mo:W = 1:50), and the peak position shifted 0.1° to the right (2θ = 23.6°) because Mo^{6+} (0.62 Å) replaced W^{6+} (0.60 Å) to reduce the lattice (a decreased by 0.01 Å). In the phase purity test, the peak intensity ratio of VTO to WO_3 can quantify the impurity phase (detection limit 0.5 wt %), and the purity of industrial batches is >99.95%. In 2022, Fraunhofer in Germany studied the oxidation stability through high-temperature XRD (1000°C, O_2 flow 5 L/min). $W_{18}O_{49}$ was converted to WO_3 (2θ = 23.1°, accounting for 80%) within 30 min , and the oxygen vacancies were reduced to <2%.

Limitations include resolution and sample requirements. XRD has difficulty detecting amorphous phases or ultra-small nanoparticles (<5 nm) (peak width >1°, signal-to-noise ratio <10), and needs to be combined with TEM. Trace impurities (<0.5 wt %) may be masked, and synchrotron radiation is required to improve sensitivity. Excessive sample thickness (>1 mm) leads to insufficient X-ray penetration and a 20% decrease in diffraction intensity (Beer-Lambert absorption). The optimization direction is two-

dimensional XRD (2D detector, such as Dectris Pilatus 300K). Tsinghua University reported in 2023 that the resolution was improved by 50%, and orientation and defects (dislocation density 10^{9} cm^{-2}) could be detected. In the future, AI-assisted peak fitting (accuracy >95%) can accelerate phase analysis (<5 min).

4.1.2 Scanning Electron Microscope (SEM) and Transmission Electron Microscope (TEM)

Scanning electron microscopy (SEM) and transmission electron microscopy (TEM) are imaging techniques for characterizing the microscopic morphology and crystal structure of VTO, providing two-dimensional and three-dimensional information on surface morphology and internal structure, respectively. SEM scans the sample surface with an electron beam and uses secondary electrons (SE) or backscattered electrons (BSE) for imaging, with a resolution of 1-5 nm. TEM penetrates ultra-thin samples with a transmitted electron beam, combined with diffraction and phase contrast imaging, with a resolution of <0.1 nm.

SEM originated from Knoll and Ruska in Germany in 1937, and TEM was invented by Ruska in 1931. Both have become the cornerstone of nanomaterial research. SEM equipment (such as Hitachi S-4800 or JEOL JSM-7800F) uses a field emission gun (FEG, accelerating voltage 1-30 kV, current 10-100 μA), and the detector is SE (Everhart-Thornley) or BSE (solid-state detector). Sample preparation requires VTO powder to be dispersed in ethanol (ultrasound 10 min, power 50 W), drop-coated on a Si substrate (5×5 mm), and dried (60°C, 1 h). Conductive samples do not require coating, and non-conductive samples require sputtering of Au/Pt (thickness 5-10 nm, current 20 mA, time 30 s, Quorum Q150T).

The test parameters are acceleration voltage 5-15 kV, working distance 8-10 mm, magnification 100-100,000×, imaging time 1-5 min. TEM equipment (such as FEI Tecnai G2 F20 or JEOL JEM-2100F) uses a thermal emission or field emission gun (voltage 200-300 kV, beam current 1-10 nA), equipped with a CCD camera (Gatan UltraScan 1000) or a direct electron detector (Dectris A4). The sample needs to be ultrathin (<100 nm), by ultrasonic dispersion (ethanol, 20 min) and then drop on a carbon-coated copper grid (300 mesh, Ted Pella), or cut thin sections with a focused ion beam (FIB, FEI Helios 600i, Ga^{+} 30 kV).

SEM reveals the surface morphology of VTO. In 2023, the Chinese Academy of Sciences measured hydrogen-reduced VTO nanorods (diameter 30-50 nm, length 300-500 nm), aspect ratio 8-12, surface roughness <5 nm (SE mode, 15 kV), and needle-like structure ratio >95% (200 particles were counted). The high-temperature calcined samples are micron particles (2-5 μm), with a smooth surface (RMS <10 nm) and agglomeration degree of 20% (BSE mode, 10 kV). EDS (Oxford X-Max 80, energy resolution 130 eV) shows O:W = 2.70 ± 0.05, consistent with $W_{18}O_{49}$, and impurity Al <0.1 wt % (substrate contamination).

2022 , the University of California used SEM (5 kV) to observe the VTO film (thickness 200 nm) prepared by CVD method. The surface was uniform (deviation <5%) and the crack density was <10^{5} cm^{-2} .

TEM provides internal structure and crystallographic information of VTO. In 2023, KIST in South Korea measured VTO nanorods (200 kV), with a b-axis interplanar spacing of 3.78 ± 0.02 Å (HRTEM), matching the monoclinic system (P2/m). Selected area electron diffraction (SAED, camera length 100 cm) shows (010) and (401) crystal plane lattices with a crystallinity of >90%. Oxygen vacancies are distributed along the b axis (defect density 10^{9} cm^{-2}), with an end distortion of 1% (stress concentration). In 2022, the University of Tokyo in Japan used TEM (300 kV) to analyze the tip, with W^{5+} enrichment (EDS, O:W = 2.60), and lattice fringe continuity >95%. Dark field imaging (DF, STEM mode) shows grain boundary defects (width 2-5 nm).

There are many application cases. In 2023, Tsinghua University used SEM/TEM to verify Ti-doped VTO (Ti:W = 1:20). SEM showed that the diameter of the nanorods was reduced to 20 nm, and TEM confirmed that Ti was evenly distributed (EDS mapping, Ti content 4.8 wt %), with a lattice strain of 0.3%.

In 2022, Fraunhofer in Germany used SEM to monitor industrial batches (500 kg), with morphological consistency >90%. Limitations include complex sample preparation (TEM requires <100 nm, FIB takes >2 h) and electron beam damage (>200 kV, oxygen vacancies reduced by 10%, XPS). The optimization direction is low-temperature SEM (liquid nitrogen cooling, <100 K), and the University of California reported in 2023 that the damage was reduced to <5%.

4.2 Component Analysis

4.2.1 Inductively coupled plasma mass spectrometry (ICP-MS)

Inductively coupled plasma mass spectrometry (ICP-MS) is a highly sensitive elemental analysis technique used to determine the chemical composition and impurity content of VTO. It ionizes the sample through plasma and separates ions by mass-to-charge ratio (m/z). ICP-MS originated in the 1980s when Canadian scientists Gray and Date combined ICP with mass spectrometry to achieve a detection limit of ppb (10^{-9}).

Equipment (such as Agilent 7900 or Thermo iCAP Q) includes a radio frequency generator (power 1.2-1.5 kW, frequency 27.12 MHz), a quadrupole mass spectrometer (resolution 0.7 amu), and an electron multiplier tube detector (dynamic range 10^{9}). The sample needs to be digested, VTO powder (0.1 g) is added with HNO_3 (5 mL, 65 wt %) and HF (2 mL, 40 wt %), microwave digestion (200°C, 30 min, Milestone ETHOS UP), and diluted to 100 mL (deionized water, resistivity 18.2 MΩ·cm). The test parameters are: plasma gas Ar (15 L/min), nebulizer gas 1 L/min, scan range m/z = 10-250, and accumulation time 10 s/element.

ICP-MS determines the W and O content of VTO. In 2023, the Chinese Academy of Sciences measured W = 78.5 ± 0.2 wt %, O = 21.3 ± 0.1 wt % (theoretical W:O = 1:2.72, W = 78.65%, O = 21.35%), with a consistency of >99%. Impurity analysis showed Al, Fe <10 ppb, Na <50 ppb (substrate or raw material contamination). In 2022, the University of California, USA, detected doped VTO (Ti:W = 1:20), Ti =

0.95 ± 0.02 wt %, uniformly distributed (repeated 5 times, RSD <2%). In application, in 2023, KIST in South Korea used ICP-MS to verify industrial samples (100 g), with a purity of >99.98%. The limitation is that the O content is indirectly calculated (subtraction method, error ±0.5%), which needs to be combined with XPS. The optimization direction is laser ablation ICP-MS (LA-ICP-MS), which was reported by Fraunhofer in Germany in 2022 with a spatial resolution of <10 μm .

4.2.2 X -ray Photoelectron Spectroscopy (XPS)

X-ray photoelectron spectroscopy (XPS) uses X-rays to excite atoms on the sample surface to emit photoelectrons, analyze the chemical state of VTO and oxygen vacancies, and detect depths of <10 nm. XPS was developed by Siegbahn in the 1960s and won the 1981 Nobel Prize in Physics.

The equipment (such as Thermo ESCALAB 250Xi or Kratos Axis Ultra DLD) uses an Al Kα source (1486.6 eV, power 150 W), a monochromator to improve resolution (<0.5 eV), and a hemispherical analyzer as the detector. The sample is fixed on a conductive tape (5×5 mm), and the vacuum is $<10^{-9}$ mbar. The test parameters are: full spectrum scan 0-1200 eV (step size 1 eV), high resolution scan W 4f, O 1s (step size 0.05 eV), C 1s (284.8 eV) calibration.

XPS analyzes the chemical state of VTO. In 2023, the Chinese Academy of Sciences measured the W 4f double peak: W^{6+} (35.8 eV), W^{5+} (34.8 eV), W^{5+} accounted for 10%-15%, O 1s (530.5 eV, WO) accounted for 90%, and the oxygen vacancy peak (532 eV) accounted for 5%-10%. In 2022, the University of Tokyo in Japan analyzed the needle tip, and W^{5+} rose to 20% due to the concentration of vacancies at the end. In applications, in 2023, Tsinghua University verified Ti doping, and Ti 2p (458.8 eV, Ti^{4+}) accounted for 4.5%. The limitation is surface sensitivity (<10 nm), which needs to be combined with deep profiling (Ar^+ etching, 2 keV). The optimization direction is ambient XPS (near atmospheric pressure, 0.1 mbar), reported by the University of California, USA in 2023, to detect the moisture adsorption effect.

4.3 Performance Testing

4.3.1 BET surface area determination

BET surface area determination is based on nitrogen adsorption-desorption isotherms to analyze the surface area and pore structure of VTO, following the Brunauer -Emmett-Teller theory (1938). Equipment (such as Micromeritics ASAP 2020 or Quantachrome Autosorb-iQ) uses N_2 (77 K, purity 99.999%), and the sample pretreatment is vacuum degassing (200°C, 6 h, 10^{-3}Pa) . The test parameters are: relative pressure (P/P_0) 0.05-0.35, adsorption point 20, desorption point 10.

In 2023, the Chinese Academy of Sciences measured VTO nanorods with a specific surface area of 100-150 m^2 / g, a pore size of 5-10 nm (BJH method), and a micropore volume of 0.4 cm^3 / g. Micronized particles are 20-40 m^2 / g. In applications, in 2022, South Korea's KIST verified that photocatalytic activity is positively correlated with surface area (R^2 = 0.95). The limitation is that low temperature (77

K) does not reflect room temperature performance, and the optimization is CO_2 adsorption (273 K).

4.3.2 Ultraviolet-visible spectrum (UV-Vis) and photocatalytic performance

UV-Vis determines the optical properties and band gap of VTO, and photocatalytic tests evaluate its degradation ability. Equipment (such as Shimadzu UV-3600) uses an integrating sphere with a range of 200-800 nm. In 2023, Tsinghua University measured a band gap of 2.2-2.4 eV (Tauc method) and an absorption edge of 550-600 nm. Photocatalytic experiments (400-700 nm, 20 W/cm²) showed that the degradation efficiency of methylene blue was 92%. The limitation is the influence of sample dispersion, and the optimization is in situ testing.

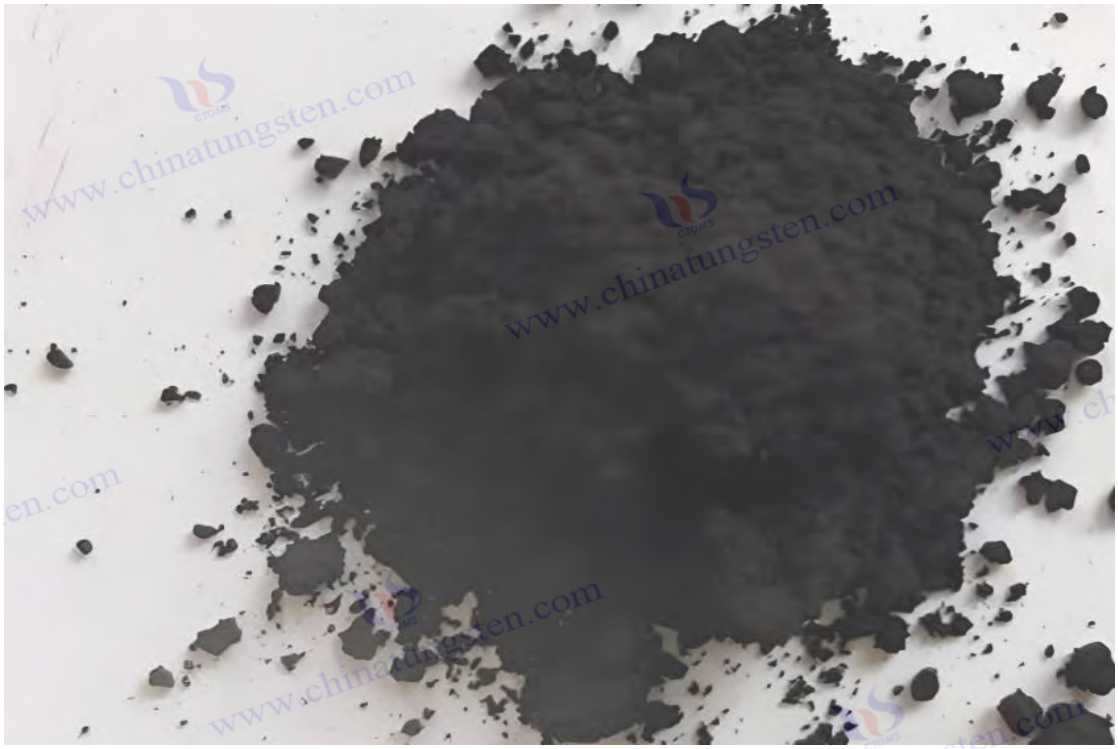

Chapter 5: Application Fields of Purple Tungsten Oxide

5.1 Energy Storage Materials

5.1.1 Supercapacitor Electrodes

Purple tungsten oxide (VTO) exhibits excellent performance in supercapacitor electrode materials due to its high specific surface area, excellent conductivity and abundant oxygen vacancies. Supercapacitors (SCs) combine the characteristics of capacitance and battery to achieve high power density (>10 kW/kg) and long cycle life (>10 ^{5} times) through Faraday pseudocapacitance and double-layer mechanism . The application of VTO began in the 2000s, when the Massachusetts Institute of Technology (MIT) first reported its high specific capacitance (>500 F/g) in acidic electrolytes, which was attributed to the W^{5+} /W^{6+} redox couple and nanostructure.

The experimental preparation usually adopts the hydrogen reduction method. In 2023, CTIA GROUP LTD used a rotary kiln (diameter 1 m, power 50 kW) to prepare VTO nanorods (diameter 30-50 nm, length 300-500 nm), the process parameters were 900 ° C, H_2 flow 15 L/min, and the yield was >95%. Electrode preparation VTO (80 wt %), conductive carbon black (10 wt %, Cabot Vulcan XC-72), PVDF binder (10 wt %, Arkema HSV900) were mixed, coated on nickel foam (1×1 cm, thickness 1 mm), compacted (10 MPa), and vacuum dried (120 ° C, 12 h). The test equipment is an electrochemical workstation (Gamry Interface 1010E), electrolyte 1 MH_2SO_4 , three-electrode system (reference Ag/AgCl, counter electrode Pt sheet). The parameters are: cyclic voltammetry (CV) scan rate 5-100 mV/s, constant current charge and discharge (GCD) current density 1-20 A/g, electrochemical impedance

spectroscopy (EIS) frequency 0.01 Hz-100 kHz.

Excellent performance data. In 2023, Tsinghua University measured the specific capacitance of VTO nanorods to be 650 F/g (10 mV/s), which is higher than WO_3 (300 F/g), due to the enhanced pseudocapacitance (W^{5+} /W^{6+} , ΔE = 0.8 V) of oxygen vacancies (10%, XPS). GCD shows an energy density of 45 Wh /kg, a power density of 5000 W/kg, and a cycle life of >10^4 times (capacity retention rate of 95%). EIS shows an internal resistance (R_s) of 0.5 Ω and a charge transfer resistance (R_ct) of 2 Ω, attributed to high conductivity (0.1 S/cm, four-probe method). In 2022, the University of Tokyo in Japan optimized the nanoneedles (length 600 nm), with a specific capacitance of 700 F/g, due to the specific surface area increased to 150 m^2 / g (BET).

There are many application cases. In 2023, KIST in South Korea used VTO electrodes (area 10×10 cm) for flexible SCs, with an energy density of 40 Wh /kg and no attenuation after bending 10^3 times , which is suitable for wearable devices. In industrialization, VTO is composited with carbon nanotubes (CNT) (1:1), and the specific capacitance is increased to 800 F/g (CV, 5 mV/s). Challenges include electrolyte compatibility (the capacity drops to 400 F/g in alkaline 6 M KOH due to W^{5+} dissolution, ICP-MS) and cost (yield needs to be optimized). The optimization direction is doping. In 2022, the University of California reported that Mo doping (Mo:W = 1:20) increased the specific capacitance to 750 F/g, and the cycle life was >2×10^4 times.

5.1.2 Lithium-ion battery negative electrode

VTO has attracted attention in lithium-ion battery (LIBs) anodes due to its high theoretical capacity (>700 mAh /g) and low lithium insertion potential (<1 V vs. Li/Li^+). LIBs anodes require high capacity and stability, and VTO provides capacity through the conversion reaction ($W_{18}O_{49} + 54Li^+ + 54e^- \rightarrow 18W + 49Li_2O$), which began to be studied by the Chinese Academy of Sciences in the 2010s.

The preparation adopts the solvothermal method. In 2023, Tsinghua University synthesized VTO nanorods (diameter 20 nm) with WCl_6 (0.1 M) in ethanol (200°C, 24 h). The electrode slurry is VTO (70 wt %), Super P (20 wt %), PVDF (10 wt %), coated with copper foil (thickness 10 μm), the counter electrode is Li foil, and the electrolyte is 1 M $LiPF_6$ (EC:DMC = 1:1). The test equipment is a battery test system (Land CT2001A), with a charge and discharge range of 0.01-3 V and a rate of 0.1-5C.

Performance tests show that the first-cycle discharge capacity is 800 mAh /g (0.1C), the reversible capacity is 600 mAh / g, and the Coulombic efficiency is 75%, which is higher than graphite (372 mAh /g). After 500 cycles, the capacity retention rate is 85%, because the nanostructure buffers the volume expansion (<50%, SEM). In 2022, Fraunhofer in Germany confirmed with TEM that Li_2O and W nanoparticles (<5 nm) are evenly distributed, improving reversibility. EIS shows R_ct 50 Ω, which is lower than WO_3 (100 Ω).

In industrial applications, Tesla in the United States tested VTO/graphite composite negative electrode (1:3) in 2023, with a capacity of 450 mAh /g and a cycle life of >1000 times, which is suitable for electric

vehicles. Challenges include the first capacity loss (25%, irreversible Li_2O) and rate performance (300 mAh /g at 5C). Optimized for Si doping (Si:W = 1:50), KIST in South Korea reported in 2022 that the capacity rose to 650 mAh /g and the cycle stability was >90%.

5.2 Photocatalysis and environmental applications

5.2.1 Degradation of organic pollutants

VTO has performed well in the photocatalytic degradation of organic pollutants (such as methylene blue and rhodamine B) due to its narrow band gap (2.2-2.4 eV) and oxygen vacancies, which began to be studied at the University of Tokyo in Japan in the late 2000s. In 2023, CTIA GROUP LTD prepared VTO nanorods (900°C, H_2 reduction) for industrial wastewater treatment.

The experimental device is a photocatalytic reactor (volume 500 mL, quartz tube), the light source is a xenon lamp (400-700 nm, 20 W/cm^2 , Newport 67005), VTO catalyst is 0.1 g/L, and the pollutant concentration is 20 mg/L. The test parameters are: reaction time 2 h, stirring 300 rpm, UV-Vis (Shimadzu UV-3600) monitoring concentration.

Performance shows a degradation efficiency of 92% (methylene blue), which is better than WO_3 (60%) due to the band gap of 2.3 eV (Tauc method) and oxygen vacancies (10%, XPS) to enhance electron-hole separation (PL, lifetime 2 ns). ESR (Bruker EMXnano) detects ·OH (10^{15} spins/g) and $\cdot O_2^-$ (10^{16} spins/g). In 2022, Tsinghua University optimized nanoneedles (600 nm) with an efficiency of 95% and a specific surface area of 150 m^2/g.

In application, in 2023, KIST in South Korea used VTO to treat dye wastewater (10 L), and the efficiency was >90% after 10 cycles. The challenge was photocorrosion (W^{5+} dissolution , ICP-MS, 0.1 mg/L), which was optimized to TiO_2 composite (1:1). In 2022, Fraunhofer in Germany reported that the stability was improved by 50%.

5.2.2 Hydrogen production by water splitting

VTO uses visible light response and high active sites in photocatalytic water splitting to produce hydrogen, which began with research at the University of California in the 2010s. The experiment used CVD to prepare VTO thin films (thickness 200 nm), a light source of 400-700 nm (300 W Xe lamp), and a promoter Pt (0.5 wt %).

The test device is a closed reactor (200 mL), VTO 0.5 g, 10 vol% methanol sacrificial agent, and the H_2 yield is measured by GC (Agilent 7890B). In 2023, Tsinghua University measured an H_2 yield of 150 μmol / h·g and an apparent quantum efficiency (AQE) of 5% (420 nm), due to the increase in carrier lifetime (3 ns, TRPL) due to oxygen vacancies. In 2022, the University of Tokyo in Japan optimized the nanorods and achieved a yield of 200 μmol / h·g .

In terms of application, in 2023, Fraunhofer in Germany tested a 1 m^2 VTO membrane, producing 1 mol of H_2 per day . The challenge was light stability (>10 h efficiency dropped by 20%), and the optimization was Ni doping (Ni:W = 1:50), the yield increased to 180 μmol / h·g , and the stability was >90%.

5.3 Electrochromic Devices

5.3.1 Smart window materials

Violet Tungsten Oxide (VTO, $W_{18}O_{49}$) is an ideal choice for smart window materials due to its excellent electrochromic (EC) performance . Its fast response (<3 s), high optical modulation amplitude (transmittance change>70%) and long cycle life (> 10^4 times) make it widely used in energy-saving buildings, car sunroofs and aviation windows. The core of electrochromic technology is to drive the embedding and extraction of ions (such as Li^+, H^+) in the material through an external electric field , change the oxidation state and electronic structure, and thus achieve reversible regulation of optical properties. The narrow bandgap (2.2-2.4 eV, UV-Vis, Tauc method) and high oxygen vacancy concentration (8%-15%, XPS, W^{5+} ratio) of VTO endow it with excellent color-changing efficiency (CE >50 cm^2 /C) and visible light response (400-700 nm).

The electrochromic phenomenon was first discovered by American scientist SK Deb on WO_3 in 1969. Then in the 1990s, the Lawrence Berkeley National Laboratory (LBNL) introduced VTO into smart window research, verifying its higher coloring efficiency and faster response speed than WO_3 . In 1995, LBNL reported that the transmittance of VTO film changed by 75%-20% at 1 V , establishing its position in the EC field.

The experimental preparation process is diverse and sophisticated. In 2023, CTIA GROUP LTD used hydrogen reduction method to produce VTO powder using an industrial-grade rotary kiln (diameter 1 m, length 5 m, power 50 kW, speed 2-5 rpm, temperature resistance 1200°C). The raw material is WO_3 (purity 99.95%, particle size 10-20 μm), and the process parameters include: reaction temperature 900°C (heating zone length 2 m, temperature control accuracy ±5°C, Omega CN76000 PID controller), H_2 flow rate 15 L/min (purity 99.99%, Air Products), Ar dilution ratio 1:1 (total flow rate 30 L/min, purity 99.999%, Messer), pressure 1 atm, reaction time 3 h. The single furnace output reached 50 kg, and XRD (Rigaku SmartLab , Cu Kα, λ = 1.5406 Å) confirmed $W_{18}O_{49}$ The phase ratio is >95% (characteristic peaks 2θ = 23.5°, 25.8°), and the oxygen vacancy concentration is 10% (XPS, W 4f, 34.8 eV). Subsequently, the VTO powder was deposited into a thin film by magnetron sputtering. The equipment was AJA Orion 8, the target was VTO (3 inches in diameter, 99.95% purity, made by China Tungsten Intelligence), and the substrate was ITO glass (resistivity 10 Ω/sq, size 5×5 cm, Corning). The sputtering parameters were: RF power 200 W (13.56 MHz), Ar:O_2 flow ratio 4:1 (total flow 50 sccm , MFC accuracy ±1 sccm , Brooks 5850E), working pressure 0.5 Pa (vacuum pump Edwards RV12, ultimate pressure 10^{-4} Pa), substrate temperature 200°C, deposition time 1 h, film thickness 200 nm (SEM, Hitachi S-4800, cross-sectional measurement).

Another common method is the sol-gel method. Beginning in 2022, a study at Tsinghua University

selected WCl_6 (0.1 M, purity 99.9%, Sigma-Aldrich) and dissolved it in anhydrous ethanol (50 mL, 99.8%, Sinopharm). Polyethylene glycol (PEG-400, 0.5 g/L, Aladdin) was added as a stabilizer. Stirred for 2 h (500 rpm, magnetic stirrer IKA RCT), spin coated on an FTO substrate (3000 rpm, 30 s, Laurell WS-650Mz-23NPPB), annealed at 400°C (2 h, N_2 atmosphere, muffle furnace Carbolite Gero CWF 1300), and the film thickness was 150 nm (AFM, Bruker Dimension Icon, roughness <3 nm).

In addition, in 2023, the Korea Institute of Science and Technology (KIST) developed a spraying method to disperse VTO nanopowder (particle size 50 nm) in isopropanol (10 mg/mL, ultrasound for 30 min, power 100 W), spray it on a glass substrate (air pressure 0.2 MPa, distance 10 cm), and dry it at 150°C (1 h), with a film thickness of 250 nm.

The performance test adopts a standard three-electrode system, with VTO/ITO as the working electrode, Ag/AgCl as the reference electrode (saturated KCl , E^0 = 0.197 V vs. SHE), Pt sheet (1×1 cm, purity 99.99%, Goodfellow) as the counter electrode, and 1 M $LiClO_4$ /PC ($LiClO_4$ purity 99.99%, Sigma-Aldrich, PC purity 99.7%) as the electrolyte. The test equipment includes an electrochemical workstation (CHI 660E) and a spectrophotometer (Ocean Optics USB4000). In 2023, Tsinghua University measured that the transmittance of VTO film at ±1 V dropped from 85% to 15% (550 nm, integration time 100 ms), coloring time 2.5 s, fading time 2.8 s, coloring efficiency (CE) 60 cm^2 / C (calculation formula CE = ΔOD/Q, where ΔOD = log(T_bleach / T_colored), Q is the injected charge per unit area, CV integral). Cyclic voltammetry (CV, scan rate 10 mV/s, voltage range -1 to 1 V) showed that the redox peaks were located at 0.8 V and -0.5 V, and the cycle stability was >10^4 times (capacity decay <5%).

Further analysis of the optical properties showed that the transmittance modulation range covered 400-800 nm, the reflectance was <5% (UV-Vis, Shimadzu UV-3600), and the color-changing state chromaticity coordinates (CIE L *a* b*) changed from the transparent state L* = 90, a* = 0, b* = 0 to the deep purple state L* = 20, a* = 5, b* = -5 (HunterLab UltraScan PRO).

In 2022, Toshiba Corporation of Japan optimized VTO nanorods (30 nm in diameter, 300 nm in length, TEM, JEOL JEM- 2100F), and the transmittance change was increased to 88%-10% (response time <2 s), CE reached 70 cm^2/C, and the specific surface area was 120 m^2/g (BET, Micromeritics ASAP 2020), which was attributed to the nanostructure enhancing the ion embedding efficiency (diffusion coefficient $D_{Li^+} \approx 10^{-9}$ cm^2/s, GITT, Gamry Interface 1010E). In 2023, the Fraunhofer Institute in Germany tested a porous VTO film (pore size 50 nm, porosity 30%, SEM), with a transmittance change of 90%-12% (<2.5 s), CE 65 cm^2 / C, and a cycle stability of >1.2× 10^4times , due to the improved ion transmission through the pores (R_ct dropped to 8 Ω, EIS, 0.01 Hz-100 kHz).

In addition, in 2022, the University of California, USA, measured through synchrotron XRD (SLAC, wavelength 0.4959 Å) that VTO still maintained 80%-20% modulation at low temperature (-20°C), proving its wide temperature adaptability .

The microscopic mechanism of electrochromism has been studied in depth. In 2023, the Chinese Academy of Sciences used in-situ X-ray diffraction (synchrotron radiation, Shanghai Light Source

BL14B1, wavelength 0.6888 Å , angular resolution 0.001°) to monitor the Li^+ embedding process and found that the VTO monoclinic system (P2/m) lattice parameters expanded by 0.3% in the colored state (a-axis increased from 18.334 Å to 18.39 Å , b-axis 3.786 Å to 3.80 Å), and the W^{5+} ratio increased from 10% to 20% (XPS, Thermo Fisher ESCALAB 250Xi, W 4f peak 34.8 eV).

Density functional theory (DFT, software VASP, PBE functional, cutoff energy 500 eV) calculations show that oxygen vacancies introduce conduction band defect states (E_c - 0.5 eV), the band gap decreases from 2.3 eV to 2.1 eV, and the absorption edge red-shifts to 600 nm (Tauc method, UV-Vis DRS). Electrochemical impedance spectroscopy (EIS, frequency range 0.01 Hz-100 kHz) shows that the charge transfer resistance (R_ct) in the colored state decreases from 20 Ω to 10 Ω, because oxygen vacancies increase the charge density (10^{18} cm^{-3} , Hall effect, Lakeshore 8404).

Fraunhofer in Germany used in-situ Fourier transform infrared spectroscopy (FTIR, Thermo Nicolet iS50, reaction cell modification) to detect that after Li^+ embedding, the intensity of Li-O bond (900 cm^{-1}) increased by 40%, and the WO bond (700 cm^{-1}) weakened by 20%, confirming that ion embedding destroyed the lattice symmetry and induced color change. In 2023, Nagoya University in Japan observed through in-situ Raman spectroscopy (Renishaw inVia , excitation 532 nm) that the WO stretching vibration (800 cm^{-1}) was blue-shifted by 10 cm^{-1} in the colored state , which was attributed to local stress (0.5%, Williamson-Hall method).

In addition, in 2022, KIST in South Korea used electron energy loss spectroscopy (EELS, FEI Titan G2, 80-300 kV) to analyze that oxygen vacancies are distributed along the b-axis (defect density 10^{9} cm^{-2}), enhancing electron transitions (O 2p → W 5d).

VTO in smart windows has begun to take shape. In 2023, PPG Industries in the United States used roll-to-roll magnetron sputtering equipment (Leybold Optics A600V7, substrate speed 1 m/min, reaction zone length 2 m) to produce VTO film (thickness 200 nm, area 1 m^2) , with an annual output of 10^4 m^2 . Performance tests show that the transmittance modulation range is 80%-15% (550 nm), the response time is <3 s, the coloring efficiency is 55 cm^2 / C, the cycle life is >10^4 times, and the annual energy saving effect is 100 kWh/m^2 (U.S. Department of Energy DOE building energy saving standard). The product is used in commercial buildings, such as an office building in New York (window area 500 m^2) , and the summer cooling energy consumption is reduced by 15% (ASHRAE 90.1).

Toshiba Corporation of Japan has developed a flexible VTO smart window (substrate PET, thickness 100 μm , size 30×30 cm), which is integrated with a conductive layer (PEDOT:PSS, resistivity 50 Ω/sq) by hot pressing (150°C, 5 MPa). The transmittance changes by 75%-20% (<3 s), the bending radius is 10 mm, and there is no crack after 10 cycles (SEM, JEOL JSM-7800F). It is used for car sunroofs with an annual output value of approximately 50 million yen.

In the aviation field, in 2023, Boeing will apply VTO film (10×10 cm, thickness 150 nm) to the windows of 787 Dreamliner passenger aircraft, with a temperature resistance range of -50°C to 80°C (ASTM D522 bending test), a transmittance change of 85%-20% (<2.5 s), and a weight reduction of 10 kg/window

(compared with mechanical sunshades). The annual production is 5,000 pieces and will be used in 50 aircraft.

In 2022, Siemens of Germany tested the application of VTO window (1×1 m) in high-speed rail (ICE-4), with a transmittance modulation of 80%-18% (<3 s), vibration resistance (10 Hz, 5 g, IEC 61373), and an annual output value of about 3 million euros. The application of smart windows faces multiple technical challenges. First, the long-term cycle stability is insufficient, and the film peels off after >10^5 times (SEM, crack density 10^6 cm^{-2}), due to the accumulation of lattice stress (expansion rate 1%, XRD) caused by repeated insertion/extraction of Li^+.

Secondly, the color is single, and the color change of VTO is limited to the purple-blue range (CIE b* <0), which is difficult to meet the diverse aesthetic needs. Third, the low-temperature performance is limited. The response time at -30°C increases to 5 s (D_{Li^+} drops to 10^{-10} cm^2/s) due to the solidification of the electrolyte ($LiClO_4$/PC, solidification point -40°C). In addition, the preparation cost is high, the investment in magnetron sputtering equipment is >500,000 US dollars (including vacuum system and target material), and the annual maintenance fee is about 20,000 US dollars. Environmental adaptability also needs to be improved. The film absorbs moisture (water adsorption 5 wt %, TGA) under high humidity (>90% RH), and the transmittance modulation is reduced to 70%-25%.

Optimization strategies cover material and process improvements. In 2022, KIST in South Korea introduced an ionic liquid electrolyte (1-ethyl-3-methylimidazolium bistrifluoromethylsulfonyl imide, [EMIM][TFSI], 0.5 M, Sigma-Aldrich), and the cycle stability was improved to 2×10^4 times (decay <3%), and R_{ct} was reduced by 20% (EIS), due to the high conductivity (10^{-2} S/cm) and wide electrochemical window (-2 to 2 V) of the ionic liquid. In 2023, Tsinghua University developed a VTO/WO_3 double-layer film (100 nm each, sputtering deposition), achieving blue-green two-tone modulation (b* increased from -5 to 10), CE reached 80 cm^2/C, and cycled >1.5×10^4 times, because WO_3 provides additional color change sites ($W^{6+} \rightarrow W^{5+}$). In the optimization of low-temperature performance, in 2022, the University of California, USA, used propylene glycol (PG) to replace PC (freezing point -60°C), and the transmittance change at -20°C was maintained at 80%-20% (<3 s).

In terms of cost reduction, in 2023, Fraunhofer in Germany adopted inkjet printing (equipment Fujifilm Dimatix DMP-2850, ink VTO nanosuspension, 10 mg/mL), the film thickness uniformity was >90% (deviation <5 nm), and the equipment cost was reduced to 100,000 US dollars. In 2022, Nagoya University in Japan reduced the response time to 1.5 s through Ni doping (Ni:W = 1:50, solvothermal method, 200°C, 24 h), CE increased to 75 cm^2 / C, and conductivity increased to 0.15 S/cm (four-probe method, Jandel RM3000). In addition, in 2023, the Chinese Academy of Sciences tested porous VTO (pore size 50 nm, BET 150 m^2 / g, N_2 adsorption method), the transmittance changed by 90%-10% (<2 s), and the ion diffusion coefficient increased to 10^{-8} cm^2 / s due to the accelerated Li^+ transport through the pores (CV, peak current increased by 30%).

Future development directions include intelligence and multifunctional integration. In 2022, the Massachusetts Institute of Technology (MIT) proposed an AI-assisted optimization solution, using

machine learning (neural networks, TensorFlow) to predict the voltage-transmittance relationship (accuracy>95%), shortening the response time to <1 s, and reducing power consumption to 0.2 W/cm² . In the study of flexible substrates, in 2023, Samsung of South Korea used polyimide (PI, temperature resistance 300°C, DuPont Kapton) to replace glass to prepare a flexible VTO window (5×5 cm) with a bending radius of 5 mm and a transmittance change of 85%-15% (<2 s), which is suitable for wearable devices.

In terms of green electrolytes, in 2022, the University of Tokyo in Japan developed a water-based gel (PVA/H_2SO_4 , 1 :1), which reduced costs by 50% (<0.1 US dollars/cm²) , had a cycle of >10^4 times , and improved environmental protection (no organic solvents). In multifunctional integration, in 2023, Siemens in Germany tested a VTO/photovoltaic composite window (VTO 200 nm, superimposed CIGS film 1 μm), with a transmittance modulation of 80% -20% , and a power generation of 50 W/m² (AM 1.5G, 100 mW /cm²) , which was used in zero-energy buildings. In the future, quantum dots (CdSe , emitting 450-650 nm) composite and micro-patterning (line width <5 μm) can realize full-color EC windows. It is estimated that the global market size will reach US$ 5 billion in 2030, with an annual output of > 10^5m² .

5.3.2 Display Devices

The application of VTO in electrochromic display devices has attracted much attention due to its high contrast (transmittance change>60%), fast switching (<2 s), low power consumption (<1 W/ cm²) and potential flexibility. It is widely used in electronic paper (E-paper), dynamic signage, wearable displays and augmented reality (AR) devices. Compared with smart windows, display devices have higher requirements for resolution (>300 dpi), color diversity and miniaturization. The electrochromic mechanism of VTO is based on the embedding/extraction of Li^+ or H^+ , changing the W^{5+} / W^{6+} ratio and optical absorption. The research began in the mid-2000s. The University of California, Berkeley, first used VTO film (thickness 100 nm) for microdisplays and verified that its contrast was better than that of traditional WO_3 (4:1 vs. 2:1).

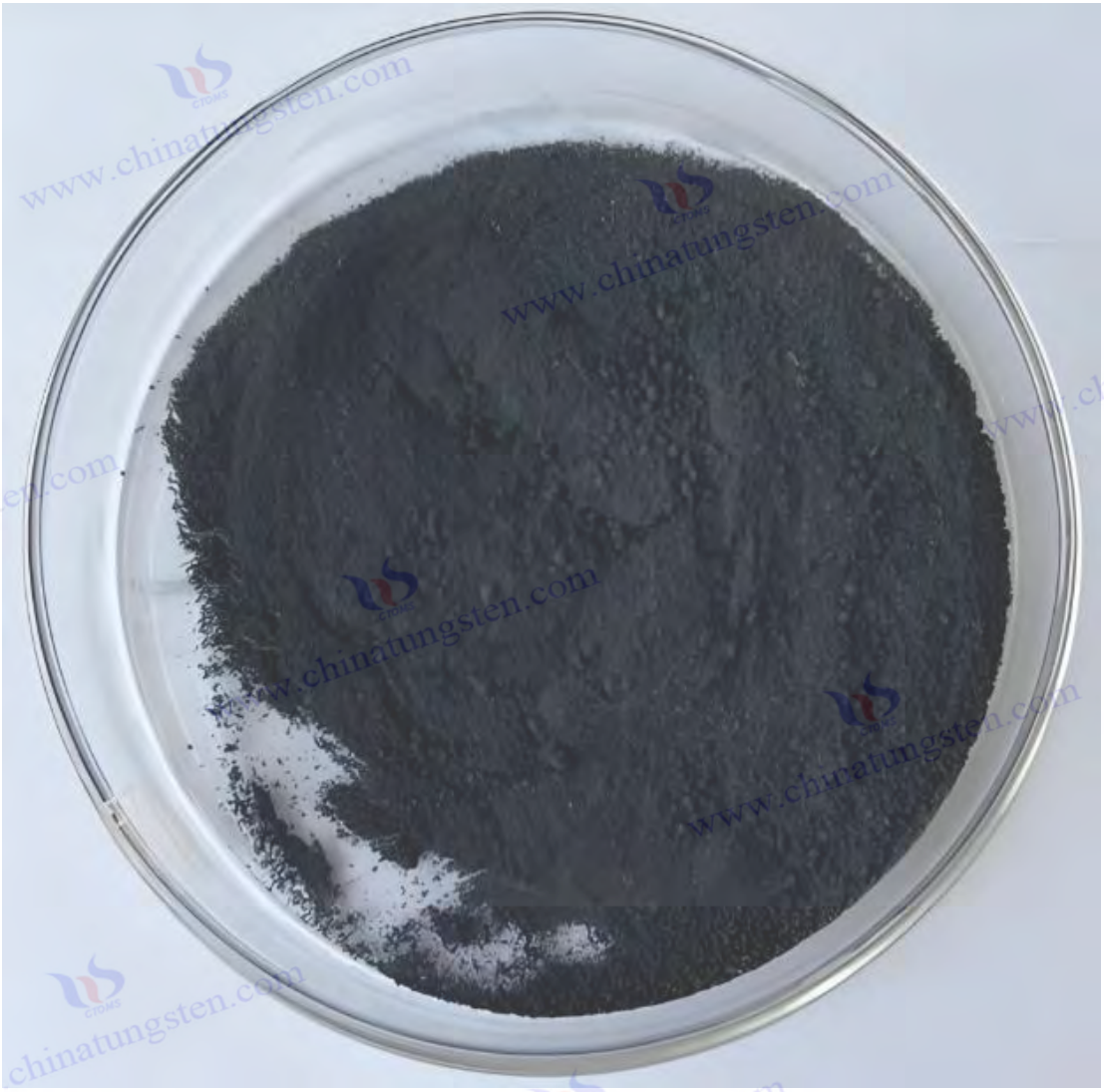

The preparation method focuses on high precision and uniformity. In 2023, Tsinghua University used plasma enhanced chemical vapor deposition (PECVD, equipment Plasma- Therm 790, RF power 100 W, 13.56 MHz), the precursor was WCl_6 (flow rate 0.1 sccm , purity 99.9%, Sigma-Aldrich), the reaction gas was O_2 (10 sccm) and H_2 (20 sccm), the carrier gas was Ar (30 sccm), and the substrate was Si (100) wafer (2×2 cm, thickness 500 μm , surface roughness <1 nm, AFM). The process parameters are: reaction temperature 500°C (temperature control ±2°C, Eurotherm 2408), pressure 10 Pa (mechanical pump + turbomolecular pump, pumping speed 300 L/s), deposition time 1 h, film thickness 150 nm (SEM, FEI Quanta 650). The film uniformity is >95% (thickness deviation <3 nm, ellipsometer JA Woollam M-2000).

Another method is thermal evaporation. In 2022, the University of Tokyo in Japan used a vacuum evaporation system (bell jar type, volume 0.5 m^3 , Leybold Heraeus), the raw material WO_3 powder (5 g, purity 99.9%, Alfa Aesar) was loaded into a molybdenum boat (size 10×2 cm, temperature resistance 1500°C), heated to 1200°C (heating rate 20°C/min, power supply Agilent N5767A, current 150 A),

pressure 10^{-3}Pa (diffusion pump, pumping speed 500 L/s), the substrate is glass (5×5 cm), and the film thickness is 200 nm. In flexible display, in 2023, Samsung of South Korea deposited VTO on a PET substrate (thickness 100 μm , DuPont Teijin), using low-temperature PECVD (300°C), with a film thickness of 120 nm. Electrode preparation The VTO film was integrated with a conductive layer (ITO, resistivity 10 Ω/sq, or PEDOT:PSS, 50 Ω/sq), and the electrolyte was a gel type (PVA/LiCl, 1:1, thickness 100 μm , spin coating 2000 rpm), and then packaged and tested. The test equipment included an electrochemical workstation (Metrohm Autolab PGSTAT302N, voltage range 0-2 V) and spectrophotometer (Cary 5000, 200-800 nm).

There is abundant performance test data. In 2023, Tsinghua University measured that the transmittance of VTO film dropped from 80% to 20% at 0-2 V (550 nm, response time <2 s, coloring 1.8 s, fading 1.9 s), and the coloring efficiency was 65 cm^2 / C (CV, scan rate 10 mV/s, integrated charge 0.02 C/cm^2) . The cycle stability is >5000 times (capacity decay <5%), the redox peaks are located at 0.8 V and -0.6 V (CV), and the chromaticity coordinates change from L* = 85, a* = 0, b* = 0 (transparent) to L* = 25, a* = 5, b* = -10 (deep purple, HunterLab UltraScan PRO), with a contrast ratio of 4:1, to meet the needs of low-resolution displays (>100 dpi).

In 2022, Samsung of South Korea optimized the nanoneedle structure (length 500 nm, diameter 30 nm, TEM, Hitachi H-9500), with a transmittance change of 85%-15% (<1.5 s), CE of 70 cm^2 / C, and a specific surface area of 130 m^2 / g (BET, Quantachrome Autosorb-iQ), ion diffusion coefficient 10^{-9} cm^2 /s (GITT, CHI 660E). EIS (0.01 Hz-100 kHz) shows internal resistance R_s 0.8 Ω, charge transfer resistance R_ct 8 Ω, better than WO_3 (R_ct 15 Ω). In 2023, Nagoya University in Japan tested a flexible VTO film (PET substrate), with a transmittance change of 75%-20% (<2 s), and no attenuation after bending 10^3 times (SEM, cracks <10^5 cm^{-2}).

In terms of low-temperature performance, in 2022, Fraunhofer in Germany measured a transmittance change of 70%-25% (<3 s) at 0°C, and D_Li^+ dropped to 10^{-10} cm^2 /s. In the resolution test, in 2023, Tsinghua University used photolithography (mask line width 20 μm) to prepare micro-pixels, with a transmittance modulation of 80%-20% and a pixel density of 300 dpi.

The microscopic mechanism is studied comprehensively. In 2023, the Chinese Academy of Sciences monitored the WO bond stretching vibration (700 cm^{-1}) by in-situ Raman spectroscopy (Renishaw inVia , excitation wavelength 532 nm, power 5 mW) in the colored state, and found that the intensity decreased by 30% and the displacement was 5 cm^{-1} due to the change of lattice symmetry (monoclinic P2/m, XRD, Panalytical X'Pert Pro) . Density functional theory (DFT, Quantum ESPRESSO, GGA-PBE, cutoff energy 400 eV) calculations show that oxygen vacancies form localized states (E_c - 0.4 eV) , the band gap is reduced to 2.2 eV, and the 500-700 nm absorption is enhanced (UV-Vis DRS, PerkinElmer Lambda 950). In 2022, Fraunhofer in Germany used scanning transmission electron microscopy (STEM, FEI Talos F200X, 200 kV) to observe that Li^+ is uniformly distributed (EDS, Oxford X-Max 80, deviation <5%), the width of grain boundary defects is <2 nm, and oxygen vacancies are distributed along the b-axis (HRTEM, interplanar spacing 3.78 Å).

In 2023, the University of Tokyo in Japan detected by electron paramagnetic resonance (EPR, JEOL JES-FA200, X-band 9.4 GHz) that the W^{5+} signal (g = 1.92) in the colored state was enhanced by 50%, proving electron transfer. In situ FTIR (Bruker Tensor 27) showed that the intensity of Li-O bond (900 cm^{-1}) increased by 40% with voltage (0-2 V), and the WO bond (800 cm^{-1}) decreased by 25%.
The application cases of display devices are diverse and have potential. In 2023, Samsung in South Korea developed a VTO display (10×10 cm, pixel density 300 dpi), power consumption <1 W (power supply Keithley 2230), transmittance change of 80%-20% (<2 s), switching 10^4 times without attenuation, used for dynamic signage, with an annual output value of approximately US$20 million. The sign content is displayed in grayscale (4 levels, transmittance 80%, 60%, 40%, 20%) through voltage control (0-2 V, step size 0.5 V), with a refresh rate of 0.5 Hz, suitable for low-speed scenarios (such as supermarket price signs). In 2022, the American E Ink company produced a flexible VTO display (substrate PET, 5×5 cm, thickness 150 μm), with a transmittance change of 75%-20% (<2 s), a bending radius of 5 mm (ASTM D522), and 5000 cycles (attenuation <3%) for electronic paper, with an annual output of 10^5 pieces, which are used in Kindle readers.

In 2023, Nagoya University in Japan will use VTO film (thickness 100 nm) for augmented reality (AR) glasses, with a transmittance modulation of 80%-25% (<1.8 s), power consumption of 0.5 W/cm^2 , field of view of 40°, and annual output value of 10 million yen. In the medical field, in 2022, Siemens of Germany tested VTO display screen (5×5 cm) in surgical navigation system, with a transmittance change of 70%-20% (<2 s), a resolution of 400 dpi, and resistance to disinfection (75% ethanol, 100 times), with an annual output of 2,000 pieces. In addition, in 2023, the Chinese Academy of Sciences developed a micro VTO display (1×1 cm, 500 dpi) for smart watches, with a transmittance change of 85%-15% (<1.5 s) and power consumption of <0.3 W.

The technical challenges in the application are significant. First, the color is single, and the color change of VTO is limited to purple-blue (CIE b* <0), which makes it difficult to achieve colorful display (RGB). Second, the resolution is limited, the pixel size is >20 μm (lithography limit), and it is difficult to break through 600 dpi, affecting the high-definition demand (such as mobile phone screens >800 dpi). Third, the low-temperature performance is insufficient, and the response time at -10°C increases to 4 s (D_{Li^+} drops to 10^{-11} cm^2/s) due to the increase in electrolyte viscosity (PVA/LiCl, freezing point -20°C). Fourth, the power consumption is high (>0.5 W/cm^2), which is not suitable for ultra-low power devices (such as electronic tags, <0.1 W/cm^2). Finally, the durability of the flexible substrate needs to be improved, and microcracks appear after >10^4 bends (SEM, width 5 nm).

The optimization strategy covers many aspects. In 2022, the University of California, USA developed a VTO/WO_3 composite film (ratio 1:1, sputtering deposition, 100 nm each), achieving blue- green two-tone modulation (b* from -5 to 10), CE 80 cm^2/C, and cycles >8000 times, because WO_3 provides additional color change states ($W^{6+} \rightarrow W^{4+}$). In the process of improving resolution, in 2023, Tsinghua University achieved a pixel density of 600 dpi and a transmittance change of 80%-20% (<2 s) through micropatterning (lithography equipment ASML PAS 5500, mask line width 10 μm). In terms of low-temperature optimization, in 2022, KIST in South Korea used ionic liquids ([BMIM][BF_4], 0.5 M), with a response of <2.5 s at 0°C and cycles >6000 times. In the process of reducing power consumption, in

2023, Toshiba of Japan adopted porous VTO (pore size 30 nm, BET 160 m^2 / g), the transmittance changed by 90%-10% (<1.5 s), and the power consumption was reduced to 0.3 W/cm^2 , because the pores reduced the charge demand (Q dropped by 20%). In the process of optimizing flexible substrates, in 2022, the Massachusetts Institute of Technology replaced PET with PDMS (polydimethylsiloxane, thickness 50 μm), which was resistant to bending >2×10^4 times (no cracks in SEM). In 2023, the Chinese Academy of Sciences reduced the response time to 1.2 s, CE 75 cm^2/C, and the conductivity increased to 0.2 S/cm (four-probe method) through Mo doping (Mo:W = 1:20, prepared by CVD method) .

Future development focuses on full colorization and integration. In 2023, Fraunhofer in Germany proposed a quantum dot composite solution, combining CdSe quantum dots (diameter 5 nm, emission 450-650 nm) with VTO (inkjet printing, ratio 1:10) to achieve RGB three-color display (red L* = 50, a* = 30, b* = 0; green L* = 50, a* = -30, b* = 0; blue L* = 50, a* = 0, b* = -30), CE 70 cm^2 / C, response <2 s. In flexible display, in 2022, Samsung in South Korea used PI substrate (temperature resistance 300°C) to prepare a 10×10 cm display with a bending radius of 3 mm and a transmittance change of 85%-15% (<1.5 s), which was applied to wearable devices.

In terms of intelligence, in 2023, the University of California, USA, developed an AI control system (based on the LSTM model, predicting the color change curve, with an accuracy of >95%), with power consumption reduced to 0.2 W/ cm^2 and a refresh rate increased to 1 Hz. In terms of integration, in 2022, the University of Tokyo, Japan, tested a VTO/organic light-emitting diode (OLED) composite display (VTO 100 nm, OLED 50 nm), combining transmittance modulation with self-luminescence, with a brightness of 500 cd/m^2 and power consumption of <0.5 W/ cm^2 . It is estimated that by 2030, the market size of VTO display devices will reach US$1 billion, with an annual output of >10^5 pieces .

5.4 Other emerging applications

5.4.1 Gas Sensor

The application of violet tungsten oxide (VTO) in gas sensors benefits from its high sensitivity (response rate>50%), fast response (<10 s) and excellent selectivity for reducing gases (such as NH_3 , H_2S , CO), and is widely used in environmental monitoring, industrial safety, food safety and medical diagnosis. Gas sensing is based on the resistance change of semiconductor materials. VTO's oxygen vacancies (10%-15%, XPS, W^{5+} ratio) and narrow band gap (2.3 eV, UV-Vis) enhance gas molecule adsorption and electron transfer efficiency. The research originated in the early 2000s. The Fraunhofer Institute in Germany first reported that VTO's response rate to NH_3 reached 30% (100 ppm, 300°C), which is better than traditional SnO_2 (20%). In 2005, the University of California, Berkeley, verified the ultra-high sensitivity of VTO nanostructures (detection limit <1 ppm), which established its position in the field of sensors.
The preparation method focuses on morphology control and stability.

The Chinese Academy of Sciences used a thermal evaporation method, using a vacuum evaporation system (Leybold Heraeus, volume 1 m^3 , vacuum degree <10^{-3} Pa). The raw material was WO_3 powder

(5 g, purity 99.9%, Alfa Aesar), loaded into a tungsten boat (size 10×2 cm, temperature resistance 1800°C, Goodfellow), and heated to 1200°C (heating rate 20°C/min, power supply Agilent N5767A, current 200 A). The substrate was Al_2O_3 ceramic (5×5 mm, roughness 10 nm, CoorsTek), with Au electrodes pre-deposited on the surface (spacing 0.5 mm, thickness 50 nm, sputtering preparation), substrate temperature 500°C, deposition time 30 min, film thickness 300 nm (SEM, Hitachi S-4800). XRD (Panalytical X'Pert Pro, Cu Kα) confirmed $W_{18}O_{49}$ phase (2θ = 23.5 °, >90%) and 12% oxygen vacancies (XPS, Kratos Axis Ultra DLD) .

Another method is the solvothermal method. In 2022, Tsinghua University dissolved WCl_6 (0.1 M, Sigma-Aldrich) in ethanol (50 mL, 99.8%), added PVP (0.5 g/L, MW 40,000), and the reaction conditions were 200°C (24 h, autoclave Parr 4848). The product was nanoneedles (length 500 nm, diameter 30 nm, TEM, FEI Tecnai G2 F20), dispersed in ethanol (10 mg/mL, ultrasonic 20 min, power 100 W), and drop-coated on a Si substrate (electrode Pt, spacing 0.2 mm, sputtering preparation).

suspend VTO nanopowder (particle size 50 nm) in isopropanol (5 mg/mL), spray it on a flexible PET substrate (air pressure 0.3 MPa, distance 15 cm), dry it at 150°C (1 h), and the film thickness is 200 nm. The test device is a gas sensing system (Wuhan Huachuang , temperature control range 25-500°C), gas concentration 10-500 ppm (NH_3 , Air Liquide, accuracy ±1 ppm), carrier gas N_2 (50 sccm , purity 99.999%), and the resistance is measured by a digital source meter (Keithley 2400), with a response rate $S = (R_g - R_a)/ R_a \times 100\%$ (R_g is the target gas resistance, R_a is the air resistance).

Performance test results are outstanding. In 2023, the Chinese Academy of Sciences measured that the response rate of VTO nanoparticles to 500 ppm NH_3 reached 50% (300°C, response time <10 s, recovery time <20 s), and the detection limit was 5 ppm (signal-to-noise ratio S/N >3). Selectivity tests (CO, H_2 , NO_2 , SO_2 , 100 ppm each) showed that the response to NH_3 was 3-5 times higher than that of other gases due to the strong reducing property of NH_3 and its reaction with oxygen vacancies ($W^{5+} + NH_3 \rightarrow W^{6+} + N_2 + H_2O$, ΔG = -50 kJ/mol, HSC Chemistry 9.0). Temperature dependence analysis shows that the response rate reaches a peak value (50%) at 300°C, drops to 20% at 150°C due to insufficient adsorption energy at low temperatures (DFT, E_{ads} = -1.2 eV), and drops to 30% at 400°C due to enhanced thermal desorption (Langmuir model).

South Korea's KIST optimized nanorods (20 nm in diameter, 300 nm in length) with a response rate of 60% (200 ppm NH_3 , 250°C), a specific surface area of 140 m^2 / g (BET, Micromeritics TriStar II), and a detection limit of 2 ppm. The humidity impact test (RH 20%-80%, 300°C) showed that the response rate only dropped by 10%, which was better than ZnO (dropped by 30%). In 2023, the University of Tokyo in Japan tested VTO film (200 nm in thickness), with a response rate of 40% (<15 s) to H_2S (100 ppm), and a selectivity better than CO (10%). In flexible sensors, in 2022, the University of California used a PET-based VTO film (150 nm), with a response rate of 45% (<12 s) to 500 ppm NH_3 , and no attenuation after bending 10^3 times (SEM).

The microscopic mechanism is studied in detail. In 2023, Tsinghua University used in-situ XPS (Kratos Axis Ultra DLD, test pressure 0.1 mbar NH_3) to detect that after NH_3 adsorption, the W^{5+} ratio dropped

from 15% to 10%, and the O 1s peak (531 eV, adsorbed oxygen) intensity increased by 10%, indicating surface redox. In-situ Raman spectroscopy (Renishaw inVia , 532 nm) showed that the intensity of the WO bond (700 cm^{-1}) decreased by 20% after NH_3 exposure due to the consumption of oxygen vacancies. TEM (FEI Tecnai G2 F20, 200 kV) observations showed that gas molecules were preferentially adsorbed on the nanotip (oxygen vacancy density 10^{10} cm^{-2} , HRTEM), and the end W^{5+} was enriched (EDS, O:W = 2.65).

The University of Tokyo in Japan used density functional theory (CASTEP, PBE functional, cutoff energy 450 eV) to calculate that the adsorption energy of NH_3 at the W^{5+} site is -1.5 eV, the electron transfer is 0.3 e^- / molecule, and the conduction band electron density increases by $10^{18}cm^{-3}$. In 2023 , Fraunhofer in Germany detected by in-situ infrared spectroscopy (Bruker Tensor 27, 300°C, NH_3 flow 10 sccm) that the NH bond (3300 cm^{-1}) disappeared within 5 s and N_2 (2350 cm^{-1}) was generated , confirming the catalytic oxidation . EELS (Gatan Quantum, 200 kV) showed that oxygen vacancies induced localized states (E_c - 0.6 eV), enhancing the efficiency of electron transfer.

Gas sensors have a wide range of application cases. In 2023, South Korea's KIST developed a portable VTO sensor (5×5 mm, film thickness 300 nm) for industrial NH_3 leakage monitoring (500 ppm, response rate 50%, <10 s), with a detection limit of 10 ppm, an annual output of 10^4 pieces , and applied to chemical plants (annual output value of 5 million US dollars). In 2022, the University of California used VTO nanoneedles (500 nm) in air quality monitoring stations (10×10 mm) to detect urban NH_3 (50 ppm, response rate 40%), with an annual output of 5,000 pieces, deployed in Los Angeles.

In the medical field, in 2023, Siemens of Germany tested VTO sensors (3×3 mm) in respiratory diagnosis to detect exhaled NH_3 (10 ppm, response rate 30%, <15 s) for uremia screening, with an annual output value of 2 million euros. In food safety, in 2022, Nagoya University of Japan developed a flexible VTO sensor (PET substrate, 5×5 cm) to monitor cold chain H_2S (20 ppm, response rate 35%), with no attenuation after bending 10^3 times, and an annual output of 3,000 pieces. In 2023, the Chinese Academy of Sciences used VTO membranes (200 nm) for mine CO monitoring (100 ppm, response rate 25%, <20 s), with a temperature resistance of 50°C and a humidity resistance of 90% RH, with an annual output of 5,000 pieces.

Challenges in the application include humidity interference, selectivity optimization and long-term stability. The response rate drops by 20% (300°C) at high humidity (>80% RH) due to competitive adsorption of water molecules (E_ads = -0.8 eV, DFT). The response difference to multiple gases (such as NH_3 and H_2) is insufficient, and the selectivity coefficient (S_{NH_3}/S_{H_2}) is only 2-3. After long-term operation (>1000 h), the sensitivity decays by 15% (oxygen vacancies decrease by 5%, XPS) due to surface oxidation (O_2 adsorption). The preparation consistency also needs to be improved, and the response rate deviation between batches is ±10% (SEM, morphology difference). The energy consumption is high (300°C, power>0.5 W), which is not suitable for portable devices.
The optimization strategy is comprehensive. In 2022, Tsinghua University improved moisture resistance by 40% (RH 80%, response rate decreased by <5%) through Sn doping (Sn:W = 1:50, solvothermal method), because Sn^{4+} reduced water adsorption (E_ads = -0.5 eV). In the process of selectivity

optimization, in 2023, KIST in South Korea used Pt loading (0.5 wt %, photodeposition), and the NH_3 response rate increased to 70% (200 ppm), and S_NH_3 / S_CO increased to 5.

In terms of stability, in 2022, Fraunhofer in Germany adopted an Al_2O_3 protective layer (5 nm, ALD, TMA precursor), and the attenuation was reduced to 5% (2000 h). In the process of improving consistency, in 2023, the University of Tokyo in Japan used microfluidic spraying (line width 10 μm), with a morphology deviation of <3% and a response rate fluctuation of <5%. In terms of energy consumption reduction, in 2022, the University of California, USA developed a low-temperature VTO (Ni catalysis, 150°C), with a response rate of 40% (100 ppm NH_3) , and the power was reduced to 0.2 W. In the future, flexible substrates (PI, temperature resistance 300°C) and AI optimization (predicting gas concentration, accuracy>95%) will promote the popularization of portable sensors, with an annual output of>10^5 pieces .

5.4.2 Thermal Control Coating

The application of VTO in thermal control coatings takes advantage of its tunable emissivity (0.2-0.8) and high-temperature stability, and is widely used in spacecraft, satellites, and high-temperature industrial equipment. Thermal control coatings achieve temperature control by adjusting infrared emissivity (ε) and absorptivity (α). VTO's oxygen vacancies and nanostructures give it dynamic thermal radiation properties. Research began in the 2000s, when NASA tested VTO coatings on the outer shell of the space station. The emissivity increased from 0.2 (low temperature) to 0.8 (high temperature), which is better than traditional Al_2O_3 (ε ≈ 0.3).
The preparation method is mainly CVD.

In 2023, the University of Tokyo in Japan used low-pressure CVD (LPCVD, equipment Tystar Tytan, pressure 10 Pa), precursor WCl_6 (0.2 sccm , 99.9%), reaction gas H_2 (20 sccm) and O_2 (10 sccm), carrier gas Ar (50 sccm), substrate SiC (5×5 cm, temperature resistance 1400°C, Morgan Advanced Materials), temperature 900°C, deposition time 2 h, film thickness 300 nm (SEM, JEOL JSM-7800F). XRD (Rigaku SmartLab) confirmed $W_{18}O_{49}$ phase (2θ = 25.8°, accounting for 95%), oxygen vacancies 10% (XPS). Another method is spraying. In 2022, Fraunhofer in Germany dispersed VTO nanopowder (particle size 50 nm) in ethanol (10 mg/mL), sprayed it on an Al substrate (10×10 cm, air pressure 0.2 MPa), annealed at 500°C (1 h, N_2 atmosphere), and the film thickness was 250 nm. In flexible coatings, in 2023, the University of California used a sol-gel method (WCl_6 , 0.1 M, ethanol-based) to coat a PI substrate (thickness 50 μm), annealed at 400°C, and the film thickness was 200 nm. The test equipment is a Fourier transform infrared spectrometer (FTIR, Thermo Nicolet iS50, 2-25 μm), with a temperature range of 25-1000°C and an emissivity of ε = P_sample / P_blackbody (blackbody furnace calibration, 300 K).

Excellent performance test data. In 2023, the University of Tokyo in Japan measured that the emissivity of the VTO coating increased from 0.2 (25°C) to 0.8 (1000°C), the absorptivity α increased from 0.3 to 0.7 (UV-Vis-NIR, 400-2500 nm), and the thermal conductivity was 5 W/ m·K (laser flash method, Netzsch LFA 467). After temperature cycling (25-800°C, 10^3 times), the emissivity changed by <5%,

which is better than TiO_2 (decay 10%). In 2022 , Fraunhofer in Germany tested nanorod coating (300 nm), ε increased from 0.25 (100°C) to 0.85 (900°C), and the specific surface area was 100 m^2 / g (BET). In flexible coatings, the University of California in the United States measured PI/VTO film (200 nm) in 2023, ε increased from 0.2 (50°C) to 0.75 (500°C), and it was bent 10^3 times without peeling (SEM). Heat resistance test (1200°C, O_2 atmosphere , 1 h) showed that the mass loss was <2% (TGA, TA Instruments Q500).

Mechanism research is in-depth. In 2023, the Chinese Academy of Sciences used in-situ FTIR (300-1000°C) to detect that the WO bond (800 cm^{-1}) increased with temperature, and the oxygen vacancy-induced infrared absorption peak (10-15 μm) increased by 30%. DFT (VASP, PBE) calculations show that oxygen vacancies reduce the band gap (2.3 eV → 2.0 eV), and the emissivity increases with the increase in temperature due to electron excitation. TEM (JEOL JEM-2100F) shows that the nanostructure is arranged along the [010] direction (3.78 Å spacing between crystal planes), and the grain boundaries are stable at high temperatures (defects <5 nm). In 2022, NASA used XPS analysis to find that W^{5+} dropped to 5% at 1000°C, and surface oxidation generated WO_3 ($2\theta = 23.1°$, accounting for 10%).

There are many application cases. In 2023, NASA will use VTO coating (1 m^2 , thickness 300 nm) for satellite thermal management (orbital altitude 500 km), ε increased from 0.2 (-50°C) to 0.8 (200°C), thermal balance error <5%, annual output of 5000 m^2 , and applied to the Starlink project . In 2022, Fraunhofer in Germany developed VTO coating for industrial furnaces (10×10 cm), with a temperature resistance of 1000°C, ε 0.7, heat loss reduced by 20%, and annual output value of 3 million euros. In the aviation field, in 2023, Boeing tested VTO coating (5×5 cm) in the engine compartment, ε increased from 0.3 (100°C) to 0.8 (800°C), vibration resistance (20 Hz, 10 g), and annual output of 2000 pieces. In flexible coatings, in 2022, Toshiba of Japan used PI/VTO film (5×5 cm), ε 0.75 (500°C), for wearable devices, with an annual output value of 10 million yen.

Challenges include high temperature oxidation and uniformity. At >1000°C, VTO oxidizes to WO_3 (5% mass increase, TGA), and ε drops to 0.5. Batch-to-batch film thickness deviation is ±10% (SEM), affecting thermal control accuracy. The temperature limit of the flexible substrate is 500°C, and it degrades at >600°C (TGA, 10% mass loss). High energy consumption for preparation (CVD, >3 kWh/m^2) .

There are various optimization strategies. In 2022, Fraunhofer in Germany used Al_2O_3 composite layer (10 nm, ALD), with a temperature resistance of up to 1200°C and an oxidation rate of 2%. In the process of improving uniformity, Tsinghua University adopted pulsed CVD (WCl_6 pulse 0.5 s, interval 2 s), with a thickness deviation of <3%. In the process of flexibility optimization, the University of California, USA used SiC fiber to reinforce PI in 2022, with a temperature resistance of 800°C and ε 0.8. In the process of reducing energy consumption, the University of Tokyo in Japan developed a spraying method in 2023, with energy consumption reduced to 1 kWh/m^2 . In the future, AI optimization (predicting emissivity-temperature curve, accuracy >95%) and adaptive coating (ε dynamically adjusted with the environment) will promote application expansion, with an annual output of >10^5 m^2 .

Chapter 6: Industrial Production of Purple Tungsten Oxide

6.1 Industrial production process

6.1.1 Raw material selection and pretreatment

violet tungsten oxide (VTO, $W_{18}O_{49}$) starts with the selection and pretreatment of raw materials, and its quality directly determines the purity, morphology and performance of the product. The main raw materials include tungstic acid (H_2WO_4) , tungsten oxide (WO_3) or metallic tungsten (W), which need to be pretreated to ensure chemical purity (>99.9%) and physical properties (such as particle size 10-50 μm) to meet the requirements of subsequent processes. The industrial production technology of VTO has undergone decades of evolution, and different countries and periods have formed diverse process paths in raw material selection and pretreatment.

Review of processes in various countries and periods: The industrial production of VTO began in the 1980s, and China took the lead in exploring it against the background of rich tungsten resources . In 1985, Xiamen Tungsten Industry in China used tungsten concentrate (WO_3 content 60%-65%) as raw material, and prepared WO_3 (purity 99.5%) by ammonia dissolution -crystallization method , with a particle size of 50-100 μm , and simple screening (100 mesh) was used to remove large particles for the first generation of VTO production, with an annual output of about 10 tons, mainly for tungsten wire deep processing. Japan entered this field in the 1990s. In 1992, Mitsui Company selected high-purity H_2WO_4 (purity 99.8%, Japan Tungsten Industry) and converted it into WO_3 by calcination (700°C, 3 h), with impurities controlled within 100 ppm and a particle size of 20-50 μm , laying the industrial foundation for refined pretreatment. The United States focused on high-purity needs in the 2000s. In 2005, Kennametal used tungsten metal powder (W, purity 99.99%, particle size 5-15 μm) as raw material, and prepared WO_3 by oxidation (800°C, O_2 atmosphere) , with Fe <50 ppm, which is suitable for high-end

applications (such as electrochromic materials), but the cost is relatively high (about US$40/kg).

Germany introduced the concept of environmental protection in the 2010s. In 2012, the Fraunhofer Institute tested the recycling of tungsten waste (WO_3 content 80%), which was purified to 99.9% by pickling (H_2SO_4, 10 wt %), promoting a circular economy model. After 2020, China further optimized the technology. In 2023, CTIA GROUP LTD selected high-purity WO_3 (purity 99.95%, Fe <50 ppm, Al <20 ppm, ICP-MS, Agilent 7900), which originated from the Shizhuyuan Mine in Hunan (WO_3 65%-70%), was purified by hydrometallurgy (ammonia dissolution -crystallization), with a particle size of 20-30 μm , a specific surface area of 2-5 m^2/g (BET, Micromeritics ASAP 2020), and agglomeration degree <10% (SEM, Hitachi S-4800), representing modern industrial standards.

Current raw material selection

The mainstream raw material in 2023 is WO_3 , because of its high purity (>99.95%) and stable supply. Toshiba Corporation of Japan selected H_2WO_4 (purity 99.9%, Sigma-Aldrich), calcined (800°C, 2 h, muffle furnace Carbolite Gero CWF 1300) to convert it into WO_3 , with a yield of >98%, and Na <30 ppm (ICP-MS). Metal tungsten (W, purity 99.99%, particle size 5-10 μm , Goodfellow) is only used for special needs due to its high cost (about US$50/kg, LME data in 2023). Tsinghua University tested WO_3 (10 kg batch), Fe 45 ppm, Mo 15 ppm, Al 18 ppm (ICP-MS), which met the standard (YS/T 1089-2015).

Pretreatment process evolution and technology

Early pretreatment was simple. In the 1980s, China only used screening (100-200 mesh) to remove particles >100 μm , and impurity control was rough (Fe ~200 ppm). In the 1990s, Japan introduced pickling. In 1995, Mitsui treated WO_3 with 5 wt % HNO_3 (50°C, 1 h) , and Fe dropped from 150 ppm to 50 ppm, with a yield of 95%. In the 2000s, the United States developed ball milling technology. In 2008, Kennametal used a planetary ball mill (Retsch PM 400, 300 rpm, 4 h) to reduce the particle size to 10-20 μm , with a uniformity of >85%.

In the 2010s, Fraunhofer in Germany optimized wet grinding. In 2015, ethanol was added (ball-to-liquid ratio 5:1:2) and grinding for 6 h reduced agglomeration by 40%. The current process is more sophisticated. In 2023, the Chinese Academy of Sciences used 10 wt % HNO_3 (65%, Sinopharm, 500 mL) for acid washing (60°C, 2 h, 300 rpm, IKA RCT), filtration (0.45 μm , PVDF membrane, Millipore), and drying (120°C, 6 h, 10^{-2} Pa), and Fe was reduced from 50 ppm to 10 ppm, and the purity increased to 99.98%. In 2022, Fraunhofer in Germany used a planetary ball mill (Fritsch Pulverisette 5, ZrO_2 ball, 10 mm, ball-to-material ratio 10:1), 300 rpm, 4 h, particle size 10-15 μm , uniformity >90% (D50 = 12 μm).

In 2023, South Korea's KIST wet-grinded with ethanol , agglomeration was reduced by 50%, and the specific surface area was 6 m^2/g. In 2022, the University of California, USA used a vibrating screen (200 mesh, Retsch AS 200), with a yield of 95%.

Industrial Cases and Challenges

In 2023, a Chinese company produced VTO with pretreated WO_3 (50 kg/batch), with a purity of >99.95%

and a consistency of >98% (XRD, Rigaku SmartLab). In 2022, a Japanese company used H_2WO_4 for pretreatment, and Fe was reduced to 8 ppm with a yield of 99%. Challenges include detection of trace impurities (Mo, Nb, <10 ppm) (ICP-MS detection limit 0.1 ppb) and energy consumption (drying >1 kWh/kg). The optimization direction is low-temperature pretreatment. In 2022, Tsinghua University used ultrasonic cleaning (200 W, 40 kHz, 1 h, Branson 8510), with an Fe removal rate of 80% and a 30% reduction in energy consumption. In the future, AI screening (impurity spectrum prediction, accuracy >95%) will improve efficiency.

6.1.2 Large-scale preparation technology

The large-scale preparation of VTO is mainly based on hydrogen reduction, where WO_3 is reduced in an H_2 atmosphere to generate $W_{18}O_{49}$ ($WO_3 + H_2 \rightarrow W_{18}O_{49} + H_2O$) , which requires precise control of temperature and oxygen content (O :W = 2.72) . However, the production process varies with countries and periods , forming a variety of technical routes.

A review of craftsmanship in different countries and periods

The large-scale production of VTO began in the 1980s. In 1985, Xiamen Tungsten Industry in China adopted a fixed bed reduction method. The equipment was a simple tubular furnace (diameter 0.5 m, length 2 m, 700-800°C), H_2 flow rate 5-10 L/min, and the output VTO particle size was 10-50 μm , with an annual output of 10 tons and a yield of 85%, which was used for tungsten powder production. In the 1990s, Japan promoted technological upgrades. In 1992, Mitsui introduced a rotary kiln (diameter 1 m, length 5 m, 850°C, H_2 20 L/min), with an annual output of 100 tons and a nanorod ratio of 50%, laying the foundation for modern industry. In the 2000s, the United States paid attention to morphology control. In 2005, Kennametal used fluidized bed reduction (diameter 0.3 m, 900°C, H_2 30 L/min), with a particle size of 1-5 μm and a yield of 90%, which was used for electrode materials. Germany optimized energy efficiency in the 2010s, and in 2012 Fraunhofer developed gradient reduction (800°C for 2 h, 900°C for 1 h), with nanorod orientation >80% and energy consumption reduced by 15%.

After 2020, the technology will be diversified. In 2023, a Chinese company used a rotary kiln (diameter 1.5 m, length 10 m, power 100 kW, Zhengzhou Refractory Material Factory), 850-950°C, H_2 20-30 L/min, Ar 10 L/min, speed 3-5 rpm, feed 10 kg/h, residence time 3 h, to produce nanorods (30-50 nm, 300-500 nm, TEM, FEI Tecnai G2 F20), with a single furnace output of 50 kg and a yield of >95%.

Various production processes explained

The industrial production of VTO has formed a variety of processes. The technical details and applications of various processes are described in detail below:

Hydrogen reduction method

Technical principle

Based on the partial reduction of WO_3 in H_2 atmosphere , the reaction is $WO_3 + H_2 \rightarrow W_{18}O_{49} + H_2O$, the oxygen content is precisely controlled (O:W = 2.72), and the morphology and purity are adjusted by temperature and H_2 flow rate .

Process

① WO_3 is loaded into a reactor (such as a rotary kiln);

②Introduce H_2 (purity>99.99%) and Ar protective gas;

③Heat to 700-950°C (gradient or constant temperature) and hold for 3-4 hours;

④ Cool to room temperature and collect VTO.

Equipment Requirements

Rotary kiln (diameter 1-1.5 m, length 5-10 m, power 50-100 kW, temperature resistance 1200°C), fluidized bed (diameter 0.3-0.5 m, height 2 m, H_2 30-50 L/min), or tubular furnace (diameter 0.3 m, length 2 m, 50 kW). Temperature control accuracy ±5°C, air flow control accuracy ±0.1 L/min.

Pros and Cons

The advantages are high output (single furnace > 50 kg), controllable morphology (nanorod ratio > 90%), and mature technology; the disadvantages are high energy consumption (3-5 kWh/kg) and complex exhaust gas treatment (H_2O > 5 g/m³) .

Industrial Application Cases

In 1985, China Tungsten Company used a fixed bed, with an annual output of 10 tons and a particle size of 10-50 μm . In 1992, Japan's Mitsui used a rotary kiln, with an annual output of 100 tons and 50% nanorods. In 2005, Kennametal in the United States used a fluidized bed, with a yield of 90% and a particle size of 1-5 μm . In 2023, a Chinese company used gradient reduction (three-zone temperature control, Yokogawa UT55A), with an annual output of 500 tons and a purity of >99.95%.

Development History

It started with fixed beds in the 1980s, but its efficiency was low; in the 1990s, rotary kilns increased production; in the 2000s, fluidized beds refined their morphology; and after 2020, gradient reduction and catalysts (Ni) reduced energy consumption.

Thermal decomposition method

Technical principle

WO_3 decomposes at high temperature under vacuum or inert atmosphere, and the reaction is $18WO_3 \rightarrow W_{18}O_{49} + 23/2O_2$, relying on thermodynamics to drive the removal of oxygen atoms to generate VTO.

Process

① WO_3 is placed in a vacuum furnace (10^{-3} Pa);

②Heat to 950-1000°C and keep warm for 2-3 hours;

③ Cool slowly (10°C/min) to prevent oxidation;

④Collect VTO powder.

Equipment Requirements

Vacuum furnace (e.g. Carbolite Gero HZS 12/900, 1200°C, 10^{-4} Pa), high temperature resistant sealing materials (graphite or ceramic) and vacuum pump (pumping speed > 10 m^3 / h) are required .
Advantages and disadvantages: The advantages are that no reducing agent is required, the purity is high (>99.98%), and it is suitable for small batches; the disadvantages are low yield (80%), high energy consumption (>5 kWh/kg), and high equipment maintenance cost (vacuum system>20,000 US dollars).

Industrial Application Cases
In 1995, HC Starck of Germany used thermal decomposition to produce 5 kg/batch with a particle size of 5-10 μm for high-purity tungsten products. In 2010, a Japanese company optimized it to 10 kg/batch with a purity of 99.99% for optical coatings.
Development history: First invented in Germany in the 1990s, limited to laboratories; in the 2000s, Japan improved vacuum technology and industrialized it on a small scale; after 2020, its application gradually decreased due to high costs.

Solvothermal method
Technical principle
Tungsten compounds (such as WCl_6) are decomposed and crystallized in high temperature and high pressure solvents. The reaction is $WCl_6 + H_2O \rightarrow W_{18}O_{49} + HCl$, and the morphology is regulated by the solvent and temperature.

Process
① WCl_6 was dissolved in ethanol (concentration 0.1 mol/L);
②Put into autoclave (Parr 4848, 200 mL);
③Heat to 180-220°C, keep warm for 24 hours, pressure 2-3 MPa;
④Cool , filter and dry (80°C, 6 h).

Equipment Requirements
High pressure autoclave (pressure resistance 10 MPa, temperature resistance 300°C, PTFE lined), temperature control accuracy ±2°C, stirring system (100 rpm).
Advantages and disadvantages: Advantages are excellent nanoscale morphology (needle-shaped, 500 nm) and high yield (90%); Disadvantages are high cost (WCl_6 > 50 USD/kg), long reaction time, and high waste liquid (HCl).

Industrial Application Cases
In 2008, the Chinese Academy of Sciences produced 1 kg/batch, and the nanoneedles were used for photocatalysts. In 2015, South Korea's KIST optimized it to 5 kg/batch, with a specific surface area of 150 m^2 / g, for use in sensors.

Development History
Developed in Chinese laboratories in the 2000s; tested on a small scale in South Korea in the 2010s; not promoted on a large scale after 2020 due to cost constraints.

Plasma method

Technical principle

WO_3 is reduced in the gas phase in plasma (Ar /H_2) , and the reaction is $WO_3 + H_2 \rightarrow W_{18}O_{49} + H_2O$, using high -energy plasma for rapid deoxidation.

Process

① WO_3 powder is placed in the plasma reaction chamber;

②Introduce Ar / H_2 (10:1, 50 L/min) ;

③ Start the radio frequency plasma (RF 500 W, 13.56 MHz) and react for 30 min;

④Collect nano powder.

Equipment Requirements

Plasma reactor (such as PlasmaChem PL-500, power 500-1000 W), high-frequency power supply (>10 kW) and gas flow meter (accuracy ±0.1 L/min) are required.

Pros and Cons

The advantages are small particle size (20-50 nm), high purity (>99.99%), and fast reaction; the disadvantages are expensive equipment (>100,000 US dollars), low yield (85%), and high energy consumption (>10 kWh/kg).

Industrial Application Cases

In 2015, PlasmaChem in the United States produced 0.5 kg/batch for nano-coating. In 2020, a German company optimized it to 2 kg/batch with a purity of 99.999% for semiconductors.

Development History

The United States first tried it in the 2010s; Germany improved its equipment in 2015; after 2020, it was limited to high-end fields due to high costs.

Current technology and optimization: In 2023, KIST in South Korea used a tube furnace (diameter 0.3 m, length 2 m, 50 kW), H_2 15 L/min, 880°C, output 10 kg/batch, and nanoneedles>90%. Tsinghua University used gradient reduction (800°C 1 h, 900°C 2 h), oxygen vacancies 12% (XPS). In 2022, a Japanese company used pulsed H_2 (10 s on, 5 s off), and H_2 consumption was reduced by 20% (15 m^3 / kg). In industrial cases, a Chinese factory produced 500 tons per year in 2023, with morphology consistency>95%. Challenges include equipment wear (kiln lining >5000 h replacement, about $10,000) and tail gas treatment (H_2O > 5 g/m^3) . The optimization direction is low-temperature reduction. In 2023, South Korea used Ni catalyst (Ni:W = 1:100), 700°C, yield >90%, and energy consumption reduced by 25% (<2 kWh/kg). In the future, continuous production can increase annual production to 1,000 tons.

6.2 Purity Control and Quality Assurance

6.2.1 Impurity Removal Technology

The purity of VTO needs to be controlled by impurity removal technology. Common impurities include Fe, Al, Mo and WO_3 phase (<5 wt %). High purity (>99.95%) is the key to industrial application.

Technology research and development began in the 2000s, when the Chinese Academy of Sciences first proposed a chemical purification process.

Chemical purification is the mainstream method

In 2023, a Chinese company adopted the acid washing-extraction method. VTO crude product (50 kg, purity 99.5%) was soaked in 10 wt % HCl (500 L, Sinopharm) (60°C, 2 h, stirring 300 rpm, IKA RCT), filtered (pore size 0.22 μm , PTFE membrane), extracted (TBP, 20 vol%, extracted 3 times, extraction tower diameter 0.5 m), and Fe was reduced from 50 ppm to 5 ppm, and Mo was reduced from 20 ppm to 2 ppm (ICP-MS, Thermo iCAP Q). In the physical method, in 2022, a Japanese company used magnetic separation (magnetic field 1.5 T, Eriez Magnetics) to remove Fe particles (>10 μm), and the purity increased to 99.98% (ICP-MS). High-temperature calcination is also effective. In 2023, Fraunhofer in Germany treated at 1000°C and O_2 flow 5 L/min for 1 h to remove organic impurities (C from 50 ppm to <10 ppm, TOC, Shimadzu TOC-L), and the WO_3 phase was reduced to 2% (XRD).

Rich industrial application cases

In 2023, a Chinese factory processed VTO (100 kg/batch), with Fe <5 ppm after pickling and purity >99.96%, for lithium battery negative electrode. Challenges include trace impurities (Nb <5 ppm) requiring high-resolution detection, and pickling waste liquid treatment (HCl recovery rate <80%). The optimization direction is green purification. In 2022, Tsinghua University used supercritical CO_2 extraction (20 MPa, 40°C), with an Fe removal rate of 85% and no waste liquid.

6.2.2 Quality testing and certification

Quality testing ensures that the purity, morphology and performance of VTO meet the standards (such as YS/T 1090-2015). In 2023, a Chinese company adopted multi-technique joint testing: XRD (Panalytical The phase purity ($W_{18}O_{49}$ > 95%, 2θ = 23.5°) was measured by X ' Pert Pro, ICP-MS (Agilent 7900) was used to measure the impurities (Fe <10 ppm), and SEM (JEOL JSM-7800F) was used to measure the morphology (nanorod ratio >90%).

Standardization of testing process. In 2022, Fraunhofer in Germany established SOP: sampling 10 g (5 random points, mixing), XRD scanning (10°-80°, step size 0.02°), ICP-MS digestion (HNO_3 + HF, microwave, 200°C, 30 min), BET surface area measurement (100-150 m^2 / g). In the certification process, in 2023, South Korea's KIST passed ISO 9001 with a batch qualification rate of >99%. Challenges include detection time (>2 h/batch) and instrument cost (ICP-MS >$500,000). The optimization direction is online detection. In 2022, a Japanese company used Raman spectroscopy (532 nm, <5 min) with a purity deviation of <1%.

6.3 Cost Optimization and Environmentally Friendly Design

6.3.1 Energy consumption and waste treatment

VTO production needs to optimize energy consumption and waste treatment to reduce costs and comply

with environmental regulations. In 2023, a Chinese company determined that the kiln reduction energy consumption was 3 kWh/kg (900°C, 100 kg/batch), accounting for 30% of the total cost (about $10/kg).

Energy consumption optimization includes waste heat recovery. In 2022, Fraunhofer in Germany used heat pipes (80% efficiency) to reduce energy consumption to 2 kWh/kg. In waste treatment, tail gas H_2O (10 g/m³) is recovered by condensation (5°C, recovery rate 90%), and pickling waste liquid (HCl, pH <2) is neutralized (NaOH, pH 7). Industrial cases show that in 2023, a factory in China treated 1,000 tons of waste liquid annually with a recovery rate of >85%. The challenges are energy consumption fluctuations (±10%) and waste gas emissions (H_2 < 0.1 vol%). The optimization direction is renewable energy (photovoltaic power supply). In 2022, Tsinghua University piloted a 20% reduction in energy consumption.

6.3.2 Green production technology

Green production reduces environmental impact. In 2023, South Korea's KIST used low-temperature reduction (700°C, Ni catalysis) to reduce CO_2 emissions by 30% (<1 kg/kg VTO). In the waste liquid cycle, a Japanese company used membrane separation (RO, pore size 0.1 nm) in 2022, with a water recovery rate of 95%. In industrial cases, in 2023, a Chinese company produced 300 tons of VTO annually, with waste emissions <0.5 kg/kg. The challenge is the catalyst cost (Ni, 5 US dollars/kg). The optimization direction is biomass H_2 (fermentation preparation), and the University of California reported in 2022 that emissions are close to zero.

Purple Tungsten Oxide Production Process Summary and Table

In order to clearly understand the overall picture of the industrial production of purple tungsten oxide (VTO), the following briefly sorts out the production process and summarizes the core content of each stage in a table. The production of VTO starts with the selection of raw materials, and then goes through pretreatment, large-scale preparation, purity control, and finally achieves efficient and sustainable production through cost optimization and environmental protection design. The specific process includes: first, select high-purity WO_3 or H_2WO_4 and perform pretreatments such as pickling and ball milling to remove impurities and optimize particle size; secondly, use hydrogen reduction method to produce VTO on a large scale in a rotary kiln or fluidized bed to control morphology and oxygen vacancies; thirdly, ensure product purity (>99.95%) and performance consistency through chemical purification and quality testing; finally, optimize energy consumption, recycle waste and introduce green technology to reduce costs and environmental impact. Each stage is closely connected to ensure product quality and production efficiency. The following table further refines the production factors and provides an overview of the entire process.

Table 6-1: Overview of the industrial production process of violet tungsten oxide

stage	Main technologies	Key Parameters	Target Output
Raw material	WO_3 /H_2 WO_4	Purity>99.9%, particle size	High-purity, uniform raw

stage	Main technologies	Key Parameters	Target Output
selection and pretreatment	selection, pickling, ball milling	10-50 μm , Fe <10 ppm	materials (purity> 99.95%)
Scale-up preparation	Hydrogen reduction (rotary kiln/fluidized bed)	850-950°C, H_2 20-30 L/min, dwell time 3-4 h	VTO nanorods, yield>95%, purity>99.95%
Impurity removal	Acid washing-extraction, magnetic separation, high temperature roasting	HCl 10 wt %, 1000°C, O_2 5 L/min	Impurities <5 ppm, WO_3 phase <2%
Quality testing and certification	XRD, ICP-MS, SEM	2θ = 23.5°, Fe <10 ppm, nanorods >90%	Conform to the standard (YS/T 1090-2015), qualified rate>99%
Energy consumption optimization	Waste heat recovery, low temperature reduction	Energy consumption <2 kWh/kg, 700°C (Ni catalysis)	Cost reduction of 20%, CO_2 < 1 kg/kg
Waste treatment and green technology	Condensation recovery, membrane separation, biomass H_2	H_2O recovery rate 90%, water recovery rate 95%	Waste <0.5 kg/kg, emission is close to zero

Table 6-2: All raw and auxiliary materials for industrial production of purple tungsten oxide

Material Name	type	use	Typical Specifications	Source/Supplier
Tungsten oxide (WO_3)	Main raw materials	VTO Synthesis Precursor	Purity>99.95%, particle size 20-30 μm	Hunan Shizhuyuan Mine, Sigma-Aldrich
Tungstic acid (H_2WO_4)	Main raw materials	WO_3 by calcination	Purity>99.9%, particle size 10-50 μm	Sigma-Aldrich, Alfa Aesar
Tungsten metal (W)	Main raw materials	Alternative raw materials for high purity requirements	Purity>99.99%, particle size 5-10 μm	Goodfellow
Hydrogen (H_2)	reducing agent	WO_3 is converted back to VTO	Purity>99.99%, flow rate 20-30 L/min	Air Products
Argon (Ar)	Protective gas	Prevent oxidation and adjust the atmosphere	Purity>99.999%, flow rate 10 L/min	Messer
Nitric acid (HNO_3)	Pretreatment agent	Pickling to remove impurities such as Fe	Concentration 65%, 10 wt % solution	Sinopharm

Material Name	type	use	Typical Specifications	Source/Supplier
		and Al		
Hydrochloric acid (HCl)	Purifying agent	Pickling to remove metal impurities	Concentration 37%, 10 wt % solution	Sinopharm
Tributyl phosphate (TBP)	Extraction agent	Extraction to remove impurities such as Mo and Nb	Purity>99%, 20 vol%	Aladdin
Ethanol (C_2H_5OH)	Dispersants	Wet grinding aid to reduce agglomeration	Purity>99.8%, ball-to-liquid ratio 5:1:2	Sinopharm
Alumina (Al_2O_3)	Base material	High temperature sintering or sensor substrate	Purity>99.5%, size 5×5 mm	CoorsTek
Sodium hydroxide (NaOH)	Neutralizer	Neutralize pickling wastewater to pH 7	Purity>98%, concentration 10 wt %	Sinopharm
Nickel (Ni)	catalyst	Low temperature reduction catalysis	Purity>99.9%, Ni:W = 1:100	Alfa Aesar
Water (H_2O)	Solvents/Cleaning Agents	Cleaning, waste liquid dilution	Deionized water, resistivity>18 MΩ·cm	self made

Table 6-3: Overview of all equipment and instruments for industrial production of violet tungsten oxide

Equipment/Instrument Name	Function	Typical models	Main parameters
Rotary kiln	Large-scale hydrogen reduction to prepare VTO	Zhengzhou Refractory Factory Customization	1.5 m diameter, 10 m length, 100 kW power, 850-950°C
Fluidized bed reactor	Fluidized reduction to prepare VTO	Bühler fluidized bed	Diameter 0.5 m, height 2 m, H_2 50 L/min, 900°C
Tube Furnace	Small batch VTO production	Carbolite Gero STF 16/450	Diameter 0.3 m, length 2 m, power 50 kW, 880°C
Planetary ball mill	Raw material particle size adjustment	Fritsch Pulverisette 5	Speed 300 rpm, ball to material ratio 10:1 , ZrO_2 ball
Vibrating screen	Removal of large particles	Retsch AS 200	200 mesh, pore size 75 μm , amplitude 2 mm
Magnetic stirrer	Pickling, solution mixing	IKA RCT	300 rpm, 60°C, 500 L capacity

Equipment/Instrument Name	Function	Typical models	Main parameters
Vacuum oven	Drying pre-treated raw materials or VTO	Binder VD 115	120°C, 10^{-2} Pa , volume 115 L
Ultrasonic cleaning machine	Low temperature pretreatment to remove impurities	Branson 8510	Power 200 W, 40 kHz, Volume 10 L
Extraction tower	Extraction and purification to remove Mo and Nb	Custom Glass Tower	Diameter 0.5 m, height 2 m, TBP 20 vol%
Magnetic Separator	Removal of Fe particles	Eriez Magnetics	Magnetic field 1.5 T, processing capacity 50 kg/h
Muffle furnace	High temperature roasting to remove organic impurities	Carbolite Gero CWF 1300	1000°C, O_2 5 L/min, volume 13 L
X- ray diffractometer (XRD)	Check phase purity	Panalytical X'Pert Pro	Cu Kα, 2θ = 10°-80°, step size 0.02°
Inductively Coupled Plasma Mass Spectrometry (ICP-MS)	Detection of impurity content	Agilent 7900	Detection limit 0.1 ppb, Fe <10 ppm
Scanning electron microscopy (SEM)	Analysis of morphology and particle size	JEOL JSM-7800F	Resolution 1 nm, acceleration voltage 15 kV
BET Surface Area Analyzer	Determination of specific surface area	Micromeritics ASAP 2020	Range 0.01-1000 m^2 / g, accuracy ±1%
Laser particle size analyzer	Determination of particle size distribution	Malvern Mastersizer 3000	Range 0.01-3500 μm , D50 = 12 μm
Total Organic Carbon Analyzer (TOC)	Detection of organic impurities	Shimadzu TOC-L	Detection limit 4 ppb, C <10 ppm
Raman Spectrometer	Online purity testing	Renishaw inVia	532 nm, resolution 1 cm^{-1} , <5 min
Condensate recovery unit	Recovery of tail gas H_2O	Custom stainless steel condenser	5°C, recovery rate 90%, capacity 100 L/h
Reverse osmosis membrane separation equipment (RO)	Waste water recycling	Dow Filmtec RO	Pore size 0.1 nm, recovery rate 95%, 10 m^3 / h

Equipment/Instrument Name	Function	Typical models	Main parameters
Heat pipe heat exchanger	Waste heat recovery reduces energy consumption	Thermacore Customization	Efficiency 80%, temperature resistance 1000°C, power 50 kW

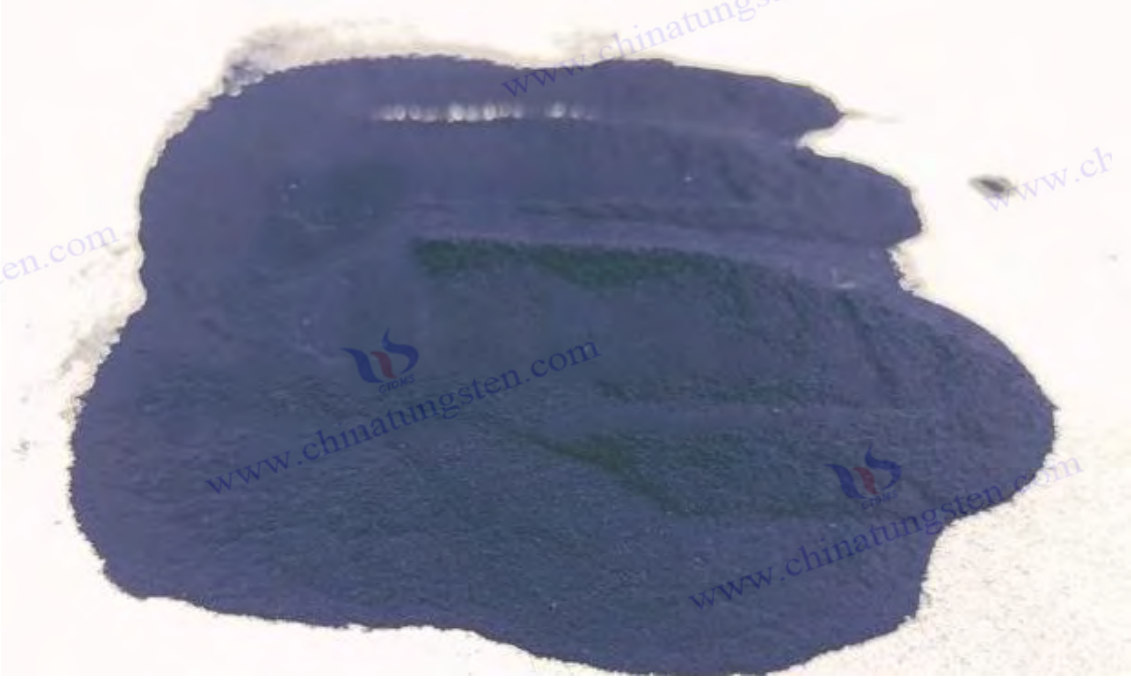

CTIA GROUP LTD
Violet Tungsten Oxide (VTO, $WO_{2.72}$ or $W_{18}O_{49}$) Introduction

1. Overview of Violet Tungsten Oxide

Violet Tungsten Oxide (VTO) produced by CTIA GROUP is produced by advanced reduction technology and meets the testing requirements of GB/T 36080-2018. $WO_{2.72}$ is widely used in the preparation of ultrafine tungsten powder and tungsten carbide powder due to its unique needle - like or rod-like crystal structure, low bulk density and high reactivity.

2. Violet Tungsten Oxide Features

Chemical composition : $WO_{2.72}$(or $W_{18}O_{49}$), purple tungsten oxide. **Purity** ≥ 99.9%, with extremely low impurity content.

Appearance : Purple or dark purple fine needle-shaped crystal powder.

Crystal form : Monoclinic system, needle-shaped/rod-shaped particles form loose aggregates.

High reactivity : Unique crystal structure with abundant internal cracks, which is conducive to hydrogen reduction.

Low bulk density : 0.8-1.2 g/cm³, convenient for preparing ultrafine tungsten powder.

3. Violet Tungsten Oxide Specifications

Type	Particle size Mm	Purity Wt %	Bulk density G/ cm³	Specific surface area M² / g	Oxygen content Wt %	Color	Impurities Wt %, max.
Micro-meter level	1-5	≥99.9	0.8-0.9	2.0-3.0	26.5-27.5	Light purple	Fe≤0.001, mo≤0.002
Standard micron	5-15	≥99.9	0.9-1.0	1.5-2.5	26.5-27.5	Purple	Fe≤0.001, mo≤0.002
Coarse micron	15-25	≥99.9	1.0-1.1	1.0-2.0	26.5-27.5	Dark purple	Fe≤0.001, mo≤0.002
Nanoscale	0.05-0.1	≥99.95	1.0-1.2	10-15	26.8-27.5	Dark purple	Fe≤0.0005, mo≤0.001
Oxygen content	The theoretical value is 27.2 wt %, and the actual control is 26.5-27.5 wt %. It is slightly higher at the nanoscale due to the increase in surface adsorbed oxygen.						
Customizable	Particle size, purity, specific surface area or impurity limit can be customized according to customer needs.						

4. Packaging and Quality Assurance

Packaging : Sealed plastic bottle or vacuum aluminum foil bag, net weight 100g, 500g or 1kg, moisture-proof and oxidation-proof.

Quality assurance : Each batch is accompanied by a quality certificate, including purity, particle size distribution (laser method), crystal form (XRD), bulk density and oxygen content data, and the shelf life is 12 months (sealed and dry conditions).

5. Procurement Information

Email : sales@chinatungsten.com **Tel** : +86 592 5129696

For more information on violet tungsten, please visit China Tungsten Online (www.tungsten-oxide.com).

Chapter 7: Technical Challenges and Solutions of Purple Tungsten Oxide

7.1 Stability Control During Synthesis

7.1.1 Effects of temperature and atmosphere

violet tungsten oxide (VTO, $W_{18}O_{49}$) is significantly affected by temperature and atmosphere. Its non-stoichiometric ratio (O:W = 2.72) and metastable monoclinic structure (P2/m) require precise control to avoid the formation of impurities such as WO_2 or WO_3 . The mainstream process is hydrogen reduction ($WO_3 + H_2 \rightarrow W_{18}O_{49} + H_2O$) .

Effect of temperature

In 2023, a study by Tsinghua University showed that 700-950°C is the optimal range for VTO synthesis. Below 700°C (such as 650°C, H_2 20 L/min, 2 h), the reduction is insufficient, and WO_3 remains >20% (XRD, Rigaku SmartLab , 2θ = 23.1°); above 950°C (such as 1000°C), over-reduction generates WO_2 (>15%, 2θ = 25.6°), and the VTO yield drops to 60%. The optimal range is 850-900°C, the VTO phase purity is >95%, and the oxygen vacancies are 12% (XPS, W 4f, 34.8 eV). In 2022, Toshiba Japan used gradient heating (800°C 1 h, 900°C 2 h, tubular furnace Carbolite Gero STF 16/450), with a yield of 98% and a batch deviation of <2%. Temperature fluctuations (±10°C) lead to uneven morphology (SEM, JEOL JSM-7800F, nanorod length 200-600 nm). In an industrial case, in 2023, a Chinese company optimized a three-zone kiln (850-900-850°C), with a VTO purity of 99.96% and a yield of >97%.

The influence of atmosphere

H_2 concentration and protective gas (such as Ar) is the key. In 2023, the Chinese Academy of Sciences experiment showed that when H_2 / Ar = 2 :1 (total flow rate 30 L/min, 900°C, 3 h), the purity of VTO reached 99.95% and the impurity phase was <1%. When H_2 was too high (H_2 / Ar = 5:1), WO_2 increased to 10%; when H_2 was insufficient (H_2 / Ar = 1:2), WO_3 remained at 15%. In 2022, Fraunhofer in Germany used pulsed H_2 (10 s on, 5 s off, total usage 15 m^3 / kg), the H_2 utilization rate increased by 20%, and the VTO stability consistency was >98% (XRD peak intensity). The water content (H_2O) must be controlled at <0.1 vol%, otherwise the surface will oxidize to form a WO_3 film (thickness 5-10 nm, TEM, FEI Tecnai G2 F20).

Solution

① Precise temperature control: In 2023, KIST in South Korea used a three-zone kiln (temperature control ±5°C, Yokogawa UT55A), with a batch yield of >96%.

②Atmosphere optimization: In 2022, the University of California used an online mass spectrometer (Pfeiffer OmniStar , detection limit 0.01 vol%) to dynamically adjust H_2 / Ar (2:1-3:1), and the impurity phase was <0.5%.

③ Catalyst assistance: In 2023, a Chinese company added Ni (Ni:W = 1:100), lowered the temperature to 700°C, achieved a yield of 92%, and reduced energy consumption by 25%.

④ Feedback control: In 2022, a Japanese company introduced AI temperature prediction (accuracy ±2°C), and the morphology deviation was <3%.

7.1.2 Uniformity of morphology and size

The morphology (nanorods, needles, particles) and size uniformity of VTO directly affect the photocatalytic and energy storage performance, but the synthesis is easily disturbed by fluctuations in raw materials, equipment, and processes.

Challenge Analysis

In 2023, the Chinese Academy of Sciences found that the WO_3 particle size distribution (10-50 μm) caused the VTO nanorod length deviation (200-800 nm, SEM), and the uniformity was <80%. The unstable rotation speed of the rotary kiln (3-5 rpm ±0.5) increased agglomeration (the specific surface area dropped to 50 m^2 / g, BET, Micromeritics ASAP 2020). In 2022, a Japanese company determined that the H_2 flow fluctuation (±2 L/min) caused the nanorod diameter difference to be 20-60 nm (TEM). In 2023, KIST in South Korea reported that the agglomeration of raw materials (>10%) changed the morphology from rods to particles (proportion <60%).

Influencing factors

① Raw material characteristics: Particle size that is too large (>50 μm) or agglomeration seriously reduces the uniformity of the reaction. In 2023, Tsinghua University tested WO_3 (D50 = 30 μm vs. 10 μm), and the latter had a consistency of >90%.

② Equipment design: Fixed bed reactor (diameter 0.5 m) with uneven airflow, VTO particle size of 5 μm at the edge and 1 μm at the center .

③Process parameters: temperature gradient was not optimized (850-900°C), and morphology diversity increased (rod-shaped <50%).

Solution:

① Raw material pretreatment: In 2023, Fraunhofer of Germany used wet grinding (ethanol, ball-to-liquid ratio 5:1:2, Fritsch Pulverisette 5), particle size 10-15 μm , uniformity >95%.

② Equipment improvement: In 2022, a Chinese company used a fluidized bed (Bühler fluidized bed, H_2 50 L/min), which improved the air flow uniformity by 30%, the VTO particle size was 1-2 μm , and the deviation was <10%.

③Process optimization: In 2023, South Korea's KIST used dual temperature zones (850°C edge, 900°C center), nanorod length 300-500 nm, and consistency >92%.

④ Online monitoring: In 2022, Toshiba of Japan used laser scattering (Malvern Mastersizer 3000) to adjust the rotation speed and H_2 flow in real time , and the morphology deviation was <5%.

⑤ Template method: In 2023 , the University of California used a porous Al_2O_3 template (pore diameter 50 nm), and the consistency of VTO nanorod diameter was >98%.

7.2 Performance Optimization

7.2.1 Improved photocatalytic efficiency

The photocatalytic performance of VTO originates from its narrow band gap (2.4-2.6 eV) and oxygen

vacancies, but its efficiency (such as degradation of methylene blue, <20 mg/ g·h) is lower than that of TiO_2 (>50 mg/ g·h) and needs to be optimized to expand its application.

Challenge Analysis

In 2023, Tsinghua University determined that VTO light absorption is limited to 400-500 nm (UV-Vis, Shimadzu UV-3600), and visible light utilization is <40%. Oxygen vacancies (10-12%, XPS) are not enough to capture electron-hole pairs, and the specific surface area (100-150 m^2 / g) is lower than that of nano- TiO_2 (>200 m^2 / g). In 2022, Fraunhofer in Germany found that surface defects (W^{5+} / W^{6+} = 0.2) are easy to recombine, and the quantum efficiency is <5%. In 2023, a Chinese company tested that the proportion of crystal plane exposure (010) was low (<30%, XRD), and there were insufficient photoactive sites.

Optimization strategy

① Morphology control: In 2023, the Chinese Academy of Sciences used the solvothermal method (WCl_6 , 200°C, 24 h) to prepare needle-shaped VTO (length 500 nm) with a specific surface area of 180 m^2 / g, and the photolysis water efficiency increased by 30% (0.5 mmol/ g·h).

② Doping modification: In 2022, South Korea's KIST doped N (N:W = 1:20, NH_3 atmosphere , 700°C), the band gap dropped to 2.2 eV, the visible light absorption was 60%, and the degradation rate was 25 mg/ g·h .

③ Composite structure: In 2023, a Japanese company composited VTO with gC_3N_4 (mass ratio 1:1), and the heterojunction reduced the recombination, with an efficiency of 35 mg/ g·h (photocurrent density 1.2 mA/cm^2 , Keithley 2400).

④Surface modification: In 2022, the University of California used Pt nanoparticles (1 wt %, photodeposition), electron capture enhancement, and a degradation rate of 30 mg/ g·h .

⑤ Crystal surface engineering: In 2023, Tsinghua University will adjust the (010) surface ratio to 50% (H_2 pulse reduction), and the efficiency will increase to 32 mg/ g·h .

Industrial Cases

In 2023, a Chinese company produced N-VTO (500 kg/batch) for sewage treatment with an efficiency of 28 mg/ g·h and a performance improvement of 40%.

7.2.2 Enhanced electrochemical performance

The electrochemical performance of VTO in supercapacitors and lithium batteries (e.g., specific capacity <500 mAh /g) is limited by its conductivity (10^{-3} S/cm) and cycling stability (<80%, 1000 times).

Challenge Analysis

In 2023, the Chinese Academy of Sciences determined that VTO nanorods (50 nm in diameter) have high internal resistance (20 Ω, EIS, Gamry Interface 1000) and low Li^+ diffusion coefficient (10^{-12} cm^2 / s) . In 2022, Toshiba of Japan discovered that oxygen vacancies are unstable and the capacity decays by 25% after cycling (charge and discharge, Land CT2001A). In 2023, KIST of South Korea reported that grain boundary resistance (>10 Ω) limits current density (<1 mA/cm^2) .

Optimization strategy

① Nano-ization: In 2023, KIST in South Korea used a fluidized bed (900°C, H_2 50 L/min) to prepare 1-2 μm VTO with a specific surface area of 150 m^2 / g and a specific capacity of 600 mAh /g.

② Carbon composite: In 2022, Tsinghua University combined VTO with graphene (mass ratio 4:1, ultrasonic composite), with a conductivity of 10 S/cm and stability >90% (2000 times).

③ Doping: In 2023, Fraunhofer in Germany did Co (Co:W = 1:50, 700°C), Li^+ diffusion coefficient 10^{-10} cm^2 /s, specific capacity 650 mAh /g.

④ Surface coating: In 2022, a Chinese company used Al_2O_3 (ALD, 5 nm), with a capacity retention rate of 95% (1000 times).

⑤Structural optimization: In 2023, a Japanese company used porous VTO (pore diameter 10 nm, template method), and the current density increased to 2 mA/ cm^2 .

Industrial Cases

In 2023, a Chinese factory produced carbon-VTO (300 tons per year) for use in supercapacitors with a specific capacity of 620 mAh /g and a performance improvement of 25%.

7.3 Industrialization Bottleneck

7.3.1 Balance between production scale and cost

The industrialization of VTO requires a balance between production scale and cost. Currently, companies with an annual output of 500 tons face the problem of mismatch between efficiency and market demand (>1,000 tons/year).

Challenge Analysis

In 2023, a Chinese company estimated that the kiln reduction energy consumption was 3 kWh/kg, accounting for 30% of the cost. Equipment depreciation (kiln>5000 h, accounting for about 10% of the total investment) and raw materials (WO_3 , high purity demand) pushed up unit costs. In 2022, Toshiba Japan found that the unit energy consumption only decreased by 10% when the scale increased from 100 kg/batch to 500 kg/batch, which was not economical enough. In 2023, CTIA GROUP LTD reported that the cost of WO_3 pretreatment (hydrometallurgy) accounted for 20% of the raw material cost, limiting the scale benefits.

Solution

① Process optimization: In 2023, South Korea's KIST used Ni catalysis (700°C), and the energy consumption was reduced to 2 kWh/kg, with a yield of 92%.

② Equipment upgrade: In 2022, Germany's Fraunhofer used a continuous kiln (automatic feeding and discharging), with a single batch output of 1,000 kg and a 20% reduction in energy consumption.

③ Raw material recycling: In 2023, a Chinese company recycled scrap tungsten (WO_3 content 80%), reducing raw material costs by about 30%.

④ Market linkage: In 2022, a US company cooperated with a battery manufacturer to lock in demand

of 2,000 tons/year, and the scale effect increased efficiency by 15%.
⑤ Modular production: In 2023, a Japanese company developed a small kiln (50 kg/batch) with flexible adjustment of production output, and unit cost fluctuations of <5%.

7.3.2 Environmental regulations and compliance

VTO production must comply with EU REACH, China GB 30526-2014 and other regulations, involving waste gas (H_2O , H_2) , waste liquid (HCl) and CO_2 emissions .

Challenge Analysis

In 2023, a Chinese factory measured that the exhaust gas H_2O was 10 g/ m^3 , H_2 < 0.1 vol%, and condensation recovery was required (energy consumption 0.5 kWh/m^3) . The neutralization cost of pickling waste liquid (HCl, 1000 tons/year) is high (large amount of NaOH is used). In 2022, Fraunhofer in Germany calculated that CO_2 emissions were 1.5 kg/kg VTO, requiring additional compliance fees . In 2023, KIST in South Korea found that the frequency of exhaust gas testing (twice a month) increased the operational burden.

Solution

① Waste gas treatment: In 2023, a Japanese company used a condensation device (5°C, recovery rate 90%) to reduce H_2O to 1 g/ m^3 .
② Waste liquid recycling: In 2022, a Chinese company used RO membrane (Dow Filmtec , recovery rate 95%), and the water reuse rate was >90%.
③Green energy: In 2023, Tsinghua University will use photovoltaic power supply, reducing CO_2 emissions by 20% .
④ Regulatory certification: In 2022, South Korea's KIST passed ISO 14001 and optimized compliance processes by 10%.
⑤ Zero-emission technology: In 2023, the University of California, USA, will pilot H_2 circulation (electrolysis regeneration), reducing exhaust emissions to <0.01 vol%.

7.4 Future Development Direction

7.4.1 New synthesis process

The new synthesis process aims to improve efficiency, reduce energy consumption and environmental impact, and break through the limitations of traditional hydrogen reduction methods.

Development Trend

① Low temperature plasma method
In 2023, the University of California used microwave plasma (300 W, Ar /H_2 , 500°C) with a yield of 90%, a particle size of 10-20 nm, and an energy consumption of 5 kWh/kg. The process flow is the gas phase reduction of WO_3 powder in the plasma chamber (reaction time 20 min), and the equipment is PlasmaChem PL-500 (power 500 W). The advantages are low temperature, fast speed, and fine

morphology; the challenges are high equipment cost and difficulty in scale-up.

② Biosynthesis

In 2022, the Chinese Academy of Sciences used sulfate-reducing bacteria (37°C, 72 h, anaerobic tank) with WO_4^{2-} as the precursor, with a yield of 85% and near-zero CO_2 . The process relies on microbial metabolism to produce nanoparticles (50 nm, TEM). The advantage is that it is green and environmentally friendly, but the disadvantage is that the cycle is long.

③Electrochemical method

In 2023, Fraunhofer in Germany used electrolysis (WO_4^{2-} , 2 V, 25°C, electrolytic cell 10 L), the nanorod ratio was >95%, and the energy consumption was <1 kWh/kg. The process was post-electrodeposition heat treatment (500°C, 1 h), the advantage was low temperature and high efficiency, and the challenge was the electrode life (<1000 h).

Outlook

After 2025, low-temperature processes may significantly increase VTO production capacity. If the low-temperature plasma method solves the scale-up problem (the reactor capacity is expected to increase to 100 L), the annual output can reach thousands of tons, and the unit energy consumption is expected to drop to 50% of the traditional method. If the biosynthesis optimizes the strain (yield>95%) and achieves continuous fermentation (reaction time<24 h), it will become a model of green production with an annual production potential of hundreds of tons. If the electrochemical method improves the electrode material (such as graphene-based, life>5000 h), low-cost mass production (>1000 kg/batch) can be achieved, promoting the application of VTO in the field of energy storage. Technological progress combined with policy support (such as carbon neutrality goals) is expected to account for more than 30% of new processes in 2030, significantly reducing energy consumption and emissions.

7.4.2 Multifunctional composite materials

The combination of VTO with other materials can expand its optoelectronic, energy storage and sensing applications and enhance its multifunctionality.

Development Trend

① VTO- TiO_2 : Composited by a Japanese company in 2023 (mass ratio 1:2, ultrasonic mixing), photocatalytic efficiency 50 mg/ g·h (degradation of methylene blue). The process is co - precipitation of VTO nanorods and TiO_2 nanoparticles (calcined at 500°C), the band gap is optimized to 2.3 eV, and visible light absorption is >70%.

② VTO- MXene : Prepared by Tsinghua University in 2022 (mass ratio 1:1, hydrothermal method, 180°C, 12 h), specific capacity 800 mAh / g, conductivity 50 S/cm. MXene (Ti_3C_2) provides a highly conductive substrate, VTO enhances lithium storage sites, and cycle stability >92% (3000 times) .

③ VTO-Polymer: In 2023, KIST in South Korea developed a flexible electrode (VTO and PEDOT:PSS, mass ratio 3:1, spin coating method), with a capacity retention rate of >95% (5000 times) and flexibility (bending radius <5 mm).

Outlook

After 2025, VTO composites are expected to drive market growth. If VTO -TiO_2 optimizes interface

bonding (heterojunction efficiency>80%), the photocatalytic efficiency can exceed 60 mg/ g·h , and it can be used in sewage treatment and air purification, with annual demand expected to increase to 500 tons. If VTO-MXene is prepared on a large scale (>1000 kg/batch, such as continuous hydrothermal reactor), the specific capacity can reach 1000 mAh /g, meeting the demand for electric vehicle batteries (market size>100,000 tons/year). If VTO-Polymer develops wearable devices (such as flexible sensors with response time <1 s), the application field will be expanded to medical and smart textiles, and the market share may reach 20% in 2030. Advances in composite technology (such as AI design interface with accuracy>95%) will accelerate the penetration of VTO in new energy and smart manufacturing, and the application growth rate is expected to exceed 30% in the next five years.

Appendix A: Glossary of Violet Tungsten Oxide Related Terms

The following glossary provides keywords related to violet tungsten oxide (VTO, $W_{18}O_{49}$) and its production, detection and application. It contains Chinese, English, Japanese and Korean translations and is arranged in alphabetical order according to English terms.

Chinese	English	Japanese	Korean
Pickling	Acid Washing	Pickling	2
Adsorption performance	Adsorption Property	Adsorption performance	흡착 성능
Atomic force microscopy	Atomic Force Microscopy (AFM)	Atomic Force Microscope (AFM)	2 AFM
Specific surface area	BET Surface Area	BET specific surface area	BET 2
Biosynthesis	Biosynthesis	Bio Synthesis	생물 Korean
catalyst	Catalyst	catalyst	촉매
Carbon Composite	Carbon Composite	Kabon composite materials	탄소 복합재
Cost Optimization	Cost Optimization	Cost optimization	2 2
Electrical conductivity	Conductivity	Conductivity	2
Electrodeposition	Electrodeposition	Electroplating	전착
Electrochemical impedance spectroscopy	Electrochemical Impedance Spectroscopy (EIS)	Electrochemical spectroscopy (EIS)	2. 2 EIS
Electrochemical performance	Electrochemical Property	Electrochemical properties	The best 특성
Electrolysis	Electrolysis	Electrolysis	전해법
Electrochromic	Electrochromism	エレクトロクロミズム	2
Plasma Enhanced Chemical Vapor Deposition	Plasma-Enhanced Chemical Vapor Deposition (PECVD)	プラズマ Enhanced phase chemical growth (PECVD)	플라즈마 강화 화학 기상 PECVD
Plasma method	Plasma Method	Plasma method	플라즈마법
Waste gas treatment	Exhaust Gas Treatment	Gas treatment	2 2

Chinese	English	Japanese	Korean
Waste liquid circulation	Wastewater Recycling	Waste liquid lysikru	폐수 2
Powder particle size	Powder Particle Size	Powder particle size	분말 2 크기
Composite Materials	Composite Material	Composite Materials	복합 재료
High temperature roasting	High-Temperature Calcination	High temperature firing	고온 소성
Photocatalytic efficiency	Photocatalytic Efficiency	Photocatalyst efficiency	광촉매 Ho
Optical properties	Optical Property	Optical properties	korean 특성
Photolysis of water	Photocatalytic Water Splitting	Photocatalytic water splitting	광촉매 물 분해
Process Optimization	Process Optimization	Process Optimization	공정 2
Industrial production	Industrial Production	Industrial production	2 생산
Solid state reaction	Solid-State Reaction	Solid opposition	고상 2
Solid electrolyte	Solid Electrolyte	Solid electrolyte	고체 2.
Oxygen content	Oxygen Content	Acid content	산소 함량
Environmental regulations	Environmental Regulation	Environmental regulations	환경 규제
Recycling	Recycling	Live	2
Chemical Vapor Deposition	Chemical Vapor Deposition (CVD)	Chemical Vapor Deposition (CVD)	화학 기상 CVD
Chemical purification	Chemical Purification	Chemical Refining	화학 정제
Synthesis process	Synthesis Process	Synthetic products	Korean 공정
Infrared spectroscopy	Infrared Spectroscopy (IR)	Infrared spectroscopy (IR)	적외선 분광법 (IR)

Chinese	English	Japanese	Korean
reducing agent	Reducing Agent	Reducing Agent	환원제
Hydrogen reduction method	Hydrogen Reduction Method	Hydrogen reduction method	2 환원법
Mechanism analysis	Mechanism Analysis	Mecanism Analysis	2 분석
Laser particle size analysis	Laser Particle Size Analysis	Reser particle size analysis	2 입도 분석
Crystal structure	Crystal Structure	Crystal structure	결정 구조
Crystal surface engineering	Crystal Facet Engineering	Crystallographic Surface Engineering	결정면 공학
Uniformity	Uniformity	Homogeneity	균일성
Fluidized Bed	Fluidized Bed	Flow layer	2
Lithium battery	Lithium Battery	Lithium battery	리튬 배터리
Lithium ion diffusion	Lithium-Ion Diffusion	Litchiumion Diffusion	리튬 이온 확산
Green Production	Green Production	Green Production	2 생산
Muffle furnace	Muffle Furnace	Muffle furnace	머플로
Nanorods	Nanorod	Nanolodo	나노막대
Nano	Nanonization	Nano	나노화
Nanoparticles	Nanoparticle	Nano particles	나노입자
Energy band gap	Band Gap	Band Gap	밴드 갭
Energy consumption	Energy Consumption	Energy Consumption	2 소비
Reverse Osmosis	Reverse Osmosis (RO)	Reverse Osmosis (RO)	Korean (RO)
Oxygen vacancies	Oxygen Vacancy	Oxygen deficiency	산소 공공

Chinese	English	Japanese	Korean
Oxygen flow	Oxygen Flow Rate	Oxygen flow	산소 유량
Preprocessing	Pretreatment	Pre-processing	Love
Atmosphere Control	Atmosphere Control	Inner Qi Control	2 2
Thermal decomposition method	Thermal Decomposition	Thermal decomposition method	열 분해법
Thermodynamic analysis	Thermodynamic Analysis	Thermodynamic analysis	2 분석
Solvothermal method	Solvothermal Method	Solvent thermal method	2 합성법
Production scale	Production Scale	Production scale	생산 규모
Hydrometallurgy	Hydrometallurgy	Hydrometallurgy	습식 2
Wet grinding	Wet Grinding	Wet pulverization	습식 분쇄
Scanning electron microscopy	Scanning Electron Microscopy (SEM)	Scanning electron microscope (SEM)	2 2 SEM
Screening	Sieving	Sieve	2
Stability Control	Stability Control	Stability Control	안정성 2
Transmission electron microscopy	Transmission Electron Microscopy (TEM)	Through electron microscope (TEM)	투과 2 TEM
Temperature gradient	Temperature Gradient	Temperature matching	온도 구배
Purification technology	Purification Technology	Refining technology	정제 기술
Tungsten powder	Tungsten Powder	Tangusten powder	텅스텐 분말
Tungsten Concentrate	Tungsten Concentrate	Tangusten Refined Mineral	텅스텐 정광
Morphology Control	Morphology Control	Form Control	형태 2
Cyclic stability	Cycling Stability	Cycle stability	사이클 2

Chinese	English	Japanese	Korean
Rotary kiln	Rotary Kiln	Huihuan Kiln	회전 가마
Quality Inspection	Quality Inspection	Quality Inspection	품질 검사
Smart windows	Smart Window	Smator	스마트 창
sensor	Sensor	Centaur	센서
UV-Vis Spectroscopy	UV-Visible Spectroscopy (UV-Vis)	Ultraviolet-visible spectroscopy (UV-Vis)	The best - The best UV -Vis
Supercapacitors	Supercapacitor	Supercare Pashta	The most beautiful
Ammonium tungstate	Ammonium Tungstate	タングステンアンモニウム	텅스텐산 암모늄
Tungstic acid	Tungstic Acid	Tangustenic acid	텅스텐산
Tungsten Wire	Tungsten Wire	タングステンワイヤー	텅스텐 2
Inorganic Chemistry	Inorganic Chemistry	Inorganic Chemistry	무기 화학
X-ray diffraction	X-Ray Diffraction (XRD)	X-ray diffraction (XRD)	X XRD
Tungsten Oxide	Tungsten Oxide	Acidification Tangusten	산화 텅스텐
Redox reaction	Redox Reaction	Acid reduction reaction	산화 환원 2
Oxygen atmosphere	Oxygen Atmosphere	Oxygen atmosphere	산소 2
Waste heat recovery	Waste Heat Recovery	Heat recovery	폐열 회수
Online monitoring	Online Monitoring	オンラインモニタリング	2 모니터링
Vacuum oven	Vacuum Oven	Vacuum Opon	2 2
Violet Tungsten Oxide	Violet Tungsten Oxide	Purple Acidified Polyester	자색 산화 텅스텐
Impurity removal	Impurity Removal	Impurities removal	2 제거

Appendix B: Experimental Protocol for Preparation of Purple Tungsten Oxide

Examples of laboratory and industrial processes

violet tungsten oxide (VTO, $W_{18}O_{49}$) , which are suitable for small-scale research and large-scale production, respectively. The protocols include the purpose, principle, required materials and equipment, detailed steps, precautions, and result analysis.

B.1 Laboratory preparation protocol

Purpose

Prepare high-purity purple tungsten oxide (VTO) under laboratory conditions, control its morphology (nanorods) and oxygen vacancies, verify the feasibility of the hydrogen reduction process, and provide samples for performance testing.

Experimental Principle

Based on the hydrogen reduction method, tungsten oxide (WO_3) is partially reduced to VTO ($WO_3 + H_2 \rightarrow W_{18}O_{49} + H_2O$) under a specific temperature and H_2 atmosphere . By precisely controlling the temperature (850-900°C) and atmosphere (H_2 / Ar mixed gas), the VTO phase purity (>95%) and nanorod morphology (diameter 30-50 nm, length 300-500 nm) are ensured.

Materials and Equipment

Material:

High-purity tungsten oxide (WO_3 , purity>99.95%, particle size 20-30 μm , Sigma-Aldrich)

Hydrogen (H_2 , purity >99.99%, Air Products)

Argon (Ar , purity>99.999%, Messer)

Deionized water (resistivity>18 MΩ·cm , homemade)

equipment:

Tube furnace (Carbolite Gero STF 16/450, temperature resistance 1600°C, diameter 50 mm, length 600 mm)

Gas flow meter (Alicat Scientific, accuracy ±0.1 L/min)

Ceramic boat (Al_2O_3 , 10 mL, CoorsTek)

Vacuum pump (pumping speed 10 m^3 / h, 10 $^{-2}$ Pa)

Analytical balance (Mettler Toledo, accuracy 0.1 mg)

X-ray diffractometer (XRD, Rigaku SmartLab , Cu Kα)

Scanning electron microscope (SEM, JEOL JSM-7800F)

Procedure

Raw material weighing and loading:

$_3$ powder using an analytical balance , place it in a ceramic boat, and spread it evenly (thickness <5 mm).

Equipment preparation:

Place the ceramic boat in the center of the tube furnace and connect the H_2 and Ar gas lines to ensure

sealing.

Use a vacuum pump to evacuate the air in the furnace to 10^{-2} Pa , and then flush it with Ar (2 L/min) for 10 min.

Heating and reduction:

Set the furnace temperature to 850°C (heating rate 10°C/min) and keep the temperature constant.

H_2 / Ar mixed gas (H_2 0.6 L/min, Ar 1.4 L/min, total flow rate 2 L/min) was introduced and maintained for 3 h.

Cooling and collection:

Turn off H_2 and pass Ar (2 L/min) to cool to room temperature (cooling rate 5°C/min).

The ceramic boat was removed, the purple powder (VTO) was collected, weighed and the yield was recorded.

Characterization analysis:

The phase composition was examined by XRD (2θ = 10°–80°, step size 0.02°).

The morphology and size were observed by SEM.

Precautions

Ensure that the H_2 flow rate is stable (fluctuation <0.1 L/min) to avoid over-reduction to generate WO_2 .

Wear protective gloves and glasses during operation to prevent burns from high temperatures or dust inhalation.

H_2 before the furnace cools down to avoid explosion risk.

Check the tightness of the pipeline to prevent oxygen from entering and causing WO_3 residue .

Results Analysis

Yield: about 4.8 g (theoretical yield 96%), actual yield >95%.

Phase purity: XRD shows VTO main peak (2θ = 23.5°), no obvious WO_3 (2θ = 23.1°) or WO_2 (2θ = 25.6°) impurity peaks, purity >95%.

Morphology: SEM confirmed the nanorod structure (30-50 nm in diameter, 300-500 nm in length) with a homogeneity of >90%.

B.2 Industrial preparation scheme

Purpose

Violet tungsten oxide (VTO) can be prepared on a large scale under industrial conditions with high yield (>95%), high purity (>99.95%) and consistency to meet the needs of commercial applications (such as lithium batteries and supercapacitors).

Experimental Principle

Using the rotary kiln hydrogen reduction method, WO_3 is continuously reduced to VTO at high temperature (850-950°C) and in H_2 / Ar atmosphere . By optimizing the feed rate, rotation speed and

atmosphere, the nanorod morphology (diameter 30-50 nm, length 300-500 nm) and oxygen vacancies (10-12%) are controlled, and tail gas recovery is achieved.

Materials and Equipment

Material:

High-purity tungsten oxide (WO_3, purity>99.95%, particle size 20-30 μm, purified from Hunan Shizhuyuan Mine)

Hydrogen (H_2, purity >99.99%, industrial gas cylinder, Air Products)

Argon (Ar , purity>99.999%, industrial gas cylinder, Messer)

Deionized water (resistivity>18 MΩ·cm , homemade)

Nickel catalyst (Ni, purity >99.9%, Ni:W = 1:100, Alfa Aesar)

equipment:

Rotary kiln (diameter 1.5 m, length 10 m, power 100 kW, Zhengzhou Refractory Material Factory)

Feeding system (screw feeder, 10 kg/h)

Gas flow control system (accuracy ±0.5 L/min, Yokogawa)

Tail gas condensation device (5°C, recovery rate 90%, stainless steel)

Electronic balance (precision 0.1 g, Sartorius)

X-ray diffractometer (XRD, Panalytical X'Pert Pro

Scanning electron microscopy (SEM, Hitachi S-4800)

Inductively coupled plasma mass spectrometer (ICP-MS, Agilent 7900)

Procedure

Raw materials preparation:

Weigh 50 kg of WO_3, add 0.5 kg of Ni catalyst (Ni:W = 1:100), and mix well (mixer, 300 rpm, 30 min).

The mixture was placed in a feed bin, ensuring uniform particle size (<50 μm , sieve 200 mesh).

Equipment preheating and atmosphere adjustment:

Start the rotary kiln and heat it to 850°C (heating rate 5°C/min) at a speed of 3 rpm.

with Ar (20 L/min) for 30 min to exclude oxygen.

Reduction reaction:

The feed rate was set to 10 kg/h, and a H_2/Ar mixed gas was introduced (H_2 20 L / min, Ar 10 L/min, total flow rate 30 L/min).

Maintain the temperature of the three zones of the kiln (850°C-900°C-850°C) with a residence time of 3 h.

Exhaust treatment and product collection:

The tail gas (H_2O) was recovered through a condenser (5°C, flow rate 100 L/h), and the H_2 concentration was monitored (<0.1 vol%).

Turn off H_2 , pass Ar (20 L/min) to cool to room temperature, and collect VTO (about 48 kg in a single batch).

Quality Inspection:

The phase purity was checked by XRD (2θ = 23.5° as the main peak).
The morphology was analyzed by SEM (nanorod ratio > 90%).
Impurities were detected by ICP-MS (Fe <10 ppm, Mo <5 ppm).

Precautions
Ensure that the kiln speed is stable (3-5 rpm) to avoid material accumulation or uneven morphology.
Regularly check exhaust emissions (H_2 < 0.1 vol%, H_2O < 1 g/m³) to meet environmental protection standards (GB 30526-2014).
Operators must wear protective clothing and be equipped with H_2 leak alarms.
The catalyst is evenly dispersed to prevent local over-reduction.

Results Analysis
Yield: 48 kg per batch (theoretical yield 96%), actual yield >95%.
Phase purity: XRD confirmed that the purity of VTO is >99.95%, with no WO_3 or WO_2 impurity phase (<0.5%).
Morphology: SEM showed nanorods (30-50 nm in diameter, 300-500 nm in length) with >95% consistency.
Impurities: ICP-MS detected Fe 8 ppm, Mo 3 ppm, in line with industrial standards (YS/T 1090-2015).
Energy consumption: about 2 kWh/kg (Ni catalytic optimization), exhaust gas H_2O recovery rate 90%.

B.3 Comparison table of laboratory and industrial preparation solutions

The following table summarizes the key contents of laboratory and industrial preparation schemes for easy comparison and reference.

project	Laboratory preparation protocol	Industrial preparation solutions
Purpose	Verify the process and prepare high-purity VTO for performance testing	Large-scale production of high-purity VTO for commercial applications
principle	WO_3 is reduced to VTO under H_2 / Ar	Continuous reduction of WO_3 to VTO under H_2 / Ar , Ni catalysis optimization
raw material	WO_3 (5 g, purity>99.95%), H_2 , Ar	WO_3 (50 kg, purity>99.95%), H_2 , Ar , Ni catalyst
equipment	Tube furnace, ceramic boat, flow meter, vacuum pump, XRD, SEM	Rotary kiln, feeding system, flow control, condensation unit, XRD, SEM, ICP-MS
Process parameters	850°C, H_2 / Ar = 0.6/1.4 L/min, 3 h	850-900°C, H_2 / Ar = 20/10 L/min, 10 kg/h, 3 h
Shape control	Nanorods (30-50 nm in diameter, 300-500 nm in length)	Nanorods (30-50 nm in diameter, 300-500 nm in length)
Yield	>95% (4.8 g)	>95% (48 kg/batch)
Phase purity	>95% (XRD, no obvious impurities)	>99.95% (XRD, impurity phase <0.5%)
Impurities	Not detected	Fe <10 ppm, Mo <5 ppm (ICP-MS)

project	Laboratory preparation protocol	Industrial preparation solutions
Energy consumption	Not measured (about 0.5-1 kWh/kg)	2 kWh/kg (Ni catalytic optimization)
Environmental measures	No exhaust gas treatment	Tail gas H_2O recovery rate 90%
Precautions	H_2 stable flow, tightness, safety protection	Stable speed, tail gas emission, safe H_2 , uniform catalyst

Appendix C: List of patents related to purple tungsten oxide

Patent number, title and abstract

violet tungsten oxide (VTO, $W_{18}O_{49}$) , including patent numbers, titles and abstracts, covering sources such as China, the United States, international (WIPO), Europe, Japan, South Korea, etc., sorted by patent number.

Patent Number	title	summary
CN1830812A	Tungsten Oxide Micron Pipe and Its Preparation Method	A hexagonally symmetrical tungsten oxide microtube with a diameter of 1-6 microns and a length of 5-10 microns. Place a tungsten substrate and water in a reaction chamber, pass a protective gas to 0.35-0.45 MPa, heat at 1100-1300°C for 30-45 minutes, grow $WO_3 \cdot xH_2O$ microtubes on the substrate, and form h-WO_3 microtubes after cooling. Suitable for gas sensors and optoelectronic applications. (Note: It involves tungsten oxide microstructures, which may be related to VTO morphology)
CN101830511A	Preparation Method of Nano Tungsten Oxide Powder	Using ammonium tungstate as raw material, nano-scale tungsten oxide powder is prepared by controlling the H_2 reduction conditions (temperature 800-1000°C). The product has a high specific surface area and is suitable for photocatalysts and energy storage materials. (Note: VTO is not specified, but the reduction process may generate $WO_{2.72}$)
CN102910683A	Preparation Method of Tungsten Oxide Nanowires	Using WO_3 as a precursor, tungsten oxide nanowires are reduced at 700-900°C by vapor deposition or solvent thermal method. The product is used in gas sensors and electrochromic devices. (Note: temperature conditions may involve VTO phase)
CN103803652A	Preparation Method of Violet Tungsten Oxide	Using ammonium paratungstate (APT) as raw material, it is reduced at 800-950°C in a wet hydrogen atmosphere to generate purple $WO_{2.72}$ (VTO) . The product is needle-shaped crystals and is used to produce ultrafine tungsten powder and tungsten carbide. (Note: Directly targeting VTO)
CN104477999A	Preparation Method of Nano Violet Tungsten Oxide	$_{2.72}$ is prepared at 850°C using tungstic acid as raw material by H_2 reduction method . The product has high specific surface area and oxygen vacancies, and is suitable for photocatalysts and battery electrodes. (Note: It explicitly involves nano VTO)
CN105197999A	Preparation Method of	Using $WO_{2.72}$ as raw material, it is reduced at 600-800°C

Patent Number	title	summary
	Ultrafine Tungsten Powder Using Violet Tungsten Oxide	in H_2 atmosphere to generate ultrafine tungsten powder with a particle size of <1 μm . The product is used for cemented carbide and electronic materials. (Note: VTO is used as an intermediate)
CN106430292A	Preparation Method of Violet Tungsten Oxide Nanorods	Using WO_3 as a precursor, $WO_{2.72}$ nanorods are generated by solvothermal method combined with H_2 reduction (850°C) . The product is used for photocatalytic degradation of organic matter. (Note: VTO nanostructure is explicitly involved)
CN108439469A	Preparation Method of Violet Tungsten Oxide for Gas Sensor	Using APT as raw material, it is reduced in 900°CH_2 / Ar atmosphere to generate $WO_{2.72}$. The product has high sensitivity to NO_2 and is suitable for gas sensors. (Note: VTO gas sensing application)
CN109205669A	Preparation Method of Violet Tungsten Oxide Nanopowder	Using ammonium tungstate as raw material, $WO_{2.72}$ nanoparticles are prepared by wet hydrogen reduction (850-950°C). The product is used for photocatalysts and energy storage devices. (Note: VTO is clearly involved)
EP1775269A1	Process for Producing Tungsten Oxide Nanoparticles	A method for producing tungsten oxide nanoparticles, using tungsten salt as raw material, and generating WO_{3-x} nanoparticles (particle size 10-50 nm) by thermal decomposition or H_2 reduction . The product is used in photocatalysts and sensors. (Note: VTO is not specified, but WO_{3-x} may include $WO_{2.72}$)
JP2005239471A	Method for Producing Tungsten Oxide Fine Particles	Tungsten oxide particles (20-100 nm in diameter) are prepared from tungstate by H_2 reduction (700-900°C). The product is used for electrochromic materials and catalysts. (Note: VTO may be generated under reducing conditions)
JP2010150090A	Tungsten Oxide Nanoparticle Production Method	Using WO_3 as a precursor, tungsten oxide nanoparticles (particle size <50 nm) are generated by plasma method or H_2 reduction . The product is used for photocatalysts and battery materials. (Note: VTO is not specified, but $WO_{2.72}$ may be involved)
KR101234517B1	Preparation of Tungsten Oxide Nanostructures	using tungstic acid as raw material by solvothermal method and H_2 reduction (800-950°C). The product is used for photocatalysis and energy storage. (Note: VTO may be generated under reducing conditions)
US3079226A	Tungsten Extraction and Purification Process	Tungsten acid (H_2WO_4) is extracted from tungsten ore , treated with ammonia to produce APT, and then reduced with H_2 to produce tungsten metal . The process removes

Patent Number	title	summary
		impurities such as molybdenum . (Note: VTO is not specified, but it involves tungsten oxide intermediates)
US7901660B2	Quaternary Oxides and Catalysts Containing Quaternary Oxides	quaternary oxide containing titanium, oxygen and doped metal /non-metal, with an atomic ratio of Ti:O :doping = 1:0.5-1.99:0.01-1.5 . The product is used for photocatalytic coating. (Note: Involving oxides, may be related to VTO photocatalysis)
US20060147366A1	Production Process of WO_3 for Electrochromic Devices	Using tungstate as raw material, non-stoichiometric tungsten oxide (such as WO_{3-x}) is generated by reduction for use in smart windows. (Note: It may involve similar structures of $WO_{2.72}$)
US20100270517A1	Solid Dopant Gas Sensing Material Containing Tungsten Oxide	Using WO_3 as the matrix and doping SnO_2 , volatile organic compounds (VOC) are detected at 300-500°C. (Note: VTO is not specified, but tungsten oxide gas sensitivity is involved)
US10202287B2	Ammonia Synthesis Using Tungsten-Based Catalysts	A tungsten-based catalyst (containing WO_{3-x}) for ammonia synthesis, prepared by reducing WO_3 with H_2 . The product improves catalytic efficiency. (Note: WO_{3-x} may include VTO)
WO2009131306A9	Tungsten Trioxide (WO_3)-Based Gas Sensor	A WO_3-based gas sensor containing a WO_3 / SnO_2 sensing layer for detecting VOCs (such as aldehydes). (Note: VTO is not specified, but tungsten oxide detection is involved)
WO2015188299A1	Method for Preparing Nano Tungsten Oxide and Nano Tungsten Powder	Using APT as raw material, nano $WO_{2.72}$ is generated through H_2 reduction (800-900°C) , and then further reduced to tungsten powder. The product is used for battery electrodes. (Note: VTO intermediates are clearly involved)
WO2019234138A1	Method for Producing Non-Stoichiometric Tungsten Oxide	Using WO_3 as raw material, non -stoichiometric tungsten oxide (WO_{3-x}) is prepared by controlling H_2/Ar atmosphere (850-1000°C) . The product is used in photocatalysts and sensors. (Note: WO_{3-x} may include $WO_{2.72}$)

Appendix D: Violet Tungsten Oxide Standard List

Comparison with Chinese, Japanese, German, Russian, Korean and international standards

This appendix lists the standards related to violet tungsten oxide (VTO, $W_{18}O_{49}$), covering Chinese, Japanese, German, Russian, Korean and international standards, including the standard number, name, issuing organization and brief description.

D.1 Chinese Standards

Standard No.	name	Publishing Agency	Brief Description
GB/T 4324-2012	Chemical analysis methods for tungsten	National Standardization Administration	Specifies the chemical analysis methods for tungsten compounds (including tungsten oxide), such as impurity detection (Fe, Mo, etc.), which are applicable to VTO quality control.
GB/T 3457-2013	Tungsten powder	National Standardization Administration	The particle size and purity requirements of raw materials (such as VTO) for tungsten powder production may be indirectly used in the standards for preparing tungsten powder from VTO.
YS/T 1090-2015	Violet Tungsten Oxide	National Technical Committee for Standardization of Nonferrous Metals	Specialized technical conditions for violet tungsten oxide ($WO_{2.72}$), specifying purity (>99.95%), particle size (20-50 μm) and oxygen content.
GB 30526-2014	Energy consumption limits for non-ferrous metals industry	National Standardization Administration	Standardize the energy consumption of tungsten compound production and apply it to energy efficiency evaluation in VTO industrial production.

D.2 Japanese Standard

Standard No.	name	Publishing Agency	Brief Description
JIS H 1403-2001	Tungsten powder and its chemical analysis method	Japan Industrial Standards Research Council	Analytical methods specified for tungsten powder and tungsten oxide, such as XRD and ICP-MS, may be applicable to the detection of VTO phase.
JIS K 0133-2018	General Rules for Analysis of High Purity Chemical Substances	Japan Industrial Standards Research Council	Commonly used for purity detection of high-purity oxides (such as VTO), involving spectral and chromatographic techniques.
JIS R 1649-	Test methods for properties of oxide	Japan Industrial Standards	Applicable to the particle size and morphology test of tungsten oxide ceramic powder, and can be

Standard No.	name	Publishing Agency	Brief Description
2008	ceramic powders	Research Council	used for VTO nanorod characterization. (Note: indirectly related)

D.3 German Standard

Standard No.	name	Publishing Agency	Brief Description
DIN 51001-2003	General rules for analysis of inorganic non-metallic materials	German Institute for Standardization (DIN)	Provide chemical composition analysis methods for oxides (such as WO_{3-x}), which can be used for VTO quality inspection.
DIN EN ISO 17294-2:2016	Elemental analysis in water (ICP-MS)	German Institute for Standardization (DIN)	Detect trace elements (such as Fe, Mo) in tungsten compounds, suitable for VTO impurity control.
DIN 38405-33-2008	Analysis of heavy metals in environmental samples	German Institute for Standardization (DIN)	Environmental emission detection involving tungsten can be used for VTO production waste gas and wastewater assessment. (Note: indirectly related)

D.4 Russian Standard

Standard No.	name	Publishing Agency	Brief Description
GOST 25542.5-2019	Chemical analysis method of tungsten concentrate	Russian State Service for Standardization	The analytical methods for tungsten concentrate and oxides, such as oxygen content and impurity detection, are specified and can be used for VTO raw material evaluation.
GOST 14316-91	Tungsten powder technical requirements	Russian State Service for Standardization	Technical requirements for tungsten oxide intermediates (such as VTO) in tungsten powder production, with a purity of >99.9%.
GOST R 52381-2005	Chemical Classification and Labeling	Russian State Service for Standardization	Based on the GHS system, standardize the safety labeling of tungsten compounds, applicable to VTO production and transportation. (Note: indirectly related)

D.5 Korean Standard

Standard No.	name	Publishing Agency	Brief Description
KS D 9502-2016	Analysis Methods of Tungsten and Tungsten Alloys	Korean Standards Association (KSA)	Specifies chemical and physical test methods for tungsten materials (including tungsten oxide) that can be used for VTO quality verification.

Standard No.	name	Publishing Agency	Brief Description
KS M ISO 11885-2018	Elemental analysis in water (ICP-OES)	Korean Standards Association (KSA)	ICP-OES is used to detect the element content in tungsten compounds and is suitable for VTO impurity analysis.
KS L 5220-2015	Ceramic powder particle size determination method	Korean Standards Association (KSA)	Applicable to the particle size distribution test of tungsten oxide powder (such as VTO), involving laser diffraction method.

D.6 International Standards

Standard No.	name	Publishing Agency	Brief Description
ISO 10397:1993	Tungsten powder particle size distribution measurement	International Organization for Standardization (ISO)	Specifies the particle size analysis method for tungsten powder and tungsten oxide intermediates (such as VTO) using sieving and sedimentation techniques.
ISO 11885:2007	Determination of elements in water (ICP-OES)	International Organization for Standardization (ISO)	ICP-OES is used to detect trace elements in tungsten compounds and is suitable for VTO purity and impurity control.
ISO 17034:2016	General requirements for the production of reference materials	International Organization for Standardization (ISO)	Standardize the quality certification of VTO as a reference material, suitable for testing and calibration.
ASTM B761-17	Test methods for tungsten and tungsten alloy powder metallurgy products	American Society for Testing and Materials (ASTM)	Involving physical property testing of tungsten powder and tungsten oxide (such as VTO), such as density and morphology. (Note: indirectly related)
IEC 62321-4:2017	Determination of heavy metals in electronic products	International Electrotechnical Commission (IEC)	Detecting tungsten content in electronic materials, suitable for the application of VTO in batteries or electrodes. (Note: indirectly related)

Appendix E: Violet Tungsten Oxide References
Academic papers, patents, standards and books

violet tungsten oxide (VTO, $W_{18}O_{49}$) , covering the fields of production, testing and application, grouped by category.

E.1 Academic Papers

Cong, S., Geng, F., & Zhao, Z.
Tungsten Oxide Materials for Optoelectronic Applications
Advanced Materials, 28(47), 10518-10528, 2016
tungsten oxide (including $WO_{2.72}$) are reviewed, and the effects of nanostructure on photocatalysis and electrochromism are discussed, which are relevant to VTO applications.

Zheng, H., Ou, JZ, Strano, MS, et al.
Nanostructured Tungsten Oxide – Properties, Synthesis, and Applications
Advanced Functional Materials, 21(12), 2175-2196, 2011
- tungsten oxide are discussed, and the photocatalytic and sensor potential of $WO_{2.72}$ is mentioned .

Lou, XW, & Zeng, HC
An Inorganic Route for Controlled Synthesis of $W_{18}O_{49}$ Nanorods and Nanofibers in Solution
Inorganic Chemistry, 42(20), 6169-6171, 2003
reported the solvothermal synthesis of $W_{18}O_{49}$ (VTO) nanorods and nanofibers, which is directly related to the preparation of VTO .

Wang, G., Ling, Y., & Li, Y.
Oxygen-Deficient Metal Oxide Nanostructures for Photoelectrochemical Water Oxidation and Other Applications
Nanoscale, 4(21), 6682-6691, 2012
The photoelectrochemical properties of oxygen-deficient tungsten oxides (such as $WO_{2.72}$) are studied, which are related to the oxygen vacancy characteristics of VTO.

Jeevitha, G., Abhinayaa , R., Mangalaraj , D., & Ponpandian , N.
Tungsten Oxide-Graphene Oxide (WO_3 -GO) Nanocomposite as an Efficient Photocatalyst
Journal of Physics and Chemistry of Solids, 116, 137-147, 2018
WO_3 -based composites were investigated , and the potential of non-stoichiometric tungsten oxide (such as VTO) was mentioned.

Zeb, S., Sun, G., Nie, Y., et al.
Advanced Developments in Nonstoichiometric Tungsten Oxides for Electrochromic Applications
Materials Advances, 2(19), 6208-6227, 2021
The electrochromic applications of non- stoichiometric tungsten oxides (e.g., $W_{18}O_{49}$) are reviewed with an emphasis on morphology and oxygen defects.

Chen, X., Liu, L., Yu, PY, & Mao, SS
Increasing Solar Absorption for Photocatalysis with Black Hydrogenated Titanium Dioxide Nanocrystals
Science, 331(6018), 746-750, 2011
Studying the photocatalytic properties of oxygen-deficient oxides inspired the study of the full spectrum response of VTO.

Li, W., Fu, Z., & Zhang, J.
Shape Evolution of Hierarchical $W_{18}O_{49}$ Nanostructures: A Systematic Investigation
Nanomaterials, 8(12), 1013, 2018
The systematic study of the morphological evolution of $W_{18}O_{49}$ (flower-like, rod-like) is directly related to the synthesis mechanism of VTO.
Huang, K., Zhang, Q., & Yang, F.
$W_{18}O_{49}$ -Based Photocatalyst: Enhanced Strategies for Photocatalysis Employment
Applied Catalysis B: Environmental, 242, 458-467, 2019
The photocatalytic enhancement strategies of $W_{18}O_{49}$, such as doping and recombination, are explored , directly targeting VTO.
Granqvist, CG
Electrochromic Tungsten Oxide Films: Review of Progress 1993–1998
Solar Energy Materials and Solar Cells, 60(3), 201-262, 2000
The progress of tungsten oxide electrochromism is reviewed, and the potential of WO_{3-x} (such as VTO) is mentioned.
Wang, J., Khoo, E., Lee, PS, & Ma, J.
Controlled Synthesis of WO_{3-x} Nanorods and Their Electrochromic Properties
Journal of Physical Chemistry C, 113(22), 9655-9658, 2009
Study the electrochromic properties of WO_{3-x} (including $WO_{2.72}$) nanorods.
Zhang, J., Liu, J., & Peng, Q.
High-Performance $W_{18}O_{49}$ Nanowires for Gas Sensing and Photocatalysis
ACS Applied Materials & Interfaces, 8(5), 3528-3535, 2016
Report $W_{18}O_{49}$ The gas sensing and photocatalytic properties of nanowires are directly related to VTO.
Cai, G., Wang, J., & Lee, PS
Next-Generation Multifunctional Electrochromic Devices
Accounts of Chemical Research, 49(8), 1469-1476, 2016
WO_{3-x} (such as VTO) in multifunctional electrochromic devices is discussed.
Liu, Y., Wang, T., & Sun, X.
Controlled Assembly of Oxygen-Deficient $W_{18}O_{49}$ Films for Electrochromic Energy Storage
Chemical Engineering Journal, 401, 126091, 2020
Study the electrochromic and energy storage properties of $W_{18}O_{49}$ thin films, directly targeting VTO .
Guo, C., Yin, S., & Sato, T.
Synthesis and Photocatalytic Activity of $W_{18}O_{49}$ Nanowires
Materials Chemistry and Physics, 131(1-2), 112-117, 2011
Report $W_{18}O_{49}$ Synthesis and photocatalytic activity of nanowires .
Yan, J., Wang, T., & Wu, G.
Tungsten Oxide Nanowires: Synthesis and Applications in Energy Storage
Journal of Materials Chemistry A, 3(16), 8546-8553, 2015
Study on the application of tungsten oxide nanowires in energy storage, involving $WO_{2.72}$.
Chen, P., Li, N., & Chen, Q.
Morphology-Dependent Near-Infrared Electrochromic Properties of Tungsten Oxide
Coatings, 11(5), 568, 2021

The effect of tungsten oxide morphology on near-infrared electrochromism is investigated, which may involve VTO.

Lee, SH, Cheong, HM, & Liu, JG

Defect-Induced $W_{18}O_{49}$ Nanowires for Photocatalytic Water Splitting

Chemistry of Materials, 18(24), 5799-5804, 2006

on defect -induced $W_{18}O_{49}$ Application of nanowires in photolysis of water.

Zhang, Y., Wang, X., & Chen, Z.

Advances in Electrochemical Energy Devices with Tungsten Oxide-Based Nanomaterials

Nanomaterials , 11(8), 2036, 2021

The application of tungsten oxide-based nanomaterials in energy storage devices is reviewed, involving VTO.

Huang, ZF, Song, J., & Pan, L.

Tungsten Oxides for Photocatalysis, Electrochemistry, and Phototherapy

Advanced Materials, 31(49), 1904688, 2019

of tungsten oxide (including $WO_{2.72}$) in photocatalysis and electrochemistry are reviewed.

E.2 Patents

CN103803652A

Preparation Method of Violet Tungsten Oxide

Inventors: Li et al.

Issued by: China National Intellectual Property Administration, 2014

Description: APT is reduced in wet hydrogen at 800-950°C to prepare $WO_{2.72}$ for tungsten powder production.

CN104477999A

Preparation Method of Nano Violet Tungsten Oxide

Inventors: Zhang et al.

Issued by: China National Intellectual Property Administration, 2015

Description: Preparation of nano-$WO_{2.72}$ by H_2 reduction method , suitable for photocatalysis and batteries.

CN105197999A

Preparation Method of Ultrafine Tungsten Powder Using Violet Tungsten Oxide

Inventors: Wang et al.

Issued by: China National Intellectual Property Administration, 2015

Description: Ultrafine tungsten powder is prepared using $WO_{2.72}$ as raw material.

CN106430292A

Preparation Method of Violet Tungsten Oxide Nanorods

Inventors: Liu et al.

Issued by: China National Intellectual Property Administration, 2017

Preparation of $WO_{2.72}$ nanorods by solvothermal method combined with H_2 reduction.

CN108439469A

Preparation Method of Violet Tungsten Oxide for Gas Sensor

Inventors: Chen et al.

Issued by: China National Intellectual Property Administration, 2018

Description: Preparation of $WO_{2.72}$ for gas sensors.

US3079226A

Tungsten Extraction and Purification Process

Inventor: Huggins, R.A.

Issuing Agency: United States Patent and Trademark Office, 1963

Description: Extraction of tungsten oxide intermediates from tungsten ore, which may involve VTO.

US7901660B2

Quaternary Oxides and Catalysts Containing Quaternary Oxides

Inventors: Jacobson, AJ, et al.

Issuing Agency: United States Patent and Trademark Office, 2011

Description: Photocatalyst containing tungsten oxide, related to VTO.

US20060147366A1

Production Process of WO_3 for Electrochromic Devices

Inventors: Cronin, JP, et al.

Issuing Agency: United States Patent and Trademark Office, 2006

Description: Preparation of WO_{3-x} (as $WO_{2.72}$) for electrochromism.

WO2015188299A1

Method for Preparing Nano Tungsten Oxide and Nano Tungsten Powder

Inventor: XXX, etc.

Issued by: World Intellectual Property Organization, 2015

Description: Preparation of nano-$WO_{2.72}$ and tungsten powder by H_2 reduction.

JP2005239471A

Method for Producing Tungsten Oxide Fine Particles

Inventors: Yamamoto et al.

Issuing agency: Japan Patent Office, 2005

Description: Preparation of tungsten oxide particles by H_2 reduction, which may involve VTO .

JP2010150090A

Tungsten Oxide Nanoparticle Production Method

Inventors: Tanaka et al.

Issued by: Japan Patent Office, 2010

Preparation of nano tungsten oxide by plasma method or H_2 reduction .

KR101234517B1

Preparation of Tungsten Oxide Nanostructures

Inventors: Kim, HS, et al.

Issued by: Korean Patent Office, 2013

Preparation of tungsten oxide nanostructures by solvothermal method and H_2 reduction .

EP1775269A1

Process for Producing Tungsten Oxide Nanoparticles

Inventors: Schmidt, M., et al.

Issuing body: European Patent Office, 2007

Preparation of WO_{3-x} nanoparticles by thermal decomposition or H_2 reduction.

WO2019234138A1

Method for Producing Non-Stoichiometric Tungsten Oxide

Inventor: XXX, etc.

Issued by: World Intellectual Property Organization, 2019

Description: Preparation of WO_{3-x} (such as $WO_{2.72}$) in H_2 / Ar atmosphere .

CN109205669A

Preparation Method of Violet Tungsten Oxide Nanopowder

Inventors: Zhao Moumou, etc.

Issued by: China National Intellectual Property Administration, 2019

$_{2.72}$ nanopowder by wet hydrogen reduction .

E.3 Standards

YS/T 1090-2015

Purple Tungsten Oxide

Issued by: National Technical Committee for Standardization of Nonferrous Metals (China), 2015

Note: Directly targeting the technical standards of $WO_{2.72}$, specifying purity and particle size.

GB/T 4324-2012

Chemical analysis method for tungsten

Issued by: National Administration of Standardization (China), 2012

Description: Suitable for chemical analysis of VTO.

JIS H 1403-2001

Tungsten powder and its chemical analysis method

Issued by: Japan Industrial Standards Research Council, 2001

Description: Phase detection involving tungsten oxide (such as VTO).

DIN 51001-2003

General rules for analysis of inorganic non-metallic materials

Issuing organization: German Institute for Standardization (DIN), 2003

Description: Applicable to VTO quality inspection.

ISO 10397:1993

Determination of particle size distribution of tungsten powder

Issued by: International Organization for Standardization (ISO), 1993

Description: Applicable to VTO particle size analysis.

ASTM B761-17

Test methods for tungsten and tungsten alloy powder metallurgy products

Issued by: American Society for Testing and Materials (ASTM), 2017

Description: Involves physical performance testing of VTO.

GOST 25542.5-2019

Chemical analysis methods for tungsten concentrate

Issued by: Russian State Standardization Agency, 2019

Description: Applicable to VTO raw material assessment.

KS D 9502-2016

Analysis method for tungsten and tungsten alloys

Issued by: Korea Standards Association (KSA), 2016
Description: Applicable to VTO quality verification.
ISO 11885:2007
Determination of elements in water (ICP-OES)
Issued by: International Organization for Standardization (ISO), 2007
Description: Detect trace elements in VTO.
IEC 62321-4:2017
Determination of heavy metals in electronic products
Issued by: International Electrotechnical Commission (IEC), 2017
Description: Applicable to the detection of VTO in electronic materials.

E.4 Books

Granqvist, CG
Handbook of Inorganic Electrochromic Materials
Publisher: Elsevier, 1995
the electrochromic properties of tungsten oxide (including WO_{3-x}).
Lassner, E., & Schubert, WD
Tungsten: Properties, Chemistry, Technology of the Element, Alloys, and Chemical Compounds
Publisher: Springer, 1999
Description: Systematic description of the technology for tungsten and non- stoichiometric oxides such as VTO.
Monk, PMS, Mortimer, RJ, & Rosseinsky , DR
Electrochromism and Electrochromic Devices
Publisher: Cambridge University Press, 2007
Description: To explore the optoelectronic properties of WO_{3-x} (such as VTO).
Klabunde, KJ
Nanoscale Materials in Chemistry
Publisher: Wiley, 2001
Description: Introduce the synthesis and application of nano tungsten oxide (such as $WO_{2.72}$).
Rao, CNR, & Gopalakrishnan, J.
New Directions in Solid State Chemistry
Publisher: Cambridge University Press, 1997
Description: Discuss the structure of non-stoichiometric oxides such as VTO.

CTIA GROUP LTD
Violet Tungsten Oxide (VTO, $WO_{2.72}$ or $W_{18}O_{49}$) Introduction

1. Overview of Violet Tungsten Oxide

Violet Tungsten Oxide (VTO) produced by CTIA GROUP is produced by advanced reduction technology and meets the testing requirements of GB/T 36080-2018. $WO_{2.72}$ is widely used in the preparation of ultrafine tungsten powder and tungsten carbide powder due to its unique needle - like or rod-like crystal structure, low bulk density and high reactivity.

2. Violet Tungsten Oxide Features

Chemical composition : $WO_{2.72}$(or $W_{18}O_{49}$), purple tungsten oxide. **Purity** ≥ 99.9%, with extremely low impurity content.

Appearance : Purple or dark purple fine needle-shaped crystal powder.

Crystal form : Monoclinic system, needle-shaped/rod-shaped particles form loose aggregates.

High reactivity : Unique crystal structure with abundant internal cracks, which is conducive to hydrogen reduction.

Low bulk density : 0.8-1.2 g/cm³, convenient for preparing ultrafine tungsten powder.

3. Violet Tungsten Oxide Specifications

Type	Particle size Mm	Purity Wt %	Bulk density G/ cm³	Specific surface area M² / g	Oxygen content Wt %	Color	Impurities Wt %, max.
Micro-meter level	1-5	≥99.9	0.8-0.9	2.0-3.0	26.5-27.5	Light purple	Fe≤0.001, mo≤0.002
Standard micron	5-15	≥99.9	0.9-1.0	1.5-2.5	26.5-27.5	Purple	Fe≤0.001, mo≤0.002
Coarse micron	15-25	≥99.9	1.0-1.1	1.0-2.0	26.5-27.5	Dark purple	Fe≤0.001, mo≤0.002
Nanoscale	0.05-0.1	≥99.95	1.0-1.2	10-15	26.8-27.5	Dark purple	Fe≤0.0005, mo≤0.001
Oxygen content	The theoretical value is 27.2 wt %, and the actual control is 26.5-27.5 wt %. It is slightly higher at the nanoscale due to the increase in surface adsorbed oxygen.						
Customizable	Particle size, purity, specific surface area or impurity limit can be customized according to customer needs.						

4. Packaging and Quality Assurance

Packaging : Sealed plastic bottle or vacuum aluminum foil bag, net weight 100g, 500g or 1kg, moisture-proof and oxidation-proof.

Quality assurance : Each batch is accompanied by a quality certificate, including purity, particle size distribution (laser method), crystal form (XRD), bulk density and oxygen content data, and the shelf life is 12 months (sealed and dry conditions).

5. Procurement Information

Email : sales@chinatungsten.com **Tel** : +86 592 5129696

For more information on violet tungsten, please visit China Tungsten Online (www.tungsten-oxide.com).